POWER QUALITY IMPROVEMNET IN DISTRIBUTION SYSTEM USING ACTIVE POWER DEVICES IN A CUSTOM POWER PARK

A Project Report

submitted by

ANVAR HUSSAIN VP

in partial fulfilment of the requirements
for the award of the degree of

MASTER OF TECHNOLOGY

DEPARTMENT OF ELECTRICAL ENGINEERING
INDIAN INSTITUTE OF TECHNOLOGY MADRAS.

MAY 2015

THESIS CERTIFICATE

This is to certify that the thesis titled **POWER QUALITY IMPROVEMNET IN DISTRIBUTION SYSTEM USING ACTIVE POWER DEVICES IN A CUSTOM POWER PARK**, submitted by **ANVAR HUSSAIN VP**, to the Indian Institute of Technology, Madras, for the award of the degree of **Master of Technology**, is a bonafide record of the research work done by him under my supervision. The contents of this thesis, in full or in parts, have not been submitted to any other Institute or University for the award of any degree or diploma.

Place: Chennai
Date:

Prof. Mahesh Kumar
Professor
Dept. of Electrical Engineering
IIT-Madras, 600 036

ACKNOWLEDGEMENTS

I take pleasure in thanking various people, who helped and supported me to carry out this work. I am thankful to those who influenced me during the course of study.

I would like to express my sincere thanks to my project guide Dr. Mahesh Kumar, for his support and guidance. His suggestions had been the source of inspiration for me during the conduct of this project.I am also grateful for the laboratory facilities provided by him in the Power Quality Simulation Laboratory, ESB 342, Department of Electrical Engineering, which facilitated my simulation work.

I would also like to thank my fellow research scholars in PQ lab especially Chandan Kumar, Narsa Reddy, Nafih Muhammad, Manoj Kumar, K. Nikhil and K. Srikanth for spending their valuable time in discussing about the project and answering my queries.

I am thankful to my classmates B. J. Rajendranth, Guru Srinivas, K. Venkateswarlu and Rajender Singh for supporting me during the course of my study.

Finally, most importantly, I wish to express my deepest gratitude and love to my parents for their unconditional support and encouragement throughout my entire education.

Anvar Hussain VP.

ABSTRACT

KEYWORDS: Custom Power; Custom Power Park; Power Quality; Voltage Sag/Swell; Harmonics; Interruption.

Custom Power Park (CPP) concept means integration of multiple custom power devices within an industrial or commercial park which offers the customers high quality and reliable power at distribution system voltage level. Custom Power Park is one of the most useful solution to prevent/mitigate voltage sag/swell, interruption and voltage and current harmonics in distribution system.

In this thesis CPP has been modelled using MATLAB/SIMULINK. The modelled CPP consists of Solid State Transfer Switch (SSTS) which is used for transferring loads to a healthy feeder when some faults occur on connected feeder, Distribution Static Compensator (DSTATCOM) which is used to mitigate current harmonic problems, Dynamic Voltage Restorer (DVR) with DC energy storage used for voltage compensation under different voltage quality disturbance such as sag/swell and harmonics and standby or backup Diesel Generator (DG) is used to supply loads under total feeder loss.

A fast sag/swell detection technique which can work even under distorted grid voltages is used for detecting the supply quality of the feeders, and an effective control scheme for the coordination of devices are also presented.

The ability of the custom power park for improving power quality under various disturbances are studied using MATLAB/SIMULINK through extensive simulation studies.

TABLE OF CONTENTS

LIST OF TABLES

LIST OF FIGURES

ABBREVIATIONS

DC	Direct Current
AC	Alternating Current
CP	Custom Power
CPP	Custom Power Park
PF	Preferred Feeder
AF	Alternate Feeder
DSTATCOM	Distribution STATic COMpensator
DVR	Dynamic Voltage Restorer
UPQC	Unified Power Quality Conditioner
SSTS	Solid State Transfer Switch
STS	Static Transfer Switch
SSCB	Solid State Circuit Breaker
SSCL	Solid State Current Limiter
PI	Proportional and Integral
PWM	Pulse Width Modulation
GTO	Gate Turn-off Thyristor
IGBT	Insulated Gate Bipolar Transistor
PCC	Point of Common Coupling
VSI	Voltage Source Inverter
ASD	Adjustable Speed Drive
PLC	Programmable Logic Controller
THD	Total Harmonic Distortion

NOTATIONS

English symbols

f	Fundamental frequency
THD_V	Total harmonic distortion in voltage
n	Harmonic number
V_n	RMS value of n'th harmonic component of voltage
v_a, v_b, v_c	Three phase instantaneous voltages
V_a, V_b, V_c	Three phase phasor voltages
v_α, v_β, v_0	Instantaneous value of $\alpha\beta 0$ reference frame voltages
v_d, v_q, v_0	Instantaneous value of $dq0$ reference frame voltages
v_{dq}	Fault detection signals in SRF
f_c	Cut-off frequency of LPF
f_{swmax}	Maximum value of switching frequency in hysteresis control
v_{a-pf}, v_{b-pf}, v_{c-pf}	Three phase instantaneous voltages of preferred feeder
v_{a-af}, v_{b-af}, v_{c-af}	Three phase instantaneous voltages of alternate feeder
R_{s-pf}, L_{s-pf}	Resistive and inductive component of preferred feeder impedance
R_{s-af}, L_{s-af}	Resistive and inductive component of alternate feeder impedance
$v_{d(p)}$, $v_{q(p)}$	Instantaneous value of dq reference frame voltages in positive sequence synchronous reference frame
v_{dp}, v_{qp}	DC value of dq reference frame voltages in positive sequence synchronous reference frame
$\overline{v}_{dp}$	Filtered value of dc component of d axis voltages in positive sequence synchronous reference frame
v_{dn}, v_{qn}	DC value of dq reference frame voltages in negative sequence synchronous reference frame
v_{dp-pf}	DC value of d axis voltages in positive sequence synchronous reference frame for preferred feeder
v_{dp-af}	DC value of d axis voltages in positive sequence synchronous reference frame for alternate feeder

$\overline{v}_{dp-pf}$	Filtered value of dc component of d axis voltages in positive sequence synchronous reference frame for preferred feeder
$\overline{v}_{dp-af}$	Filtered value of dc component of d axis voltages in positive sequence synchronous reference frame for alternate feeder
$\overline{v}_{a0}$, $\overline{v}_{a+}$, $\overline{v}_{a-}$	Instantaneous zero, positive and negative sequence voltages
$\overline{V}_{a+}$	Phasor value of positive sequence voltage
$\overline{i}_{a0}$, $\overline{i}_{a+}$, $\overline{i}_{a-}$	Instantaneous zero, positive and negative sequence currents
C_{dc1}, C_{dc2}	DC link capacitance's of DSTATCOM
K_p, K_i	Proportional and integral gains for DC link voltage controller
V_{dc1}, V_{dc2}	Voltage across capacitance's C_{dc1}, C_{dc2}
V_{dcref}	Reference DC link voltage of DSTATCOM
V_{dcD}	DC link voltage of DVR
R_f, L_f	Resistive and inductive component of filter inductance
v_{sa}, v_{sb}, v_{sc}	Three phase instantaneous voltages at PCC of DSTATCOM
i_{sa}, i_{sb}, i_{sc}	Three phase instantaneous source currents at PCC of DSTATCOM
i_{la}, i_{lb}, i_{lc}	Three phase instantaneous load currents at PCC of DSTATCOM
i^*_{fa}, i^*_{fb}, i^*_{fc}	Three phase instantaneous filter reference currents
i_{fa}, i_{fb}, i_{fc}	Three phase instantaneous filter injected currents
P_{lavg}	Average load power of L1
T	Period of the instantaneous power waveform
P_{loss}	Switching losses in DSTATCOM
v_{la}, v_{lb}, v_{lc}	Three phase instantaneous voltages at terminal of load L3
v_{ta}, v_{tb}, v_{tc}	Three phase instantaneous voltages before DVR injection transformer
R_{se}, L_{se}, C_{se}	Resistance, inductance and capacitance of DVR filter
h_i, h_v	Hysteresis bands for DSTATCOM, DVR
v_{fa}, v_{fb}, v_{fc}	Three phase instantaneous voltages injected by DVR
$v^*_{d\ ref}$, $v^*_{q\ ref}$, $v^*_{0\ ref}$	Voltages to be injected by DVR in $dq0$ reference frame
v^*_{fa}, v^*_{fb}, v^*_{fc}	Three phase instantaneous voltages to be injected by DVR
$v_{L\ max}$	Desired value of voltage magnitude in each phase of load L3
$Z_{l1\ a}$, $Z_{l1\ b}$, $Z_{l1\ c}$	Impedance's of each phases of the unbalanced load
Z_{l1d}	Impedance of the DC load
Z_{l2}, Z_{l3}	Impedance of the loads L1, L2, L3

Greek symbols

$\phi+$	Phase angle between voltage and current injected in degrees
θ	Transformation angle from $\alpha\beta 0$ to $dq0$ reference frame
ω	Fundamental frequency in radians/second
Δt	Sampling interval for differentiation
ξ	Damping ratio of filter
ω_n	Natural frequency of filter

CHAPTER 1

INTRODUCTION

This chapter presents the background and motivation behind the work carried out in this project. It discusses the need of power quality improvement in a distribution systems briefly, then it briefly introduces the concept of Custom Power Park. This is followed by the project objectives and limitations. Finally an outline about the organization of thesis is provided at the end of the chapter.

1.1 Background

In recent years both industrial, commercial electrical consumers have reported a rising tide of mis-adventures related to power quality. The major cause of power quality problems are from today's automated equipments, electrical drives or robots, automated manufacturing lines or machine tools, Programmable Logic Controllers (PLC) or power supplies in personnel computers. They and their likes are far vulnerable to the disturbances in distribution systems than their previous generation electromechanical equipments, less automated production and information systems.

For the reason described above, there is growing interest in equipment for mitigation of power quality disturbances, especially power electronic based devices called custom power devices.

Custom Power (CP) is power electronic based solution for improving power quality disturbances, CP devices such as SSTS, DSTATCOM and DVR are applied in the distribution system for protecting an entire plant, feeder or a group of customers or loads. Custom Power Park (CPP) is a new concept in improving power quality which is able to offer customers high quality power and to meet the needs of sensitive and critical loads within an industrial/commercial park [1]. The concept requires integration of multiple custom power devices which have previously deployed independently. These devices compensate for power quality disturbances to protect sensitive loads as well as improve

service reliability. The custom power park concept requires integration of state of art power quality devices within an utilities distribution system which could provide tenants with electronically controlled, cost effective, nearly undisturbed energy: energy corrected for major sags, swells, harmonics, interruption and other disturbances. Here in this work SSTS, DSTATCOM and DVR are the state of art technologies installed to coordinate each other and monitor power supply so as to mitigate disturbances. The distinguished features of these devices i.e., ability of SSTS for transfer of loads between two feeders, harmonic and reactive power compensation capability of DSTATCOM and voltage compensation capability of DVR can be combined to create a new system that can provide improved quality of electrical service as per the requirement of customers.

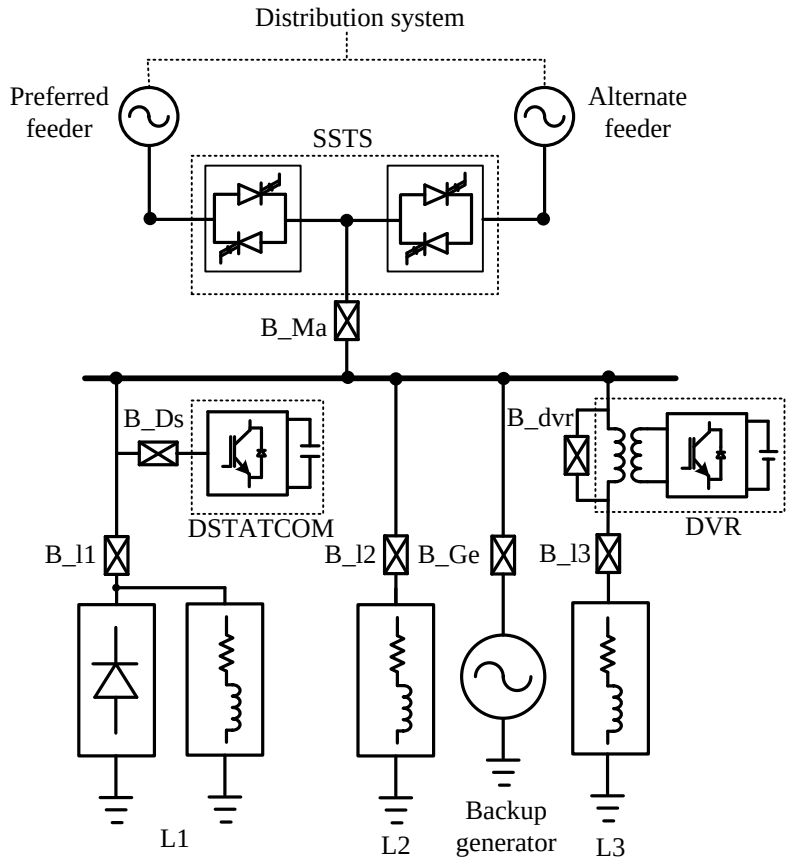

Figure 1.1: Single line diagram of CPP used in study.

The custom power park model studied in this work has three loads L1, L2 and L3 and each receives different power quality levels CP-1, CP-2 and CP-3. All loads in the park will get the benefit of SSTS which will transfer the loads to an alternate feeder if some kind of fault is detected on preferred feeder. The DSTATCOM is connected in shunt with load L1 which is a unbalanced and nonlinear load, it will compensate for

the current harmonics and unbalance. DVR is connected in series with load L3, DVR protects this load against sag/swell. The loads L2 andL3 will get benefit of diesel generator which will comes to operation under total feeder loss. A fast control algorithm for detection of the power quality disturbances is also presented. The single line diagram of the CPP model used for simulation is as shown in Fig. 1.1.

The major power quality problems taken in to consideration in this work are balanced voltage sag/swell, unbalanced voltage sag/swell current and voltage harmonics and interruption. To maintain power quality there should be proper coordination between devices used in the CPP. Hence it demands use of fast acting controllers so as to make detection and mitigation of power quality disturbances very fast.

1.2 Project Objectives and Scope

The project involves design and modelling of various custom power devices and its controllers along with a common control strategy to maintain different power quality levels in the CPP.

The major objectives of this work are:

- Design and simulation of different custom power devices which includes SSTS, DSTATCOM and DVR for mitigating power quality problems such as voltage and current harmonics voltage sag/swell and interruption.
- Combining the custom power devices and Diesel Generator (DG) to form a custom power park where the customers will get different power quality levels according to their requirements.
- Developing an efficient control algorithm for proper coordination of devices used in custom power park

1.3 Organization of Thesis

Chapter 1 presented a brief introduction about motivation behind this work and it also discusses about the objectives of the work.

Chapter 2 presents literature review which has mainly three sections, the first part briefs about different power quality problems, their causes and effects on the power system. The second section discusses about different custom power devices and their operating principles. The final section describes about gives an idea about the custom power park and its different topologies present in literature, It also explains some techniques used for fault detection in custom power park.

Chapter 3 discusses about design and modelling of different custom power devices. The operation of SSTS, voltage sag/swell detection method and its control are explained in the first part of this chapter. Operation DSTATCOM and its reference current generation are described in second part. The final part is discusses about the DVR and its control.

Chapter 4 presents the modelling of Custom Power Park, it also discusses about the control algorithm used for control and coordination of the custom power devices in CPP.

Chapter 5 presents the simulation results. The operation of the CPP and effectiveness of the control algorithm used for coordination of devices are also discussed with the help of simulation results.

and **Chapter 6** summarizes the work carried out in this project and it also gives an outlook of further research that can be carried out based on this thesis

CHAPTER 2

LITERATURE REVIEW

This project is to model a Custom Power Park (CPP) for improving power quality of sensitive and critical loads, before going to details of CPP it is necessary to have an idea about the different power quality problems, their causes and effects on power system operation.

2.1 Introduction to Power Quality

Power quality in electrical networks is one of the most concerned areas of electric power systems. Institute of Electrical and Electronics Engineers (IEEE) standard IEEE 1100 defines power quality [2] as "The concept of powering and grounding sensitive electronic equipments in a manner suitable for the equipment." The power quality has serious implications for customers, utilities and electrical equipment manufacturers. A simple word power quality is the set of electrical boundaries that allow a device to function in its intended manner without significant loss of performance.

2.2 Power Quality Problems, Causes and Effects

Power quality and its related issues are most concern nowadays. The ideal power supply voltage should maintain a steady magnitude and a perfect sinusoidal wave shape without any interruptions. Any phenomena that will alter ideal situation are classified as disturbances. the widespread use of electronic equipments such as information technology equipments, PLC's, Adjustable Speed Drives (ASD) and energy efficient lighting systems will cause harmonics in currents as well as voltages [2]. Further more conventional loads such as large arc furnaces and welding machines cause voltage fluctuations, voltage unbalance and flicker. The increased sensitivity of industrial as well as domestic processes to power quality problems requires the availability of electric power with

quality in every sector. The most critical areas which will be affected by poor power quality are continuous process industries and information technology systems where a disturbance may cause huge financial loss and consequently it will leads to loss of productivity and competitiveness. Although many efforts are taken by the utility for reducing power quality related problems some customers require a higher level of power quality than that is available from modern electrical distribution networks. This implies some measures must be taken to improve the power quality which will be mostly done by incorporating custom power devices in the distribution systems. A variety of disturbances such as harmonics, transients, outages, sags, swells, and flicker can be associated with the term "power quality" [2]. The various terminologies used in power quality studies are given as follows.

2.2.1 Voltage Sag

Voltage sag or dip can be defined as short duration reduction in voltage level between 10 and 90% of the nominal rms voltage at power frequency for a duration of one half cycle to one minute [3]. Voltage sags are mostly caused by connection of heavy loads, start-up of large motors and fault in customer installations. Starting of large induction motors can result in voltage dip as it draws a starting current which can be up to 10 times the rated full load current. The consequences of voltage sag are disconnection and loss of efficiency in rotating electrical machines; tripping of electromagnetic relays and malfunctioning of computer or microprocessor based control systems.

2.2.2 Voltage Swell

Voltage swell can be defined as the momentary increase in voltage level at power frequency outside the nominal tolerances for more than one half cycle and typically less than few seconds [3]. Voltage swell's are mainly because of line faults, badly dimensioned power sources and incorrect tap setings in tap changers in substations. A single line to ground fault can result in voltage swell in healthy phases. Swell can also result from energisation of large capacitor banks. The consequences of voltage swell are flickering of lighting and screens, data loss and stoppage of sensitive equipments.

2.2.3 Interruptions

An interruption can be defined reduction in line voltage or current to less than 10 % of nominal value not exceeding 1 minute. Interruption can be classified in to two depending on their duration as given below:

2.2.3.1 Very Short Interruption

Very short interruption is defined as total interruption of electric supply few milliseconds to one or two seconds [2]. Normally very short interruptions happens because of insulation failures, lightning, system faults, equipment failures and flashover. The consequences of very short interruptions are loss of information and malfunctioning of data processing equipments tripping of protection devices and stoppage of power for sensitive equipments.

2.2.3.2 Long Interruption

Long interruption are defined as loss of utility power lasting more than 2 minutes due to major local area or regional area electrical events in the power system networks [2]. These are caused by equipment failures storms and objects striking on transmission line or poles, power system faults and control malfunctioning. The consequences long interruption are total stoppage of all the equipments.

2.2.4 Transients

Transients are defined as the very fast variation of voltage values for duration from several microseconds to few milliseconds [3]. The variation may reach thousands of volts even in low voltage systems. Transients are of two types as given below:

2.2.4.1 Impulsive Transients

An impulsive transient is brief unidirectional variation in voltage current or both on a power line. These are caused due to lightning, switching of inductive loads and disconnection of heavy loads. The consequences of impulsive transients are destruction of

electronic equipment, failure of insulation materials, data processing errors and electromagnetic interference [4].

2.2.4.2 Oscillatory Transients

An oscillatory transient is a brief bidirectional variation in voltage, current or both on a power line. These are caused due to power factor correction capacitors, switching of inductive loads and transformer ferro resonance. The consequences of oscillatory transients are failure of insulation materials, overheating of cables and equipments and electromagnetic interferences [4].

2.2.5 Harmonic Distortion

Harmonic distortion is caused by non linear devices in the power system. A non linear device is one which current is not proportional to applied voltage, while the applied voltage is perfectly sinusoidal the resulting current is distorted. Increasing the voltage by few percent may cause the current to double and take on different wave shape. Non linear loads include ASD's, arc furnaces and electric power converters [3], [4]. Any periodic distorted waveforms can be expressed as sum of sinusoid's with different magnitudes and phases having frequencies that are multiples of power system frequency. Harmonics are also caused due to electric machines operating above the knee of magnetization curve, arc furnaces, welding machine rectifiers and non linear loads. The consequences of harmonics are increased probability of occurrence of resonance, overheating of cables and equipments, neutral current over load in three phase systems, loss of efficiency in electric machines and electromagnetic interference with communication systems.

Harmonic levels can be described by calculating Total Harmonic Distortion (THD) which measures the complete harmonic spectrum with magnitudes and phase angles of individual components. THD is the summation of all harmonic components of the voltage or current waveform compared against the fundamental component of the voltage or current wave.

Voltage THD (THD_V) is given by:

$$THD_V = \frac{\sqrt{\sum_{n=2}^{\infty} V_n^2}}{V_1} \tag{2.1}$$

where,

V_1 is the rms value of fundamental component (V),

V_n is the rms value of harmonic component 'n' (V),

and $n = 2, 3....., \infty$.

2.2.6 Voltage Fluctuation

Voltage fluctuations are systematic variation of voltage or a series of random changes in voltage magnitudes which lies in the range of 0.9 to 1.1 pu [4]. The voltage fluctuations are caused due to frequent start or stop of electric motors, oscillating loads and arc furnaces. The consequences of voltage fluctuations are under voltages and flickering of lighting and screens.

2.2.7 Noise

Noise is defined as super imposing of high frequency signals on the wave form of power system frequency [4]. Noise is caused due radiation due to welding machines, electromagnetic interferences, arc furnaces and improper grounding. The effects of noise mainly are disturbances on sensitive electronic equipments and data processing errors.

2.2.8 Voltage Unbalance

Voltage unbalance is defined as voltage variation in three phase systems in which the voltage magnitudes and phase angle difference between the phases are not equal [4]. Voltage unbalance is caused due to large single phase loads and incorrect distribution of single phase loads in three phase systems. The voltage unbalance will leads to the existence of negative sequence component which is harmful to all three phase loads. The most affected loads are three phase induction machines.

2.3 Custom Power Devices

The concept of Custom Power was introduced by N.G Hingorani in 1995 for improving performance electric distribution systems. The concept of custom power is similar to Flexible AC Transmission Systems (FACTS) the former is used in distribution systems while the latter is used in transmission systems. The custom power devices are power electronic based controllers in distribution systems to supply high quality and reliable power to customers [5]. Just as FACTS devices improve the reliability of power transmission systems by enhancing power transfer capability and stability custom power devices enhances the power quality in distribution systems. Due to increase in load demand and increased use of power electronics in equipments custom power devices becoming a relevant part of electric distribution networks. A custom power solution may include provision for

- Tight voltage regulation including protection against short duration sag's or swell's.
- Low harmonic voltage and current.
- No power interruption.
- Acceptance of non linear loads without effect on terminal voltage [6].

The power electronic controllers used in custom power solution can be classified in to two types, they are network reconfiguring type and compensating type [6].

2.3.1 Network Reconfiguring Type Custom Power Devices

The network reconfiguring type custom power devices are mainly GTO or thyristor based devices used for current limiting, current breaking and load transferring, they are Solid State Current Limiter (SSCL), Solid State Circuit Breaker (SSCB) and Solid State Transfer Switch (SSTS) [6]. SSCL is commonly used for the purpose of limiting fault current, it consists of a back to back connected GTO switches, inductor for limiting fault current and ZnO arrester connected as shown in Fig. 2.1(a), when a fault is detected it inserts the inductor in series with the power line or cable so as to limit the fault current. SSCB is a high speed switching device applied to reduce large current because of fault in distribution systems. Its structure is similar to SSCL except that a back to back connected thyristor switch is connected in series with the inductor. SSTS is

used for protecting sensitive loads against voltage sag or swell. It is composed of two GTO or thyristor blocks connected anti parallel connected, each block consists of three such pairs corresponding to three phases of the system. As shown in Fig. 2.1(b) it is

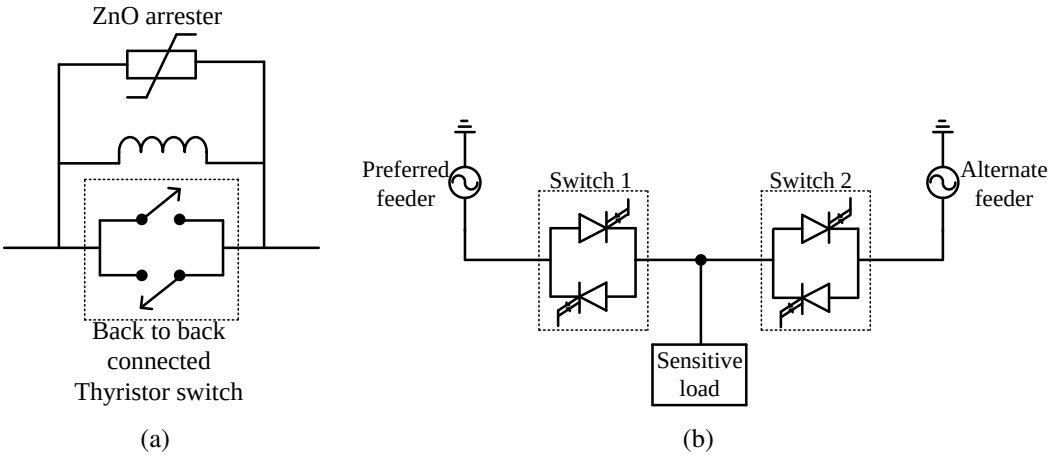

Figure 2.1: Schematic diagrams of: (a) SSCL. (b) SSTS [6].

connected to two different power sources namely Preferred Feeder (PF) and Alternate Feeder (AF). Under normal conditions, PF feeds the load through switch 1, when a fault occurs in the PF load is transferred to AF through switch 2. The transfer time of SSTS varies from 0.25 to 0.5 cycles of fundamental frequency.

2.3.2 Compensating Type Custom Power Devices

The compensating type custom power devices are VSI based and used for active power filtering, load balancing, power factor correction and voltage regulation. There are mainly three types of compensating type custom power devices, they are Distribution Static Compensator (DSTATCOM), Dynamic Voltage Restorer (DVR) and Unified Power Quality Conditioner (UPQC) [7]. A DSTATCOM is generally used active power filtering load balancing and power factor correction. In it's most basic form DSTATCOM consists of a dc capacitor, an inverter and an interface filter to connect the output of inverter at the load terminals as shown in Fig. 2.2(a). When DSTATCOM operated in current control mode it supply's the harmonic and reactive part of the load current so that current drawn from the supply is perfectly balanced and in phase with the system voltage. In voltage control mode DSTATCOM supply's the reactive power required by the load so as to maintain the voltage at the load terminal a constant. The DVR is a controller that is commonly used for mitigation of voltage sags/swells at the point of

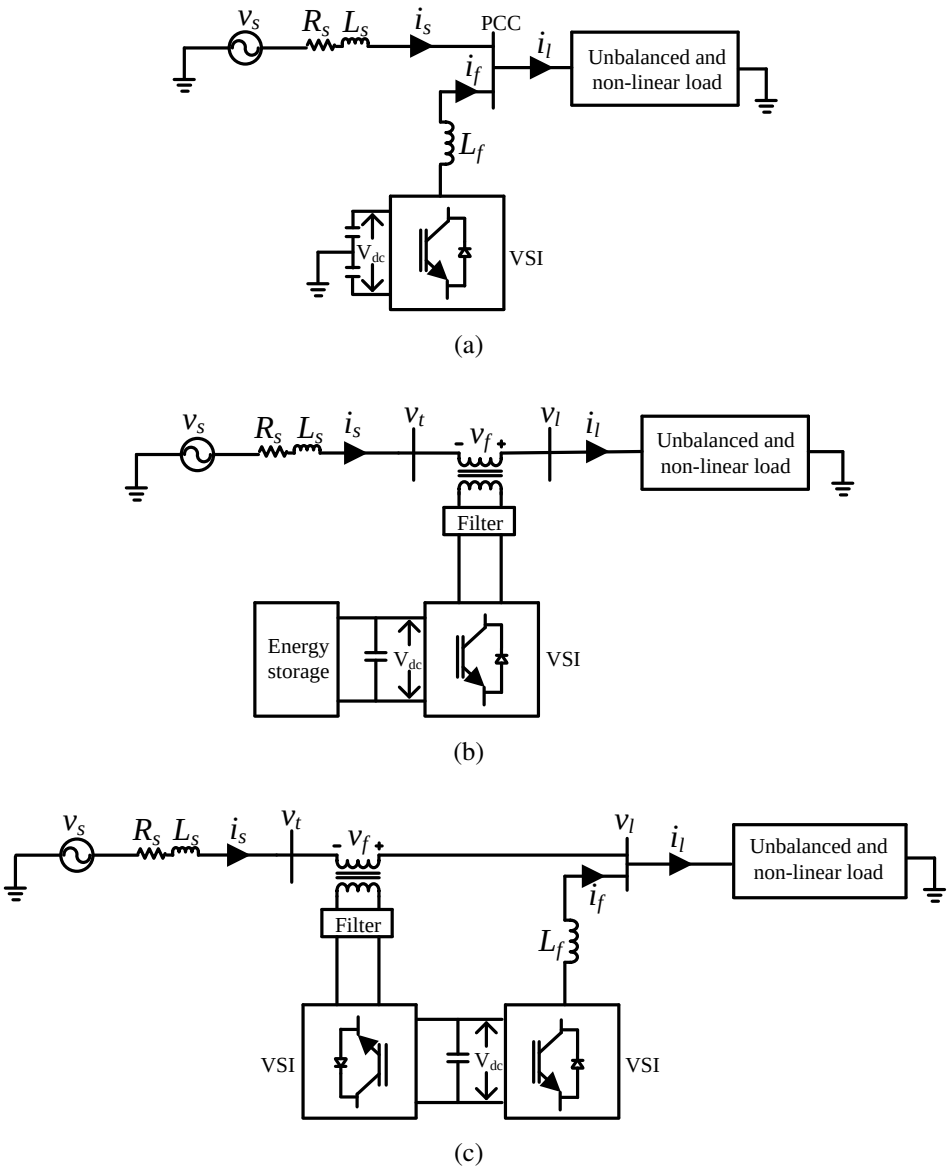

Figure 2.2: Schematic diagrams of: (a) DSTATCOM. (b) DVR. (c) UPQC [7].

connection. The DVR employs the same blocks as the DSTATCOM, except that a coupling transformer is connected in series with the ac system. Fig. 2.2(b) represents the schematic diagram of DVR. The main functions of DVR are voltage regulation, compensation for voltage sags and swells and unbalance voltage compensation for 3-phase systems. The VSI generates a three phase ac output voltage which is controllable in phase and magnitude. These voltages are injected into the ac distribution system in order to maintain the load voltage at the desired voltage reference. UPQC is a combination of DSTATCOM and DVR as shown in Fig. 2.2(c). UPQC allows mitigation of both voltage and current related power quality problems for a sensitive load to which it is connected.

2.4 Custom Power Park

The concept of custom power park have been introduced in [1] by N. G Hingorani. All customers of the park benefit from high-quality power supply which, in the basic form, is superior to the normal power supply from a utility. The electrical power to the park is supplied through two feeders from two independent substations. Both these feeders are joined together via a Solid State Transfer Switch (SSTS) that can make a subcycle transfer from the preferred feeder (PF) to the alternate feeder (AF) such that the duration of any voltage dip can be reduced to less than 10 ms. In addition, one or more VSI based devices are used to eliminate harmonic currents and voltages, to correct voltage sag/swell and for power factor correction.

In [8] A. Ghosh discussed about the concept of an mini-custom power park in which voltage at CPP bus is tightly regulated by a DSTATCOM. The park has three loads namely L1, L2 and L3, a DSTATCOM which is operated in voltage control mode and a Diesel Generator (DG) which is used as a backup to supply the loads on the occasion of total feeder loss. The schematic diagram of this mini-custom power park is as shown in Fig. 2.3. In [9], same author compared performances of two different compensating devices in a mini-custom power park. The performance of DSTATCOM and DVR which are operated independently along with an SSTS in a mini-custom power park is investigated.

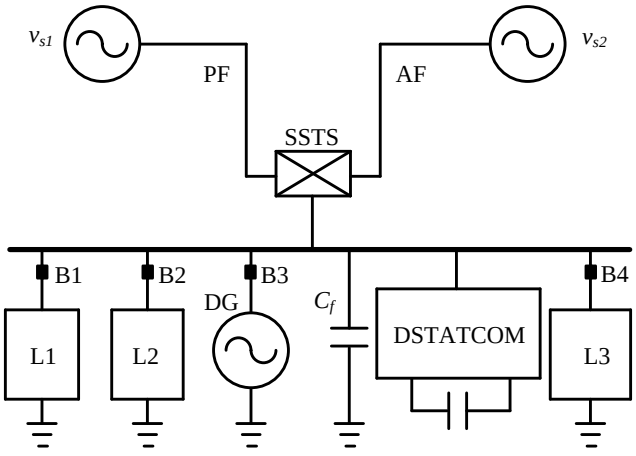

Figure 2.3: Schematic diagram of mini-custom power park [8].

In [10] an extended custom power park is presented which has both current and voltage quality improving devices. The park has four loads LA1, LA2, LAA and LAAA. The load LA2 is dc load and an APF is connected in shunt with it mitigates the harmonic

current drawn by the load. LAAA is the most critical load and a DVR is connected in series with it maintains the voltage across it as a constant. DG provides the power to loads LAA and LAAA under total feeder interruption. The Fig. 2.4 shows the single line diagram of the extended custom power park.

A custom power park with distributed generation is presented in [12]. Instead of diesel generator used in [10], DVR and distributed generation are used to supply the critical loads during interruption. The park has four loads LA1, LA2, LAA and LAAA. APF is used to mitigate the harmonic currents drawn by the load LA2. DVR is connected in series with the load LAAA, it is supported by distributed generation (DG) along with a DC/DC boost converter as in Fig. 2.5.

The another important part in a Custom Power Park is the method which is used for detection of the voltage sag, swell, interruption and other power quality problems. The voltage sag's/swells can be detected by measuring the peak value or rms value, it can also be done using Fourier based methods. Most commonly used method is based on Synchronous Reference Frame (SRF) based algorithm which is used for controlling custom power park in [12]. The block diagram for identification of sag or swell in feeders using SRF is as shown in Fig. 2.6.

The SRF based algorithm for involves transforming the three phase voltage to a positive sequence synchronous rotating frame based on abc to dq transformation for achieving sag detection.

$$\begin{bmatrix} v_d \\ v_q \end{bmatrix} = K_s \begin{bmatrix} v_a \\ v_b \\ v_c \end{bmatrix} \tag{2.2}$$

where

$$K_s = \frac{2}{3} \begin{bmatrix} sin(\theta) & sin(\theta - 120) & sin(\theta + 120) \\ cos(\theta) & cos(\theta - 120) & cos(\theta + 120) \end{bmatrix} \tag{2.3}$$

$$\theta(t) = \int_0^t \omega(\xi) d\xi + \theta(0) \tag{2.4}$$

where v_a, v_b and v_c are preferred or alternate feeder phase to neutral voltages, v_d and

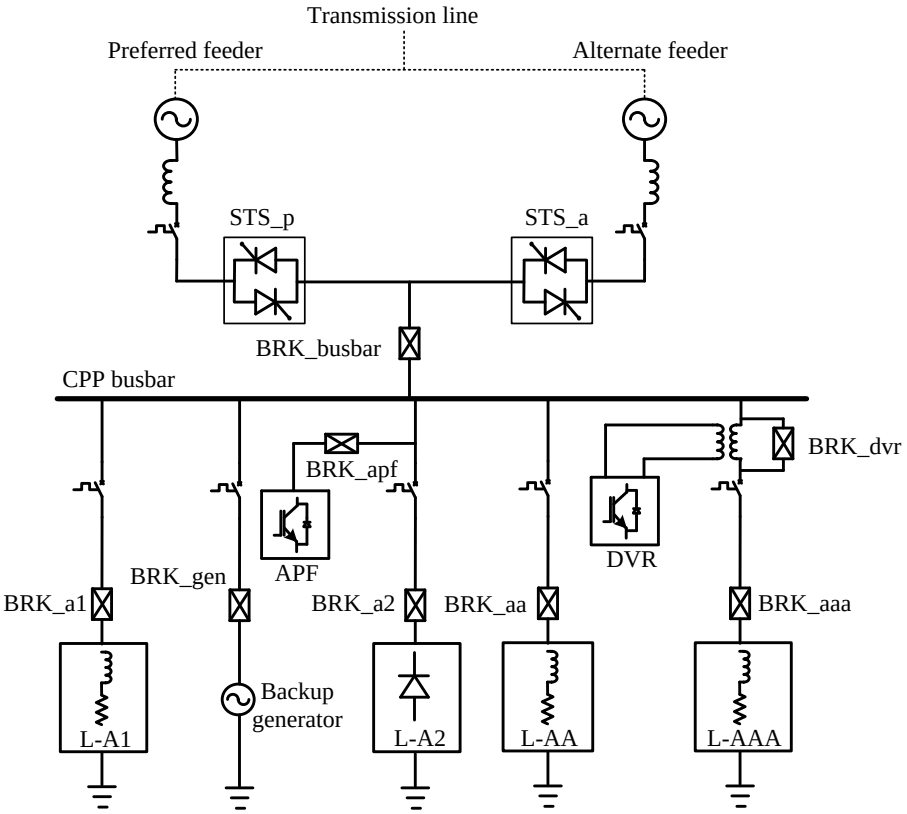

Figure 2.4: Single line Diagram of extended CPP [10].

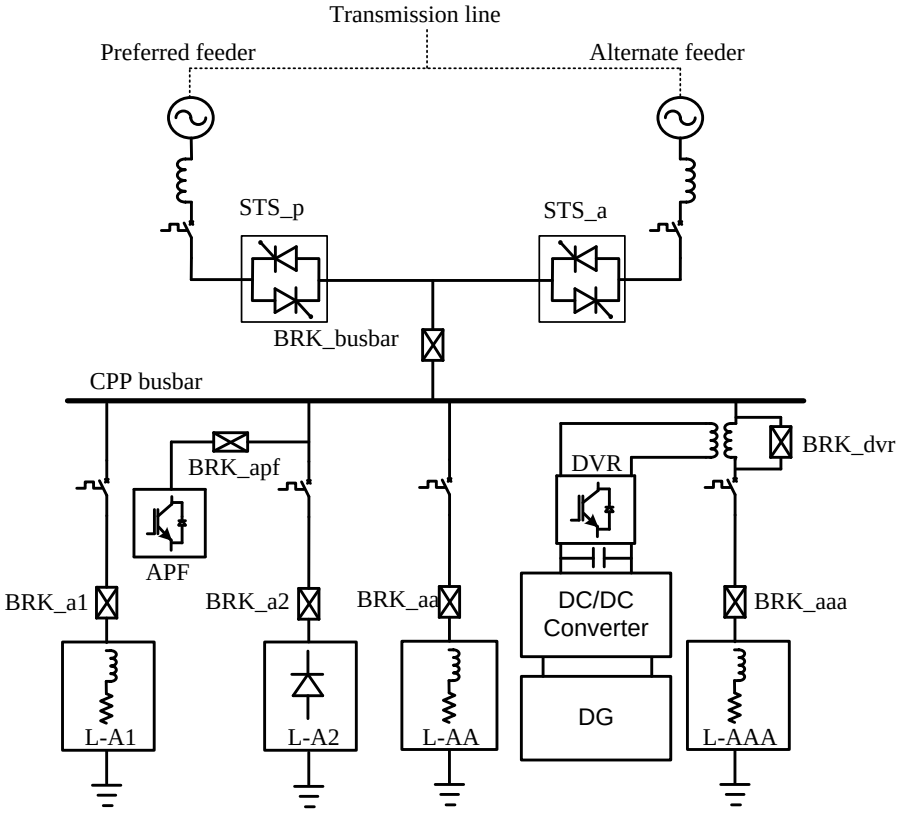

Figure 2.5: Single line diagram of CPP with DG unit [12].

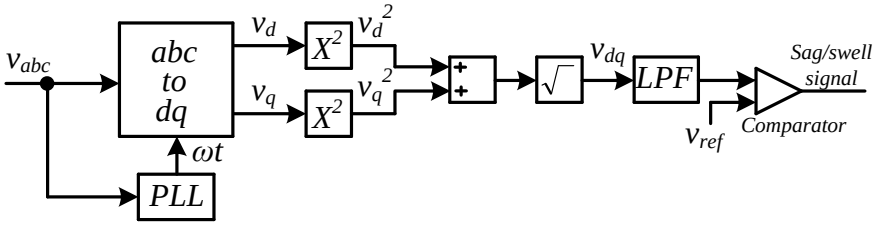

Figure 2.6: Block diagram of SRF based sag or swell detection.

v_q are the corresponding dq components, ω is the rotating frame angular frequency and $\theta(t)$ is transformation angle.

The voltage disturbance can be detected based on v_{dq} which is given by

$$v_{dq} = \sqrt{v_d^2 + v_q^2} \tag{2.5}$$

In this method v_{dq} is filtered with a LPF (f_c = 50 Hz) and the output of LPF is compared with a reference voltage v_{ref} to detect the sag or swell and to generate transfer signals. As a LPF with cut-off frequency, f_c = 50 Hz is used the response time for the detection of the power quality disturbances will be more and hence the time taken for switching between the feeders after occurring a disturbance will increase.

The another method used for voltage imperfection detection is single phase dq theory which detects both single phase and three phase voltage imperfections such as balanced or unbalanced sag/swell with better performance than SRF based voltage imperfection detection [14]. The block diagram for identification of sag or swell in feeders using single phase dq theory is as shown in Fig. 2.7. In this method each single phase

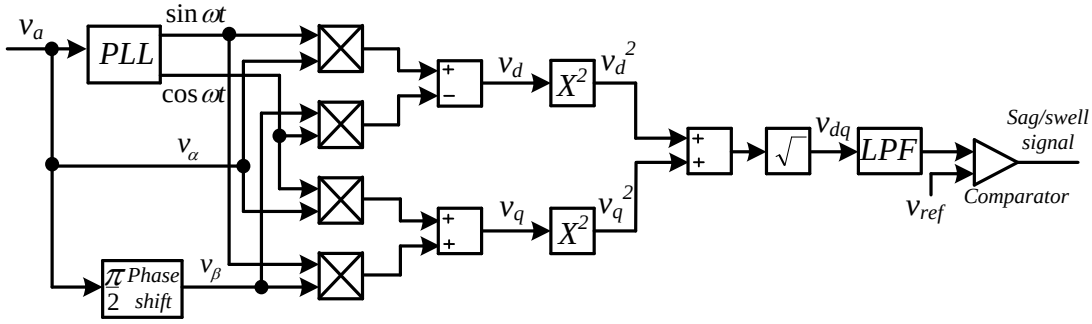

Figure 2.7: Block diagram of single phase dq theory based sag or swell detection.

voltages are converted to two phase stationary voltages ($\alpha\beta$ reference frame) by giving a phase shift of $\pi/2$ with the help of (2.6), then they are converted to dq reference frame

using (2.7), and signal v_{dq} is generated as in (2.5).

$$\begin{bmatrix} v_\alpha \\ v_\beta \end{bmatrix} = \begin{bmatrix} v(\omega t) \\ v(\omega t \pm \frac{\pi}{2}) \end{bmatrix} \tag{2.6}$$

$$\begin{bmatrix} v_d \\ v_q \end{bmatrix} = \begin{bmatrix} cos(\omega t) & -sin(\omega t) \\ sin(\omega t) & cos(\omega t) \end{bmatrix} \begin{bmatrix} v_\alpha \\ v_\beta \end{bmatrix} \tag{2.7}$$

and again

$$v_{dq} = \sqrt{v_d^2 + v_q^2}$$

v_{dq} is filtered using a LPF and output of the LPF is compared with the reference signal v_{ref} to generate the sag or swell signal for this phase, and signals from both the three phases are used for transfer signal generation. This method can give good response as compared to SRF based method as it can detect balanced and unbalanced sag's or swell's, but the requirement of detection in all the three phases of two feeders makes the control complicated.

2.5 Summary

This chapter has given an overview about power quality, power quality terminologies, custom power devices and custom power park. It also discussed about some control strategies used for detecting voltage imperfections in custom power park. The next chapter discusses about the operation, modelling and control of the custom power devices used in this work and the proceeding chapter discusses about the operation and control of the custom power park.

CHAPTER 3

MODELLING OF SSTS, DSTATCOM AND DVR

Solid State Transfer Switch (SSTS), Distribution Static Compensator (DSTATCOM) and Dynamic Voltage Restorer (DVR) are the different devices used in the custom power park. The modelling of SSTS and its transfer signal generation, modelling of DSTATCOM and its reference current generation using instantaneous symmetrical component theory, dc link design and filter inductance design and modelling of DVR, its control and filter design are discussed in this chapter.

3.1 Solid State Transfer Switch

The increasing sensitivity of customer equipment to voltage variations has given rise to use of custom power devices in distribution system. One of the most effective custom power device is Solid State Transfer Switch (SSTS). If an alternate feeder exists or can be provided to a critical load at reasonable cost, SSTS can transfer the load bus to an alternate feeder and sensitive load experiences only a shallow sag of short duration. Obviously SSTS is not effective in the case of a utility complete outage and cannot provide power conditioning, if both feeders sag simultaneously as might be the case of fault near a point where two utility joins.

The voltage sag magnitude and duration at the load terminals depend directly on the SSTS control scheme. Hence voltage detection and transfer need to be as fast as possible. Furthermore the transfer and gating logic must assure that in no case paralleling of the sources will occur, which would case severe damage to the thyristor switches [16].

In this work GTO based solid state transfer switch is used for simulation study. GTO has several disadvantages like the magnitude of latching, holding currents is more compared to conventional thyristors of the same rating, on state voltage drop and the associated loss is more, due to multi-cathode structure of GTO triggering gate current is higher than that required for normal thyristor, gate drive circuit losses are more and

its reverse voltage blocking capability is less than the forward voltage blocking capability. Though GTO is having these disadvantages, using GTO makes the control and switching circuitry simple as no external commutation circuitry is required for turning off the GTO.

While designing an SSTS to have a reliable system the following three modes of operation should be taken in to account:

1. ***Normal mode*:** Under normal circumstances the control system should ensure that the preferred feeder is connected to the load terminals.
2. ***Power failure mode*:** When the preferred feeder voltage fails or drops below a reference value the system should check whether the alternate feeder is having better voltage than preferred feeder. If the alternate feeder is having better voltage then it should transfer the load automatically to the alternate feeder.
3. ***Return mode*:** When the power at the preferred feeder returns SSTS should transfer the load back to the preferred feeder.

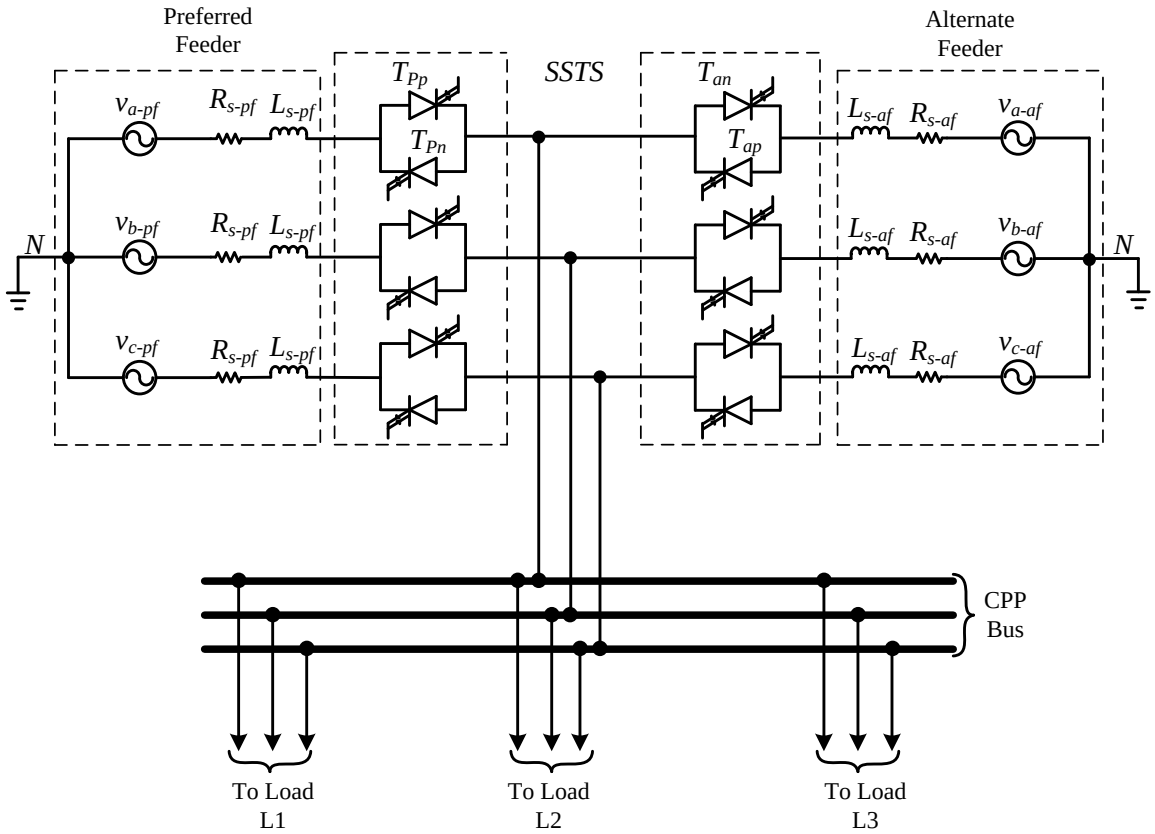

Figure 3.1: Power circuit of SSTS used for simulation study.

Fig. 3.1 shows the power circuit of SSTS used for the simulation study. Two feeders, preferred and alternate are connected to the Custom Power Park (CPP) bus, to supply the loads of the park. When a sag or swell occurs at the preferred feeder the loads will

be transferred to alternate feeder within a short time span. Next section explains the control theory used for the detection of voltage disturbances.

3.1.1 Voltage Sag/Swell Detection

The function of control unit is to monitor the voltage quality of both feeders, to detect voltage sag or swell in the system and to transfer the load from one feeder to another if required. The each phase voltage from both the feeders are the inputs to the control unit and outputs are gating pattern for the preferred and alternate feeder GTO switches. Under normal conditions the control unit triggers only the GTO's of the preferred feeder (T_{p_p} and T_{p_n}). If the preferred feeder does not meet the voltage requirements, the control unit will transfer the load bus to the alternate feeder if it meets the voltage requirements. This is accomplished by taking off gate signals from T_{p_p} and T_{p_n} GTO's and triggering T_{a_p} and T_{a_n}.

The control unit consists of synchronously rotating reference frame based voltage transformation and a switching pulse generation logic based on the output of voltage transformation unit. The total 'operating time' of the SSTS depends on this voltage sag or swell detection logic and the time taken to transfer the load from one switch to another. So to have a fast operation the voltage sag or swell detection should happen quickly, this will be explained here and the switching logic will be explained while discussing operation of custom power park.

The SRF based voltage detection is discussed in Section 2.4. As shown in Fig. 2.6 the output v_{dq} is filtered using a LPF (f_c = 50Hz) and the filtered signal is compared with a reference value to generate sag or swell signal. However this method introduces a delay in the output because of LPF which is used to filter out the ripples causing faulty transfer signals.

In this study an improved method is used for the control of SSTS which uses the method described in [19] and [20] for sag/swell detection under distorted grid voltages. This involves transforming the phase voltages firstly to a stationary reference frame ($\alpha\beta$) using Clarke transformation [21] and then to synchronous rotating frame (dq) using Park transformation [22]. The dq voltages in the synchronous reference frame and their relationship with $\alpha\beta$ reference frame are shown in Fig. 3.2.

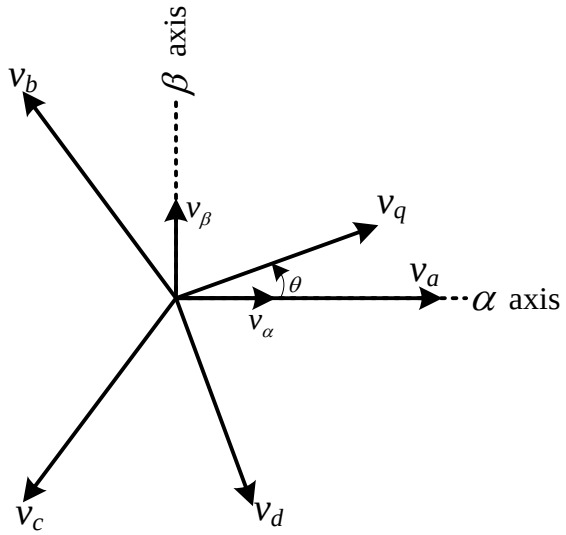

Figure 3.2: Voltages in stationary reference frame and SRF.

We can get the phase voltages transformed to dq values of the positive sequence synchronous rotating frame using equations (3.1), (3.2) and (3.3).

$$R(\theta) = \begin{bmatrix} sin(\theta) & -cos(\theta) \\ cos(\theta) & sin(\theta) \end{bmatrix} \tag{3.1}$$

$$C = \begin{bmatrix} 1 & \frac{-1}{2} & \frac{-1}{2} \\ 0 & \frac{\sqrt{3}}{2} & \frac{-\sqrt{3}}{2} \end{bmatrix} \tag{3.2}$$

$$\begin{bmatrix} v_{d(p)} \\ v_{q(p)} \end{bmatrix} = \frac{2}{3} R(\omega t) C \begin{bmatrix} v_a \\ v_b \\ v_c \end{bmatrix} \tag{3.3}$$

$R(\theta)$ rotates the stationary reference frame quantities by a phase angle θ, if $\theta = \omega t$, it represents the SRF. The subscript (p) in (3.3) represents that the value is in positive sequence synchronous rotating frame and d, q represents the d-axis and q-axis values of voltages. For a positive sequence synchronous rotating frame positive sequence component rotates in counter clockwise direction and negative sequence component rotates in clockwise direction. So the positive sequence voltage becomes dc component and negative sequence become 100 Hz (for 50 Hz network frequency) component. The d and q components of the voltage for a balanced and unbalanced voltage sag is as shown

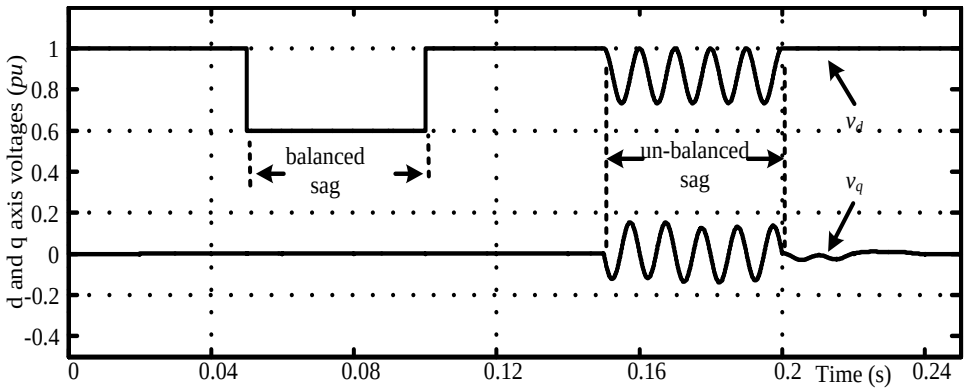

Figure 3.3: The d and q axis components of voltage for balanced and unbalanced sags.

in Fig. 3.3.

From Fig. 3.3 it is clear that for a balanced sag or swell the d and q components will be dc value and for unbalanced sag/swell the d axis voltage is in a shifted sinusoidal form and q axis voltage is a sinusoid, both the signals are with a frequency double the network frequency as they are part of negative sequence components appearing in supply voltages.

From Fig. 3.3 it is clear that during an unbalanced sag starting from $t = 0.15\ s$ (here it is a single phase unbalanced sag of 40%) both d and q axis components contain components having same amplitude and frequency 2ω. The sag detection method is based on shifting the q axis 2ω component by -90 degrees and adding this to the d axis voltage. Shifting is done using a discrete differentiator, and as a result 2ω component is eliminated, this result can be filtered using an LPF of high cut-off frequency (f_c = 1 kHz), so a fast voltage detection can be achieved. But as we are using a differentiator if the grid voltage is distorted the rate of change will become very high so faithful detection cannot be achieved. So it is important to design the cut-off frequency of LPF so as to work under distorted grid voltages. Before going to the design of LPF let's discuss mathematically how we can achieve the cancellation of the negative sequence components present in v_d, for that equation (3.3) can be rewritten once again,

$$\begin{bmatrix} v_{d(p)} \\ v_{q(p)} \end{bmatrix} = \frac{2}{3} R(\omega t) C \begin{bmatrix} v_a \\ v_b \\ v_c \end{bmatrix}$$

The above equation contains positive sequence dc components and negative se-

quence 100 Hz components which can be expressed as

$$\begin{bmatrix} v_{d(p)} \\ v_{q(p)} \end{bmatrix} = \begin{bmatrix} v_{dp} \\ v_{qp} \end{bmatrix} + R(-2\omega t) \begin{bmatrix} v_{dn} \\ v_{qn} \end{bmatrix} \tag{3.4}$$

In equation (3.4) the subscripts p and n represents the value of original positive and negative sequence components respectively, which are dc components. To detect sag/swell only these components are sufficient, the procedure to extract the dc components is as follows:

Differentiating equation (3.4) we will get

$$\begin{bmatrix} \dot{v_{d(p)}} \\ \dot{v_{q(p)}} \end{bmatrix} = -2\omega R(\frac{\pi}{2}) R(-2\omega t) \begin{bmatrix} v_{dn} \\ v_{qn} \end{bmatrix} \tag{3.5}$$

The differential of $R(\omega t)$ can be derived to be $-2\omega R(\frac{\pi}{2})R(-2\omega t)$, v_{dp} and v_{qp} are constants so their differential will be zero. Multiplying both sides of (3.5) by $R(\frac{\pi}{2})$ and dividing it by -2ω gives (3.6).

$$\frac{-1}{2\omega} R(\frac{\pi}{2}) \begin{bmatrix} \dot{v_{d(p)}} \\ \dot{v_{q(p)}} \end{bmatrix} = R(\pi) R(-2\omega t) \begin{bmatrix} v_{dn} \\ v_{qn} \end{bmatrix} \tag{3.6}$$

Adding (3.4) and (3.6) we will get

$$\begin{bmatrix} v_{d(p)} \\ v_{q(p)} \end{bmatrix} - \frac{1}{2\omega} R(\frac{\pi}{2}) \begin{bmatrix} \dot{v_{d(p)}} \\ \dot{v_{q(p)}} \end{bmatrix} = \begin{bmatrix} v_{dp} \\ v_{qp} \end{bmatrix} \tag{3.7}$$

From (3.7) the dc component of positive sequence d axis voltage can be written as

$$v_{dp} = v_{d(p)} + \frac{1}{2\omega} \dot{v_{q(p)}} \tag{3.8}$$

The discrete differentiation of the signal $v_{q(p)}$ is achieved as follows, if we are considering a sampling interval Δt at any arbitrary time t_1

$$\dot{v_{q(p)}}[t_1] = \frac{v_{q(p)}[t_1] - v_{q(p)}[t_1 - \Delta t]}{\Delta t} \tag{3.9}$$

The Δt is used in (3.9) should be higher than the sampling time used for simulation to achieve good result.

The v_{dp} signal generated in (3.8) can be passed through a LPF and can be compared with reference voltage v_{ref} to generate sag or swell signal. If the supply voltage is undistorted we can use a LPF with high cut-off frequency to filter out the high frequency components that comes from differential result. In practical cases the supply voltage will be distorted, the most common harmonics in voltage are 250 Hz which forms the negative sequence and 350 Hz which forms the positive sequence. Both these components will come in dq reference frame as 300 Hz components. Other most probable harmonic frequencies are 550 Hz and 650 Hz which will come in dq reference frame as 600 Hz components. Therefore the component v_{dp} is invalid if supply voltage contain harmonics.

To figure out this problem the LPF cut-off frequency (f_c) is designed, taking into account harmonic frequencies. However, in the design criteria will consider only the lowest frequency or 300 Hz component and the higher frequency need not be taken into account, due to the frequency response of LPF [20]. To filter out 300 Hz the filter cut-off frequency can be selected as

$$f_c = \frac{6f}{2} \tag{3.10}$$

where f is the supply frequency. The block diagram of voltage sag or swell detection logic is as shown in Fig. 3.4 and Fig. 3.5 represents the different output signals when a single phase sag of magnitude $0.4\ pu$ occurred in the feeder between 0.15 and 0.2 second's.

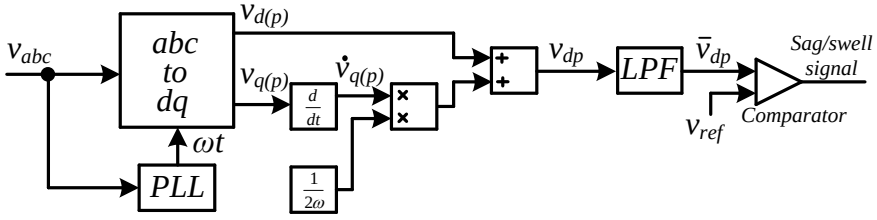

Figure 3.4: Block diagram of voltage sag/swell detection.

The Fig. 3.5(a)-(d) shows the various components in generating the fault detection signals. An unbalanced sag of 40% is started at $t = 0.15\ s$, during the sag the sinusoidal

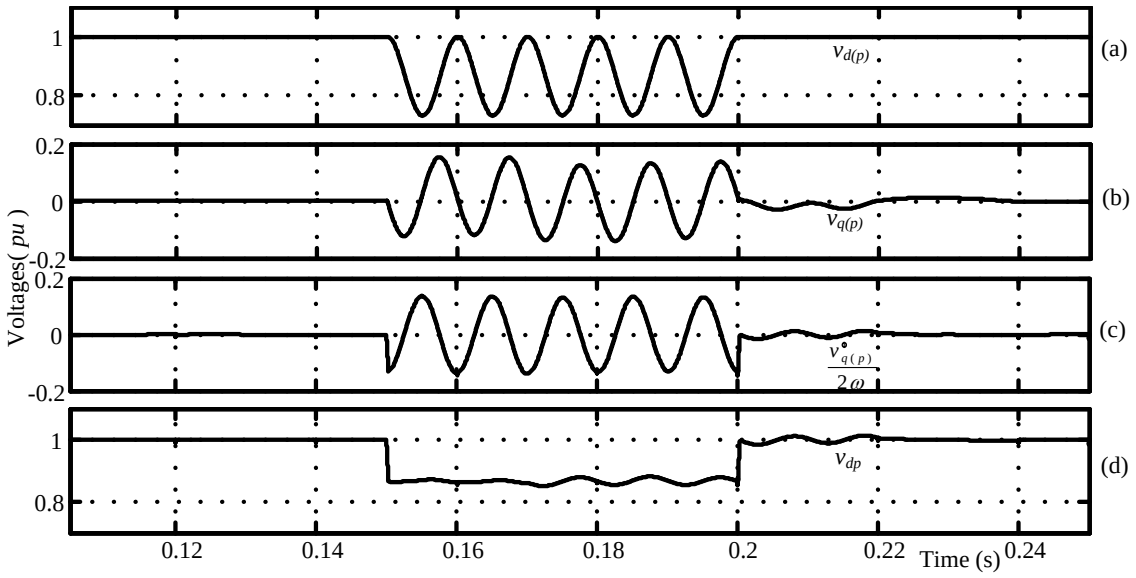

Figure 3.5: Example waveforms for $0.4\ pu$ single phase sag: (a) $v_{d(p)}$. (b) $v_{q(p)}$. (c) $v_{d(p)}^{\cdot}/2\omega$. (d) v_{dp}

.

components in the signal $v_{d(p)}$ and $v_{q(p)}^{\cdot}/2\omega$ are exactly in phase opposition, so if we add those to the sinusoidal components of frequency 100 Hz get's canceled out and the remaining part is the dc component v_{dp}. This v_{dp} can be used for detection of both balanced and unbalanced faults after filtering with the LPF designed in (3.10).

3.1.2 Control of SSTS

A schematic diagram of SSTS with its control unit is as shown in Fig. 3.6. Voltage detection part consists of two sag/swell detection unit discussed in Fig. 3.4, each for the respective feeders. The outputs of the two LPF's $\overline{v}_{dp-pf}$ and $\overline{v}_{dp-af}$ are given two the switching logic which will generate the gating signals for the preferred and alternate feeders. Switching logic has several outputs which is used for breaking and making the loads of the Custom Power Park and it acts as a master control for the other devices. The overall control algorithm used in switching logic will be discussed in Chapter 5.

The other issue that is to be discussed the minimum voltage dip or rise that can be detected using this method. As we discussed the output of LPF in Fig. 3.4, $\overline{v}_{dp}$ will give the magnitude of the positive sequence voltage of the input supply. Following procedure is adopted for finding the limits of sag/swell detection.

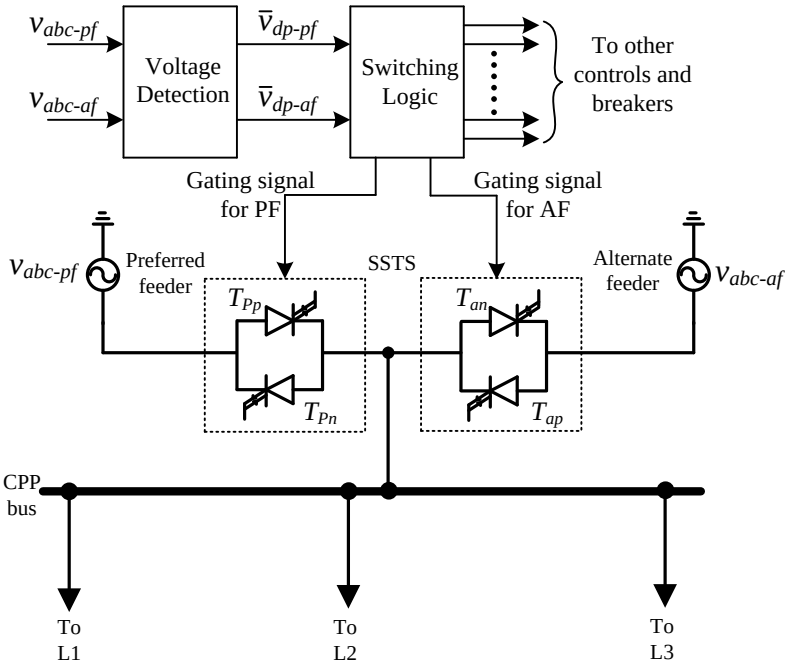

Figure 3.6: Schematic diagram of the SSTS and its control unit.

The instantaneous symmetrical components of a three phase system can be given by

$$\begin{bmatrix} \overline{v}_{a0} \\ \overline{v}_{a+} \\ \overline{v}_{a-} \end{bmatrix} = \frac{1}{3} \begin{bmatrix} 1 & 1 & 1 \\ 1 & a & a^2 \\ 1 & a^2 & a \end{bmatrix} \begin{bmatrix} v_a \\ v_b \\ v_c \end{bmatrix} \tag{3.11}$$

where,

$\overline{v}_{a0}$, $\overline{v}_{a+}$ and $\overline{v}_{a-}$ are the zero, positive and negative sequence components of voltage. v_a, v_b and v_c are the voltages of three phases and $a = e^{j2\pi/3}$ or $(1\angle 120^o)$.

We can represent three phase voltage as phasor's, $v_a = |V_a| \angle 0^o$, $v_b = |V_b| \angle -120^o$ and $v_c = |V_c| \angle 120^o$, then the positive sequence component can be expressed as

$$\overline{v}_{a+} = \frac{v_a + a \times v_b + a^2 \times v_c}{3} \tag{3.12}$$

if we substitute the values of voltage phasor's and a,

$$\overline{v}_{a+} = \frac{|V_a| \angle 0^o + 1\angle 120^o \times |V_b| \angle -120^o + 1\angle -120^o \times |V_c| \angle 120^o}{3}$$

and after simplification we will get

$$\overline{v}_{a+} = \frac{|V_a| + |V_b| + |V_c|}{3} \angle 0^o \tag{3.13}$$

so the magnitude of positive sequence voltage is the average of the three phase voltage magnitudes, so we can write $\overline{v}_{dp}$ as

$$\overline{v}_{dp} = \left|\overline{V}_{a+}\right| = \frac{|V_a| + |V_b| + |V_c|}{3} \tag{3.14}$$

Using (3.14) we can get the minimum value of voltage dip that can be detected by this method. In per units (3.14) can be written as

$$\overline{v}_{dp(pu)} = \frac{\left|V_{a(pu)}\right| + \left|V_{b(pu)}\right| + \left|V_{c(pu)}\right|}{3} \tag{3.15}$$

This voltage is compared with the reference detect the voltage sag's or swell's, the lower limit for detection of sag is 0.9 pu. So the it can detect the balanced voltage sag of if $\overline{v}_{dp(pu)}$ goes below 0.9 pu. To find the lower limit for two phase sag we can substitute $\left|V_{a(pu)}\right| = \left|V_{b(pu)}\right|$ and $\left|V_{c(pu)}\right| = 1$ in (3.15) and equating it to 0.9, we will get the limit as 0.85 pu. If we substitute $\left|V_{b(pu)}\right| = \left|V_{c(pu)}\right| = 1$ in (3.15) and equating it to 0.9, we will get the lower limit for single phase sag as 0.7 pu. So this detection scheme cannot detect single phase sags with magnitude between 0.7 and 0.9 pu and two phase sags with magnitude between 0.85 and 0.9 pu. This disadvantage can be improved by increasing the reference limit for detection of sags to a higher value from 0.9 pu.

3.2 Distribution Static Compensator

Fig. 3.7 shows the power circuit of DSTATCOM used in the simulation study of Custom Power Park. The loads may be a lagging power factor load or unbalanced load or nonlinear load or combination of all these loads. For reducing ripples in the compensating current interfacing inductors (L_f) are used in the AC side of VSI and R_f represents the resistance of the interfacing inductor. The harmonic and reactive currents (i_f) are injected by the DSTATCOM to cancel the harmonic and reactive part of load currents (i_l). So the harmonic, unbalance and reactive components in the source currents (i_s) are compensated by the DSTATCOM. The main parts of the power circuit are a dc link with split capacitor topology, 3-leg VSI with IGBT switches and interface inductor. The reference currents for DSTATCOM are generated using instantaneous symmetrical component theory and hysteresis band PWM control is used for generating switching

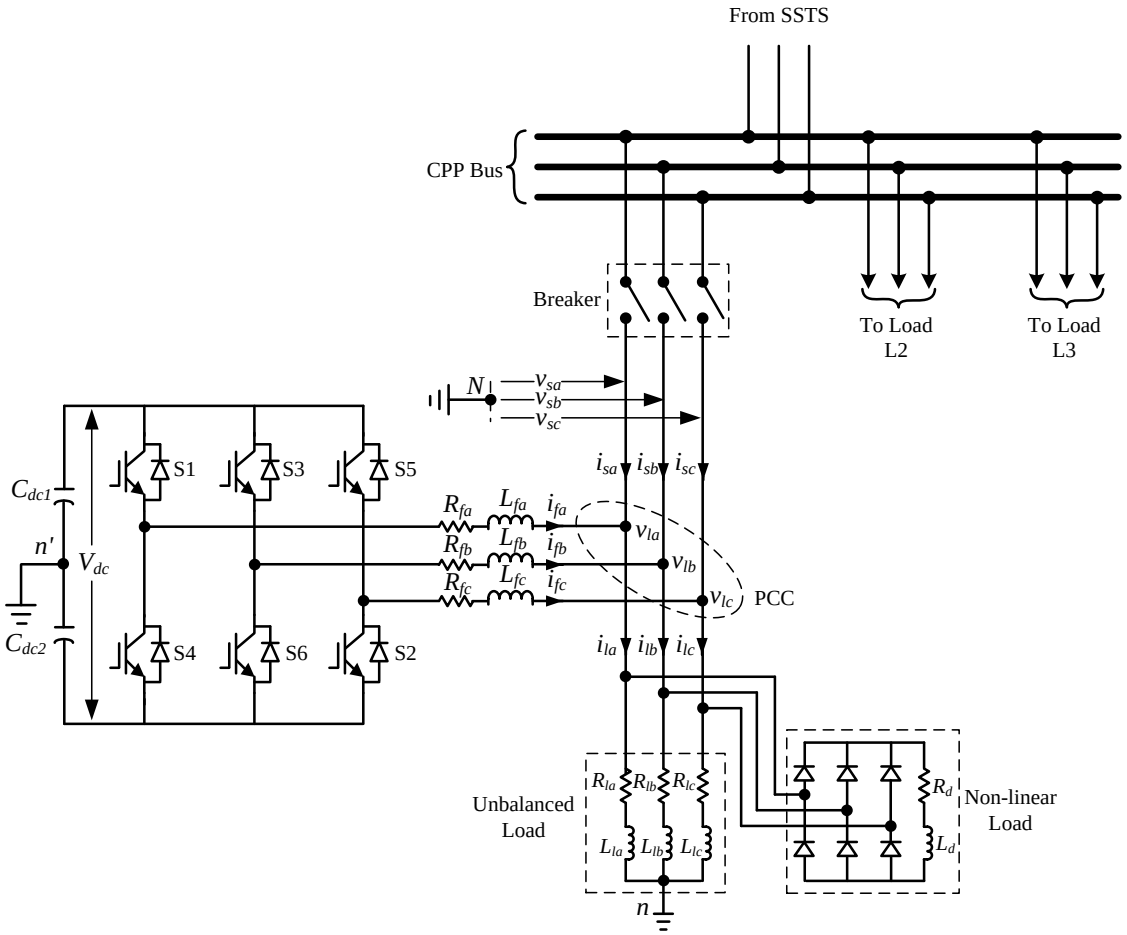

Figure 3.7: Power circuit of DSTATCOM used in the CPP.

pulses for the VSI. This section explains about the design of various components in the power circuit and the control of the DSTATCOM.

3.2.1 Selection of DC Link Voltage and Capacitance

The compensation capability of DSTATCOM greatly depends on the voltage rating of dc link capacitor. In general DC link voltage must be much higher than the peak value of line to neutral voltages. This is done in-order to achieve better performance at the peak value of supply voltage. In [23] authors discusses that in-order to achieve better compensation the dc link voltage should be greater than 1.6 times the peak value of the system voltage. When the dc link voltage is below this limits there is insufficient voltage to drive the current through filter inductance so as to track the reference currents.

The value of DC energy storage capacitor is governed by the decrease in dc link voltage upon the application of load and rise in dc link voltage on removal of load [23].

It is preferred to use higher value of dc link capacitance as it will also reduce the ripples in dc link voltage. A PI controller is used to maintain the dc link voltage as constant, higher value of capacitance may increase the rise time of this controller. So capacitor value is selected such that it is not too high as to increase the response time of the controller.

3.2.2 Selection of Filter Inductance

The proper selection of interface inductor plays an important role in satisfactory operation of the VSI in DSTATCOM. The value of shunt inductance should be low to allow the required harmonic frequency and it should be high enough to block the switching frequency components. If the dc link voltage, maximum switching frequency and hysteresis band are selected then the value of interface inductor L_f is given by [23]:

$$L_f = \frac{1.6V_m}{4h_i f_{swmax}} \tag{3.16}$$

where,

V_m is the maximum value of supply voltage (V).

h_i is hysteresis band (A), and

f_{swmax} is the maximum value of switching frequency (Hz).

3.2.3 Reference Current Generation Using Instantaneous Symmetrical Component Theory

Instantaneous symmetrical component theory is used for unbalance load compensation, harmonic compensation and reactive power compensation. The control algorithm using instantaneous symmetrical component theory can compensate any kind of unbalance and harmonics in loads provided we have a high bandwidth current source to track the reference current generated using this theory.

For any three phase voltages or currents instantaneous symmetrical components are defined as follows:

for currents

$$\begin{bmatrix} \bar{i}_{a0} \\ \bar{i}_{a+} \\ \bar{i}_{a-} \end{bmatrix} = \frac{1}{3} \begin{bmatrix} 1 & 1 & 1 \\ 1 & a & a^2 \\ 1 & a^2 & a \end{bmatrix} \begin{bmatrix} i_a \\ i_b \\ i_c \end{bmatrix} \tag{3.17}$$

similarly for voltages

$$\begin{bmatrix} \overline{v}_{a0} \\ \overline{v}_{a+} \\ \overline{v}_{a-} \end{bmatrix} = \frac{1}{3} \begin{bmatrix} 1 & 1 & 1 \\ 1 & a & a^2 \\ 1 & a^2 & a \end{bmatrix} \begin{bmatrix} v_a \\ v_b \\ v_c \end{bmatrix} \tag{3.18}$$

The load currents shown in Fig. 3.7 (i_{la}, i_{lb} and i_{lc}) are unbalanced and nonlinear. We have to achieve three objectives using instantaneous symmetrical component theory based reference current generation [24], they are :

1. To provide balanced supply current (i_{sa}, i_{sb} and i_{sc}) such that its zero sequence component ($\bar{i}_{a0}$) is zero.

$$i_{sa} + i_{sb} + i_{sc} = 0 \tag{3.19}$$

2. To have a desired power factor angle (ϕ_+) between the positive sequence supply voltage ($\overline{v}_{a+}$) and positive sequence supply current ($\bar{i}_{a+}$).

$$\angle \overline{v}_{a+} = \angle \bar{i}_{a+} + \phi_+ \tag{3.20}$$

3. Power supplied from the source (p_s) must be equal to the average load power (P_{lavg}).

$$p_s = v_{sa} i_{sa} + v_{sb} i_{sb} + v_{sc} i_{sc} = P_{lavg} \tag{3.21}$$

Using (3.17) and (3.18) we can write (3.20) as follows

$$\angle \left(\frac{1}{3} \left[v_{sa} + a v_{sb} + a^2 v_{sc} \right] \right) \;=\; \angle \left(\frac{1}{3} \left[i_{sa} + a i_{sb} + a^2 i_{sc} \right] \right) + \phi_+ \tag{3.22}$$

By substituting the value of a L.H.S and R.H.S of (3.22) can be written as

$$
\begin{aligned}
\text{L.H.S} &= \angle\frac{1}{3}\left[\left(v_{sa}-\frac{v_{sb}}{2}-\frac{v_{sc}}{2}\right)+j\frac{\sqrt{3}}{2}\left(v_{sb}-v_{sc}\right)\right] \\
&= tan^{-1}\frac{\frac{\sqrt{3}}{2}\left(v_{sb}-v_{sc}\right)}{\left(v_{sa}-\frac{v_{sb}}{2}-\frac{v_{sc}}{2}\right)} \\
&= tan^{-1}\frac{C_1}{C_2} \qquad (3.23) \\
\text{R.H.S} &= \angle\frac{1}{3}\left[\left(i_{sa}-\frac{i_{sb}}{2}-\frac{i_{sc}}{2}\right)+j\frac{\sqrt{3}}{2}\left(i_{sb}-i_{sc}\right)\right]+\phi_+ \\
&= tan^{-1}\frac{\frac{\sqrt{3}}{2}\left(i_{sb}-i_{sc}\right)}{\left(i_{sa}-\frac{i_{sb}}{2}-\frac{i_{sc}}{2}\right)}+\phi_+ \\
&= tan^{-1}\frac{C_3}{C_4}+\phi_+ \qquad (3.24)
\end{aligned}
$$

Where C_1, C_2, C_3 and C_4 are $\frac{\sqrt{3}}{2}\left(v_{sb}-v_{sc}\right)$, $v_{sa}-\frac{v_{sb}}{2}-\frac{v_{sc}}{2}$, $\frac{\sqrt{3}}{2}\left(i_{sb}-i_{sc}\right)$ and $i_{sa}-\frac{i_{sb}}{2}-\frac{i_{sc}}{2}$ respectively.

and now from (3.24) and (3.24)

$$tan^{-1}\frac{C_1}{C_2}=tan^{-1}\frac{C_3}{C_4}+\phi_+$$

taking tan on both sides

$$\frac{C_1}{C_2}=tan\left(tan^{-1}\frac{C_3}{C_4}+\phi_+\right) \qquad (3.25)$$

Substituting values of C_1,C_2,C_3 and C_4 in (3.25) and rearranging we will get

$$
\begin{aligned}
&\left\{\left(v_{sb}-v_{sc}\right)+\beta\left(v_{sb}+v_{sc}-2v_{sa}\right)\right\}i_{sa} \\
+&\left\{\left(v_{sc}-v_{sa}\right)+\beta\left(v_{sc}+v_{sa}-2v_{sb}\right)\right\}i_{sb} \\
+&\left\{\left(v_{sa}-v_{sb}\right)+\beta\left(v_{sa}+v_{sb}-2v_{sc}\right)\right\}i_{sc} &= 0 \qquad (3.26)
\end{aligned}
$$

where $\beta=\frac{tan\ \phi_+}{\sqrt{3}}$. Now if we take $v_{s0}=3\left(v_{sa}+v_{sb}+v_{sc}\right)$ (3.26) can be rewritten as

$$
\begin{aligned}
&\left\{\left(v_{sb}-v_{sc}\right)-3\beta\left(v_{sa}-v_{s0}\right)\right\}i_{sa} \\
+&\left\{\left(v_{sc}-v_{sa}\right)-3\beta\left(v_{sb}-v_{s0}\right)\right\}i_{sb} \\
+&\left\{\left(v_{sa}-v_{sb}\right)-3\beta\left(v_{sc}-v_{s0}\right)\right\}i_{sc} &= 0 \qquad (3.27)
\end{aligned}
$$

Equations (3.19),(3.21) and (3.27) forms a system of linear equations with variables i_{sa},

i_{sb} and i_{sc}, which can be solved to get the source reference currents as follows.

$$\begin{aligned} i_{sa} &= \frac{(v_{sa}-v_{s0})+\beta\,(v_{sb}-v_{sc})}{\sum_{j=a,b,c} v_{sj}^2 - 3v_{s0}^2} P_{lavg} \\ i_{sb} &= \frac{(v_{sb}-v_{s0})+\beta\,(v_{sc}-v_{sa})}{\sum_{j=a,b,c} v_{sj}^2 - 3v_{s0}^2} P_{lavg} \\ i_{sc} &= \frac{(v_{sc}-v_{s0})+\beta\,(v_{sa}-v_{sb})}{\sum_{j=a,b,c} v_{sj}^2 - 3v_{s0}^2} P_{lavg} \end{aligned} \tag{3.28}$$

The above equation represents the reference source currents that is to be drawn from the source after DSTATCOM connection.

If we consider source voltages as balanced then v_{s0} will be zero, so (3.28) will become

$$\begin{aligned} i_{sa} &= \frac{v_{sa}+\beta\,(v_{sb}-v_{sc})}{\sum_{j=a,b,c} v_{sj}^2} P_{lavg} \\ i_{sb} &= \frac{v_{sb}+\beta\,(v_{sc}-v_{sa})}{\sum_{j=a,b,c} v_{sj}^2} P_{lavg} \\ i_{sc} &= \frac{v_{sc}+\beta\,(v_{sa}-v_{sb})}{\sum_{j=a,b,c} v_{sj}^2} P_{lavg} \end{aligned} \tag{3.29}$$

Applying Kirchoff's law at PCC we will get the filter reference currents as

$$\begin{aligned} i_{fa}^* = i_{la} - i_{sa} = i_{la} - \frac{v_{sa}+\beta\,(v_{sb}-v_{sc})}{\sum_{j=a,b,c} v_{sj}^2} P_{lavg} \\ i_{fb}^* = i_{lb} - i_{sb} = i_{lb} - \frac{v_{sb}+\beta\,(v_{sc}-v_{sa})}{\sum_{j=a,b,c} v_{sj}^2} P_{lavg} \\ i_{fc}^* = i_{lc} - i_{sc} = i_{la} - \frac{v_{sc}+\beta\,(v_{sa}-v_{sb})}{\sum_{j=a,b,c} v_{sj}^2} P_{lavg} \end{aligned} \tag{3.30}$$

These currents (3.30) are given as the reference currents to the VSI which will generate the filter currents (i_{fa}, i_{fb} and i_{fc}).

3.2.4 Generation of P_{loss} to Maintain DC Link Voltage

To have perfect current tracking we have to maintain the dc voltages (V_{dc1} and V_{dc2}) across the capacitors (C_{dc1} and C_{dc2}) must be maintained at reference value (V_{dcref}).This has to be achieved by drawing some power from the source. In order to accommodate this the real power drawn from the source is not equal to the average value which is given in (3.21), it should also contain the average power lost in the DSTATCOM circuit

[25]. P_{loss} can be generated through a suitable PI controller such that average dc link voltage $(V_{dc1} + V_{dc2})$ is maintained a constant. In steady state $(V_{dc1} + V_{dc2})$ will be equal to V_{dc} which is the average DC link voltage of DSTATCOM. P_{loss} is given as follows

$$P_{loss} = K_p\, e_{vdc} + K_i \int e_{vdc} dt \tag{3.31}$$

where $e_{vdc} = 2V_{dcref} - (V_{dc1} + V_{dc2})$ is the voltage error. The terms K_p and K_i are proportional and integral gains respectively.

The value of P_{loss} generated using (3.31) can be incorporated in (3.30) to draw additional amount of real power from the source. The new reference filter current considering P_{loss} is given as follows:

$$\begin{aligned}
i^*_{fa} &= i_{la} - \frac{v_{sa} + \beta\,(v_{sb} - v_{sc})}{\sum_{j=a,b,c} v^2_{sj}}\,(P_{lavg} + P_{loss}) \\
i^*_{fb} &= i_{lb} - \frac{v_{sb} + \beta\,(v_{sc} - v_{sa})}{\sum_{j=a,b,c} v^2_{sj}}\,(P_{lavg} + P_{loss}) \\
i^*_{fc} &= i_{la} - \frac{v_{sc} + \beta\,(v_{sa} - v_{sb})}{\sum_{j=a,b,c} v^2_{sj}}\,(P_{lavg} + P_{loss})
\end{aligned} \tag{3.32}$$

For unity power factor operation ϕ_+ will be zero hence β also will be zero, so the reference filter currents will become

$$\begin{aligned}
i^*_{fa} &= i_{la} - \frac{v_{sa}}{\sum_{j=a,b,c} v^2_{sj}}\,(P_{lavg} + P_{loss}) \\
i^*_{fb} &= i_{lb} - \frac{v_{sb}}{\sum_{j=a,b,c} v^2_{sj}}\,(P_{lavg} + P_{loss}) \\
i^*_{fc} &= i_{la} - \frac{v_{sc}}{\sum_{j=a,b,c} v^2_{sj}}\,(P_{lavg} + P_{loss})
\end{aligned} \tag{3.33}$$

The average load power P_{lavg} can be computed by using a moving average filter which runs over a window of one period (T) of data points as follows

$$P_{lavg} \;=\; \frac{1}{T}\int_{t1}^{t1+T} (v_{sa} i_{sa} + v_{sb} i_{sb} + v_{sc} i_{sc})\, dt \tag{3.34}$$

where $t1$ is an arbitrary time instant.

3.2.5 Hysteresis Band PWM Control

The hysteresis band PWM is basically an instantaneous feedback current control method of PWM where the actual current continuously tracks the reference current within a specified hysteresis band.

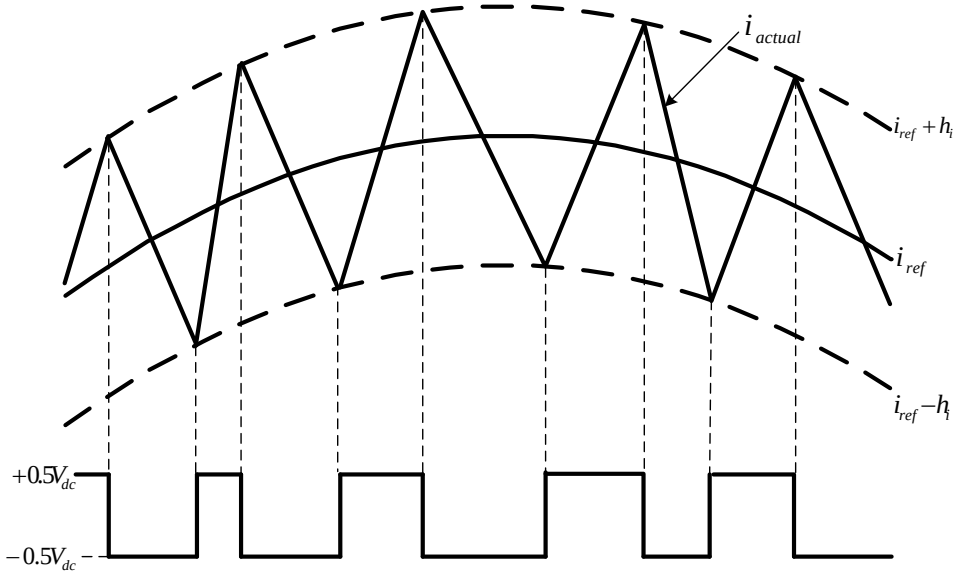

Figure 3.8: Principle of hysteresis band PWM.

The Fig. 3.8 explains the operating principle of the hysteresis band PWM. The control circuit generates a current wave of desired shape, and it is compared with the actual filter current. As the current exceeds a prescribed hysteresis band the upper switch in the half bridge is turned off and lower switch is turned on, as a result the output voltage changes from $+0.5V_{dc}$ to $-0.5V_{dc}$ and the current starts to decay. As the current crosses the lower limit the lower switch is turned off and upper switch is turned on.

The control algorithm is as follows for phase a in Fig. 3.7

if $i_{actual} \geq i_{ref} + h_i$

$S1$ OFF

$S4$ ON

else if $i_{actual} \leq i_{ref} - h_i$

$S1$ ON

$S4$ OFF

else if $i_{ref} - h_i \leq i_{actual} \leq i_{ref} + h_i$

Retain the status of switches.

Where i_{actual} is the actual filter current, i_{ref} is the reference filter current and h_i is the hysteresis band, $S1$ and $S4$ are the switches corresponding to phase a. The actual current wave is thus forced to track the reference wave within the hysteresis band by back and fourth switching of the upper and lower switches.

3.2.6 Control of DSTATCOM

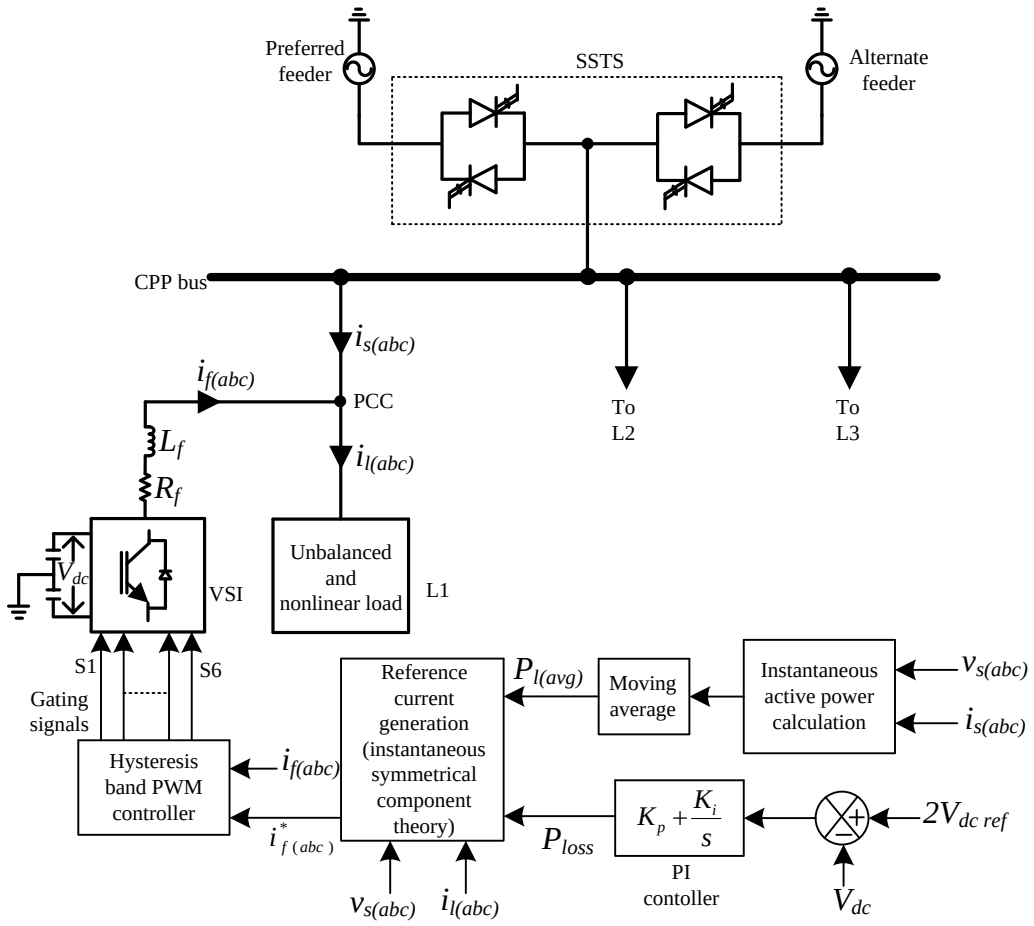

Figure 3.9: Schematic diagram of DSTATCOM with its control unit.

Fig. 3.9 shows the schematic diagram of DSTATCOM and its control unit. It uses (3.21) to calculate the instantaneous active power supplied from the source. To calculate the average load power a moving average filter which runs over a window of one cycle as mentioned in (3.34) is used. The P_{loss} is generated by comparing the DC voltage with a reference value and using a PI controller as in (3.31). Reference currents are generated using instantaneous symmetrical component theory as in (3.33). Hysteresis band PWM current controller is used to generate switching pulses for the VSI. The DSTATCOM is connected to the load L1 in the custom power park which is unbalanced and nonlinear.

The load currents ($i_{l(abc)}$) are unbalanced and nonlinear, after the connection of DSTATCOM at load terminal the source currents ($i_{s(abc)}$) will be balanced and sinusoidal.

3.3 Dynamic Voltage Restorer

DVR is a custom power device used to eliminate supply side voltage disturbances. DVR maintains load voltage at a desired magnitude and phase by compensating voltage sags/swells, voltage unbalances and voltage harmonics at the point of common coupling. It can also be used for maintaining voltage for short duration during interruption provided it is having sufficient energy storage at its dc side [26].

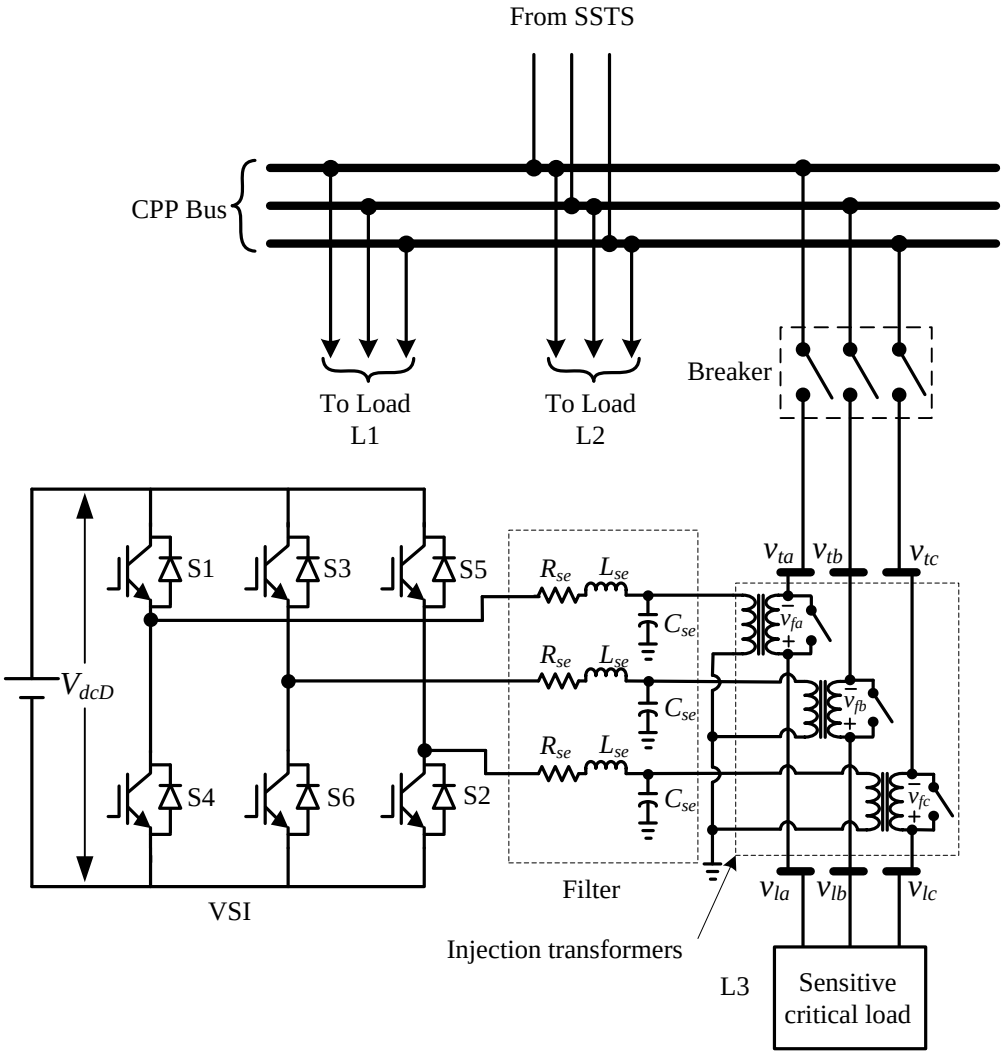

Figure 3.10: Power circuit of DVR.

The power circuit of DVR is as shown in Fig. 3.10. DVR mainly has the following parts:

1) ***Voltage source inverter***: Voltage Source inverters used in DVR usually are of low voltage rating and high current rating as a step-up injection transformer boosts the voltage the voltage level.

2) ***Injection transformer***: Injection transformers can be connected in delta/open or star/open winding configuration in the distribution line. The star/open winding connection allows injection of positive, negative and zero sequence voltages where as delta/open winding allows only the injection of positive and negative sequence voltages.

3) ***Passive filter***: The filtering scheme in DVR can be placed either in high voltage side or at the inverter side of series injection transformer. The advantage of inverter side is that it is on the low voltage side of the transformer and it is close to harmonic source. The filtering scheme considered in this work pertains to that at the inverter side. Using this scheme higher order harmonics can be prevented from entering to the transformer thus reducing the voltage stress on transformer.

4) ***Energy storage with DC capacitor***: A regulated constant DC supply is employed in DVR with the help of an energy storage system and DC/DC converter. Generally battery, flywheel or SME's etc. are used to provide the real power for compensation. Compensation using real power is required when a large voltage sag occurs. A DC capacitor is provided to get a stiff dc voltage to the inverter. In this work the entire combination of energy storage, DC/DC converter and capacitor is not considered, they are modelled by a simple DC voltage source.

5) ***Bypass switches***: Bypass Switches are provided to protect DVR from load faults, large inrush currents and to bypass the transformer under normal operation.

3.3.1 Reference Voltage Generation

The DVR has a control circuit which continuously monitor the terminal voltages (v_{ta}, v_{tb} and v_{tc}) and generate the reference signals (v^*_{fa}, v^*_{fb} and v^*_{fc}) that is to be injected by the DVR to compensate the sag, swell and harmonics. The reference voltage generation is based on Synchronous Reference Frame (SRF) theory [27]. The measured

terminal voltages are converted from abc to $dq0$ reference frame using the following Park's transformation.

$$\begin{bmatrix} v_{td} \\ v_{tq} \\ v_{t0} \end{bmatrix} = \frac{2}{3} \begin{bmatrix} sin(\theta) & sin(\theta - 120) & sin(\theta + 120) \\ cos(\theta) & cos(\theta - 120) & cos(\theta + 120) \\ \frac{1}{2} & \frac{1}{2} & \frac{1}{2} \end{bmatrix} \begin{bmatrix} v_{ta} \\ v_{tb} \\ v_{tc} \end{bmatrix} \tag{3.35}$$

Where θ is given as follows

$$\theta(t) = \int_0^t \omega(\xi) d\xi + \theta(0) \tag{3.36}$$

ω is the rotating frame angular frequency. The abc reference frame voltages and $dq0$ reference frame voltages are related as in Fig. 3.2.

The desired load voltages in $dq0$ reference frame is given as follows:

$$\begin{bmatrix} v_{ld} \\ v_{lq} \\ v_{l0} \end{bmatrix} = \begin{bmatrix} v_{L\ max} \\ 0 \\ 0 \end{bmatrix} \tag{3.37}$$

Where $v_{L\ max}$ is the desired value of load voltage magnitude in each phase. The reference voltages in $dq0$ reference frame can be obtained by subtracting (3.35) from (3.37) and is as follows

$$\begin{bmatrix} v^*_{d\ ref} \\ v^*_{q\ ref} \\ v^*_{0\ ref} \end{bmatrix} = \begin{bmatrix} v_{ld} \\ v_{lq} \\ v_{l0} \end{bmatrix} - \begin{bmatrix} v_{td} \\ v_{tq} \\ v_{t0} \end{bmatrix} \tag{3.38}$$

The reference voltages in abc reference frame can be obtained by transforming the $dq0$ reference quantities back to abc reference frame using inverse Park's transformation as follows.

$$\begin{bmatrix} v^*_{fa} \\ v^*_{fb} \\ v^*_{fc} \end{bmatrix} = \begin{bmatrix} sin(\theta) & cos(\theta) & 1 \\ sin(\theta - 120) & cos(\theta - 120) & 1 \\ sin(\theta + 120) & cos(\theta + 120) & 1 \end{bmatrix} \begin{bmatrix} v^*_{d\ ref} \\ v^*_{q\ ref} \\ v^*_{0\ ref} \end{bmatrix} \tag{3.39}$$

The reference voltages generated using (3.39) are given to a PWM generator to ob-

tain the switching pulses for the VSI. The reference voltages could be balanced, unbalanced and it can even have harmonics depending on the terminal voltage ($v_{t(abc)}$). The same hysteresis band PWM control explained in Subsection 3.2.5 is used for generating the switching pulses for the VSI [28].

The sag/swell detection signals are generated from the control circuitry of the SSTS explained in Subsection 3.1.2. If both $\overline{v}_{dp-pf}$ and $\overline{v}_{dp-af}$ goes below the sag detection limit then only the sag will affect the Custom Power Park bus. DVR needs to inject the voltage under this condition and when there is harmonics in supply voltage.

The reference voltages in dq reference frame for DVR during interruption is as follows:

$$\begin{bmatrix} v^*_{d\ ref} \\ v^*_{q\ ref} \\ v^*_{0\ ref} \end{bmatrix} = \begin{bmatrix} v_{L\ max} \\ 0 \\ 0 \end{bmatrix} \tag{3.40}$$

The reference voltages in abc reference frame can be obtained by transforming the $dq0$ reference quantities back to abc reference frame using inverse Park's transformation as follows.

$$\begin{bmatrix} v^*_{fa} \\ v^*_{fb} \\ v^*_{fc} \end{bmatrix} = \begin{bmatrix} sin(\theta') & cos(\theta') & 1 \\ sin(\theta' - 120) & cos(\theta' - 120) & 1 \\ sin(\theta' + 120) & cos(\theta' + 120) & 1 \end{bmatrix} \begin{bmatrix} v_{L\ max} \\ 0 \\ 0 \end{bmatrix} \tag{3.41}$$

Where $\theta' = \omega t' + \theta$, θ is the phase angle at the starting of interruption, it is taken to get a synchronized output with the supply voltage and t' is taken as 0 at the starting of interruption and it will increase from there onwards.

3.3.2 Selection of Passive Filter Parameters

The output of VSI will contain switching frequency which will be in the order of few kHz. It has to be filtered out so that the load voltage is distortion free. LC filter is used for this purpose, which is as shown in Fig. 3.11.

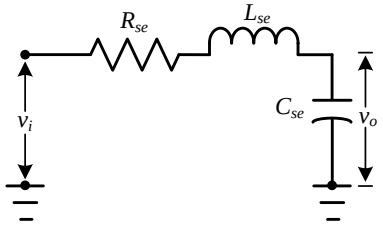

Figure 3.11: LC low pass filter.

The transfer function of the low pass filter is as follows

$$\begin{aligned} \frac{v_o(s)}{v_i(s)} &= \frac{1/(L_{se}C_{se})}{s^2 + s(R_{se}/L_{se}) + 1/(L_{se}C_{se})} \\ &= \frac{\omega_n^2}{s^2 + 2\xi\omega_n s + \omega_n^2} \end{aligned} \tag{3.42}$$

where,

$\omega_n = \frac{1}{\sqrt{L_{se}C_{se}}}$, the natural frequency of filter.

$\xi = \frac{R_{se}}{2}\sqrt{\frac{L_{se}}{C_{se}}}$, the damping ratio.

If the source voltage has some harmonics then that also to be compensated by the DVR. So the filter cut-off frequency should be higher than the highest order harmonic component that is to be compensated. LC parameters are chosen such a way that it passes the fundamental component and required harmonics. Higher value of C_{se} will reduce the ripples in output voltage. R_{se} is selected so as to provide sufficient damping.

3.3.3 Control of DVR

Fig. 3.12 shows the schematic diagram of DVR with its control unit. The control unit has a 3 phase PLL for extracting the instantaneous phase angle of the voltage, reference voltage is generated as explained in Subsection 3.3.1 and hysteresis band PWM controller is used for generating the switching pulses for the VSI. The switching frequency components present in the VSI output is filtered using a LC low-pass filter. The filtered output contains the required harmonics and fundamental frequency components which are injected through the injection transformer with a polarity as shown. A bypass switch is used to protect the DVR from load faults, large inrush currents and to bypass the transformer under normal operation.

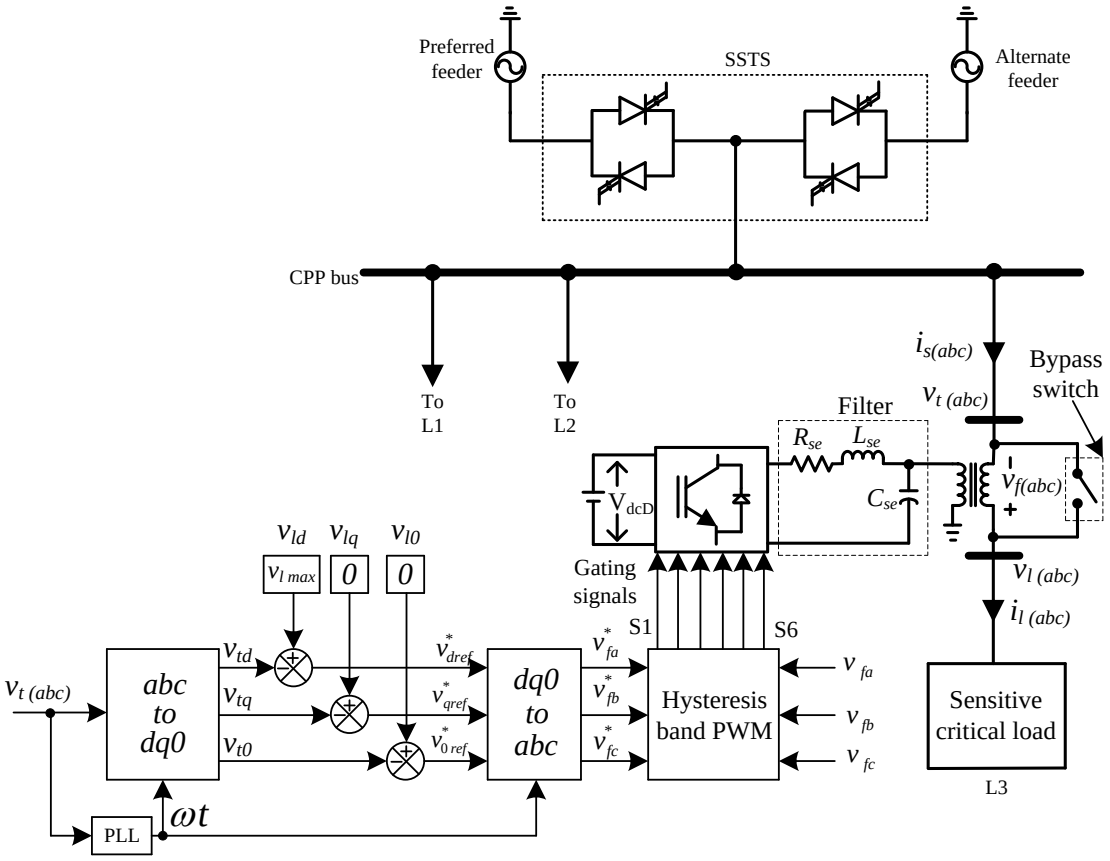

Figure 3.12: Schematic diagram of DVR and its control.

3.4 Summary

This chapter explained the operation, modelling and control of custom power devices used in this study. In first section the modelling of SSTS, voltage sag/swell detection algorithm are discussed, then operation of DSTATCOM and its reference current generation are explained and in final section the operation of DVR and its are discussed. The next chapter explains how these devices can be coordinated in a custom power park.

CHAPTER 4

MODELLING OF CUSTOM POWER PARK AND ITS CONTROL

In previous chapter the operation and control of different custom power devices like SSTS, DSTATCOM and DVR are discussed in detail. This chapter explains how these devices can be coordinated to form a Custom Power Park (CPP). In a custom power park all customers will get a higher quality supply which is superior to the normal power which is available from the utility. The CPP presented in this work differs from the conventional studies in the following aspects

- It has devices to improve both current and voltage related power quality problems i.e., DSTATCOM and DVR as compared to [8] and [9].
- It uses an improved control algorithm which can work even under distorted grid voltage for detecting power quality disturbances.
- Voltage detection scheme used in the control of custom power park has better response time than that in [12] and [14].

4.1 Modelling of Custom Power Park

The custom power park offers high quality power of three different grades namely CP-1, CP-2 and CP-3 to the customers for meeting the requirements of various sensitive and critical loads. Fig. 4.1 shows the power circuit of the custom power park used for the simulation study. It has network reconfiguring custom power device i.e., SSTS which is connected to preferred and alternate feeders, two compensating custom power devices i.e., DSTATCOM and DVR, three different loads L1, L2 and L3 named as the grades of power they are receiving and a diesel generator which can be used as the backup supply in the case of total feeder loss.

SSTS protects the custom power park bus from the voltage related problems such as voltage sags, swells and interruption by transferring the loads to a healthy feeder within a time span of 4-8 milli-seconds. The control unit is responsible for monitoring

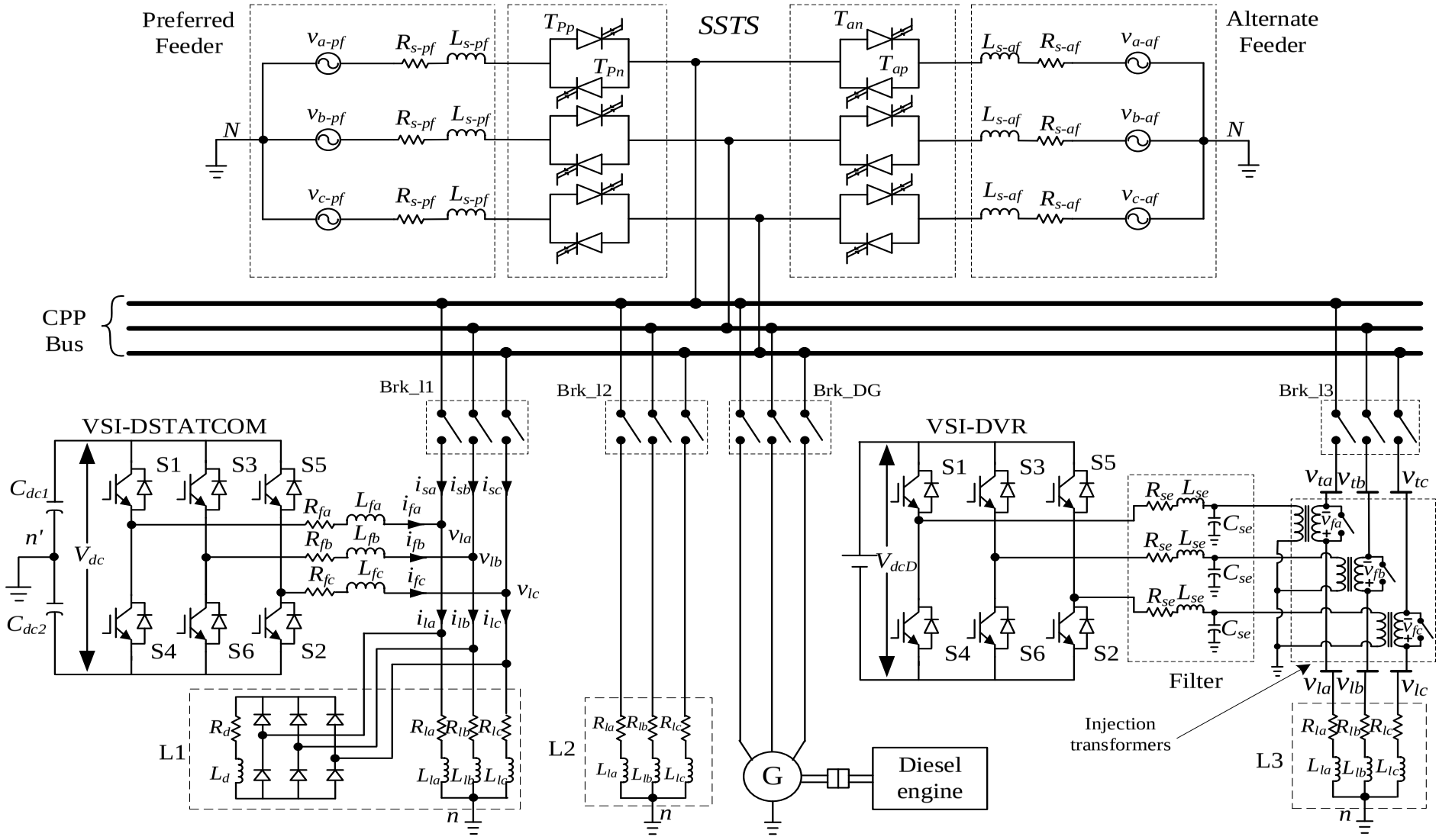

Figure 4.1: Power circuit of the custom power park.

the voltage quality of both feeder voltages and making the decision to transfer the loads whenever it is necessary. The voltage quality is monitored based on the modified SRF theory as explained in Subsection 3.1.1. If the preferred feeder meets the specified requirements then the CPP bus will be connected to it and if it doesn't the loads will be transferred to alternate feeder.

DSTATCOM mitigates Current harmonics and compensate for the reactive power required by the load L1. Shunt connected 3 leg VSI with split capacitor topology on the DC side is used in the DSTATCOM power circuit. Switching frequency components in the output of VSI are filtered using first order inductance filter. The reference currents for the DSTATCOM are generated using instantaneous symmetrical component theory as explained in Subsection 3.2.3. So the load L1 will get a sag well free and current harmonic free power which is the least qualified power in the custom power park.

DVR is connected in series with the load L3 by means of three single phase transformers and has capable of compensating voltage related problems such as voltage sag swell and harmonics. A SRF based reference voltage generation as explained in Subsection 3.3.1 is used for the DVR. The voltage sag and swell are detected as explained in Subsection 3.1.1. DVR needs to compensate only when both the feeders are subjected to sag or swell and when voltage harmonics are present in the feeder which is connected to the custom power park bus. The DC energy support for the DVR is increased so that it can maintain the voltage across the load L3 nearly to nominal value for few seconds which is considered as start-up time for diesel generator under total feeder loss. After this few seconds diesel generator will be connected to the bus and it starts supplying the loads L2 and L3

There are three different grades of qualified powers in Custom Power Park they are Custom Power-1 (CP-1), Custom Power-2 (CP-2) and Custom Power-3 (CP-3).

Custom Power-1 (CP-1): CP-1 is the basic quality value added power in the CPP. It is high quality power compared to the normal power in distribution system arises from the fact that the park has two incoming feeders. SSTS ensures that feeder with superior power is selected in less than a half cycle. There will be still voltage dips which are common to the both feeders resulting from the faults in transmission system. It also gets benefit from the DSTATCOM which will compensate the current harmonics there by reducing harmonic distortion at the load L1 and it also compensates the reactive

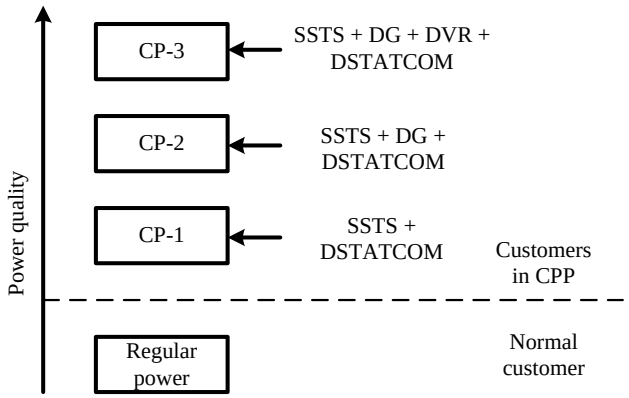

Figure 4.2: The grades of power in custom power park.

power required by this load. The following are the improvements which CP-1 got over the normal utility power:

1. 60-80 % reduction in voltage dips.
2. Rare occurrence of interruption.
3. Active power and harmonic filtering.

Custom Power-2 (CP-2): CP-2 also receives same basic qualified power as CP-1 which is harmonic free and sag well free if any one of the feeders is in good condition, apart from that it also receives benefit from a standby Diesel Generator (DG) which comes in to operation in about 10-20 seconds in the case of total feeder loss caused by transmission system faults. So this load losses power only during this 10-20 seconds which is the start-up and synchronization delay for the diesel generator.

Custom Power-3 (CP-3): CP-3 power quality is above and over the grade of CP-2, it is harmonic free, sag/swell free, voltage unbalance free and long interruption free. It also receives the benefit of DVR which adds right amount of voltage to the feeder voltage to ensure that the load voltage is free from sag/swells and voltage harmonics. During long interruption if there is some start-up for the diesel generator DVR is supposed to maintain the voltage across this load near to the nominal value.

An overview of the grades of powers compared to normal power is as shown in Fig. 4.2. The loads in custom power park are categorized to three according to the grades of power they are receiving, they are L1, L2 and L3. The load L1 is unbalanced and it can contain the DC loads also, L2 is the senstive load which is assumed to be balanced and L3 is critical sensitive load which is also balanced. L1, L2 and L3 will

Table 4.1: Grades of powers required by different customers.

Grades of Power	Types of Customer
CP-1	Shopping centers, office buildings, plastic company, computer hardware companies.
CP-2	Software development companies, pathology and other testing facilities
CP-3	Semiconductor manufacturing, hospitals, life support systems

get the power grades CP-1, CP-2 and CP-3 respectively. There are different customers in custom power park and they require different grades of power. The Table 4.1 shows the types of customers and their requirements of the power quality as interpreted from [1].

4.2 Control of Custom Power Park

When different types of devices are operated to solve multiple power quality disturbances simultaneously proper control and coordination of devices are necessary for the flexibility of the system. Some control functions can be centralized from a common platform. This common platform for the proposed custom power park uses the modified SRF theory explained in Subsection 3.1.1. Using this theory we can extract the DC component positive sequence d axis voltage v_{dp} as per the following expression

$$v_{dp} = v_{d(p)} + \frac{1}{2\omega} \dot{v_{q(p)}} \tag{4.1}$$

where,

$v_{d(p)}$ is the d axis voltage in SRF.

$v_{q(p)}$ is the q axis voltage in SRF.

and ω is the angular frequency.

This signal v_{dp} may contain high frequency noises because of the differentiator used in the detection scheme, which can be filtered using a low-pass filter. If the grid voltage contains harmonics this problem become more severe as the rate of change of harmonic components will be very much higher than that of fundamental component. Considering that the most common harmonics in voltage are 250 Hz which forms the negative

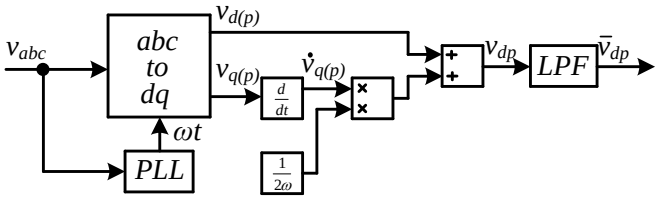

Figure 4.3: Block diagram for generation of fault detection signal.

sequence and 350 Hz which forms the positive sequence, this will appear as 300 Hz component in dq reference frame a cut-off frequency of 150 Hz is chosen for the LPF. So harmonic and higher frequency components will be attenuated and output of the LPF $\overline{v}_{dp}$ will be pure DC component which will be used for fault detection.

The block diagram used for the generation of fault detection signal $\overline{v}_{dp}$ is as in Fig. 4.3. As we are using higher cut-off frequency for the low pass filter the detection time will be less than the control schemes presented in [12] and [14]. Custom power park has two feeders namely preferred and alternate feeder. So we will be having two fault detection signals as in (4.1) in the control part corresponding to this feeders. For preferred feeder:

$$v_{dp-pf} = v_{d(p)-pf} + \frac{1}{2\omega} \dot{v_{q(p)-pf}} \tag{4.2}$$

and for alternate feeder:

$$v_{dp-af} = v_{d(p)-af} + \frac{1}{2\omega} \dot{v_{q(p)-af}} \tag{4.3}$$

where the the pf and af terms in suffixes corresponds to preferred feeder and alternate feeder respectively. These outputs in (4.2) and (4.3) can be filtered to get fault detection signals $\overline{v}_{dp-pf}$ and $\overline{v}_{dp-af}$ corresponding to preferred and alternate feeders respectively. The normal, sag, swell and interruption can be detected by comparing the per-unit value of $\overline{v}_{dp}$ with reference values as given below :

- If the per-unit value of $\overline{v}_{dp}$ is in between $0.9\ pu$ and $1.1\ pu$ then it is said to be operating in **normal** mode (less than 10% sag/swell).
- If the per-unit value of $\overline{v}_{dp}$ is in between $0.5\ pu$ and $0.9\ pu$ then it then it considered as **sag** (dip in voltage magnitude between 10% and 50%).
- If the per-unit value of $\overline{v}_{dp}$ is in between $1.1\ pu$ and $1.5\ pu$ then it then it considered as **swell** (rise in voltage magnitude between 10% and 50%).

- If the per-unit value of $\overline{v}_{dp}$ is less than $0.5\ pu$ or greater than $1.5\ pu$ then it considered as **interruption** (dip in voltage magnitude below its 50% or rise in voltage magnitude above its 50%).

Considering that custom power park is having two incoming feeders and a diesel generator which is having some start-up delay, the following 8 cases of operation are possible in the proposed custom power park.

1. Less than 10% sag/swell at preferred and alternate feeder (normal operation).
2. Less than 10% sag/swell at preferred feeder and between 10% and 50% sag/swell at alternate feeder.
3. Less than 10% sag/swell at preferred feeder and more than 50% sag/swell at alternate feeder.
4. Between 10% and 50% sag/swell at preferred feeder and less than 10% sag/swell at alternate feeder.
5. More than 50% sag/swell at preferred feeder and less than 10% sag/swell at alternate feeder.
6. Between 10% and 50% sag/swell at preferred and alternate feeder.
7. More than 50% sag/swell at preferred feeder and alternate feeder and diesel generator is starting-up.
8. More than 50% sag/swell at preferred feeder and alternate feeder and after diesel generator start-up.

The power quality monitoring and controlling system of the custom power park is having three parts, the first part will generate the fault detection signals $\overline{v}_{dp-af}$ and $\overline{v}_{dp-af}$, the second part will identify the cases described above and the third part will switch the devices in the park depending on the identified operating case.

There are two inputs to the first part of the control system, they are the each phase voltages of preferred and alternate feeders and this will generate the fault detection signals. The second part is having three inputs, the first one is the fault detection signal from the preferred feeder ($\overline{v}_{dp-pf}$), second is the fault detection signal from alternate feeder ($\overline{v}_{dp-af}$) and third one is dg_ready signal which will be issued by the diesel generator when the conditions for connecting it to the park bus are satisfied after getting a dg_start signal. The third part will generate the switching signals depending on the case identified in second part. It will generate for the switching signals SSTS and load breakers, control signals for the DSTATCOM and DVR and start/stop signals for the

Table 4.2: Different conditions for identification of operating cases/modes.

Cases	$\overline{v}_{dp-pf}$ (pu)	$\overline{v}_{dp-af}$ (pu)	dg_ready
1	$0.9 < \overline{v}_{dp-pf} \leq 1.1$	$0.9 < \overline{v}_{dp-af} \leq 1.1$	0
2	$0.9 < \overline{v}_{dp-pf} \leq 1.1$	$0.5 < \overline{v}_{dp-af} \leq 0.9$ or $1.1 < \overline{v}_{dp-af} \leq 1.5$	0
3	$0.9 < \overline{v}_{dp-pf} \leq 1.1$	$\overline{v}_{dp-af} \leq 0.5$ or $\overline{v}_{dp-af} > 1.5$	0
4	$0.5 < \overline{v}_{dp-pf} \leq 0.9$ or $1.1 < \overline{v}_{dp-pf} \leq 1.5$	$0.9 < \overline{v}_{dp-af} \leq 1.1$	0
5	$\overline{v}_{dp-pf} \leq 0.5$ or $\overline{v}_{dp-pf} > 1.5$	$0.9 < \overline{v}_{dp-af} \leq 1.1$	0
6	$0.5 < \overline{v}_{dp-pf} \leq 0.9$ or $1.1 < \overline{v}_{dp-pf} \leq 1.5$	$0.5 < \overline{v}_{dp-af} \leq 0.9$ or $1.1 < \overline{v}_{dp-af} \leq 1.5$	0
7	$\overline{v}_{dp-pf} \leq 0.5$ or $\overline{v}_{dp-pf} > 1.5$	$\overline{v}_{dp-af} \leq 0.5$ or $\overline{v}_{dp-af} > 1.5$	0
8	$\overline{v}_{dp-pf} \leq 0.5$ or $\overline{v}_{dp-pf} > 1.5$	$\overline{v}_{dp-af} \leq 0.5$ or $\overline{v}_{dp-af} > 1.5$	1

diesel generator. Different cases that will be identified in the second stage will be one among the cases described above, the Table 4.2 summarizes conditions under which different cases are detected. In order to avoid for detecting multiple case number for same fault detection signals some limits are forced to be less than ($<$) instead of less than or equal to ($\leq$).

In normal mode that is less than 10% sag/swell at both the feeders the park bus will be connected to the preferred feeder and all the loads L1, L2 and L3 will be connected to the bus. DSTATCOM will be operating to compensate the harmonics and reactive power required by the load L1 and DVR will remain as idle. The operation will be same as normal mode in second and third case also. The fourth and fifth case corresponds to a sag/swell and interruption respectively at the preferred feeder, under this condition the

Table 4.3: ON/OFF status of the devices in each operating cases/modes.

Cases	SSTS_PF	SSTS_AF	L1	L2	L3	DSTATCOM	DVR	DG
1	ON	OFF	ON	ON	ON	ON	OFF	OFF
2	ON	OFF	ON	ON	ON	ON	OFF	OFF
3	ON	OFF	ON	ON	ON	ON	OFF	OFF
4	OFF	ON	ON	ON	ON	ON	OFF	OFF
5	OFF	ON	ON	ON	ON	ON	OFF	OFF
6	ON	OFF	ON	ON	ON	ON	ON	OFF
7	ON	OFF	OFF	OFF	ON	OFF	ON	OFF
8	OFF	OFF	OFF	ON	ON	OFF	OFF	ON

park bus will be supplied from the alternate feeder and all the loads will be connected to the bus. The DVR needs to operate only in sixth and seventh cases. Sixth case corresponds to a sag/swell which lies in between 50% and 90% of nominal value, under this condition the preferred feeder will be connected to the bus. The loads L1 and L2 will get the supply quality which corresponding to that of preferred feeder but L3 voltage will be same as pre-sag voltage as the DVR starts operating.

The case 7 corresponds to interruption at both the feeders, so the control system will issue a start signal to the generator which is denoted as dg_start and it continuously monitor the dg_ready signal which is an output of the diesel generator which will become active when the diesel generator is ready to get connected to the bus. During this diesel generator start-up period the DVR will maintain the voltage across load L3 near to its nominal value. The custom power park bus will be connected to the preferred feeder this time to get the reference for the DVR voltage which is injected in series. After getting the dg_ready signal the diesel generator will be connected to the bus and it will supply the loads L2 and L3. The Table 4.3 shows the ON/OFF status of the devices for different cases of operation.

The complete flow chart of the custom power park control system is as shown in Fig. 4.4. Here '1' corresponds to 'ON' condition or operating condition of the each devices and '0' corresponds to 'OFF' or no operation condition of the devices. The inputs to the control system are each phase voltages of preferred and alternate feeders and dg_ready signal. Using the measured phase voltges first part will generate the voltage sag/swell detection signal, second stage use this two signals and dg_ready signal for identifying

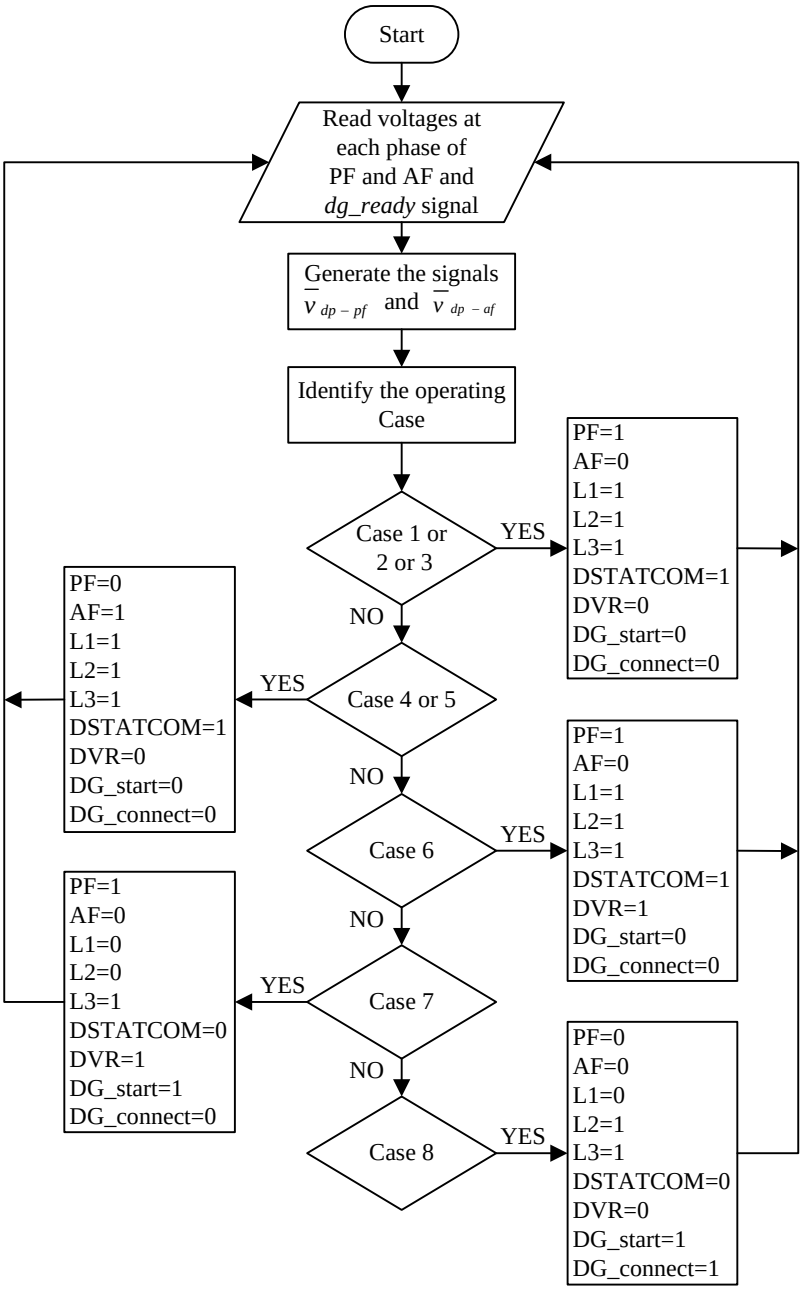

Figure 4.4: Flow chart of the CPP control.

the operating case and third part will generate the switching and control signals.

The Fig. 4.5 shows a schematic of custom power park with its complete control system. It consists of a common control for detection of faults and it will switch the devices according to the power quality of the feeders. DSTATCOM will compensate for harmonics, reactive power and unbalance in load L1, which uses instantaneous symmetrical component theory for generation of reference voltage. DVR will compensate for sag, swell and voltage harmonics and it maintains constant voltage across L3. The back up diesel generator will supply the loads L2 and L3 when a long interruption occurs.

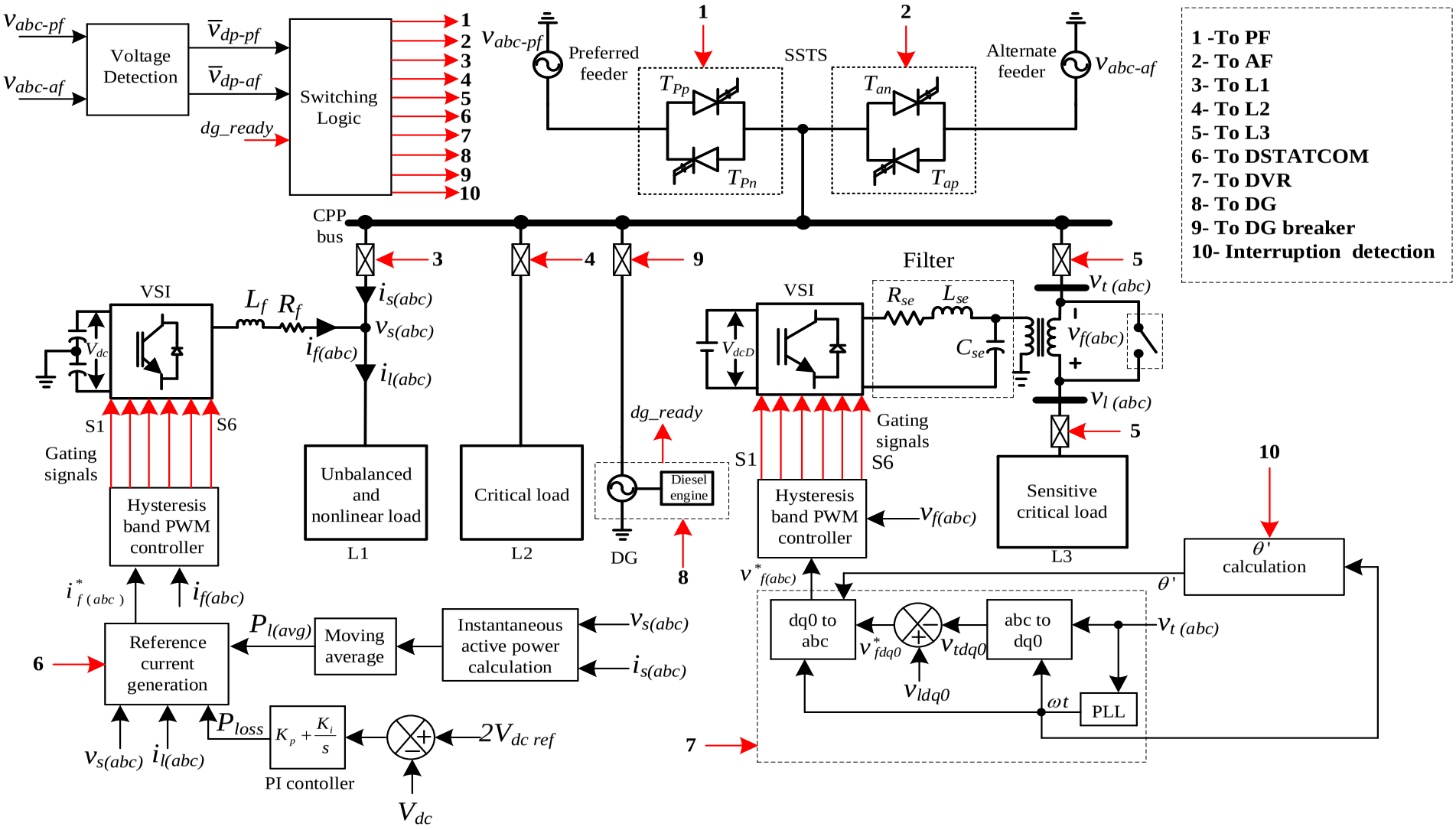

Figure 4.5: Schematic diagram of CPP and its control.

4.3 Summary

This chapter discussed about the operation and control of the custom power park and it also discussed about the different power quality levels that are obtained in the custom power park and how they can be obtained. The next chapter presents the performance of the proposed custom power park under different voltage and current quality disturbances.

CHAPTER 5

SIMULATION STUDIES

The proposed Custom Power Park is simulated using MATLAB-SIMULINK and the performance of the control algorithm and coordination of different devices for different operating conditions such as current/voltage harmonics, voltage sags, swells and interruptions occurred on preferred and alternate feeders. The circuit scheme used for simulation study is as in Fig. 4.1. The control algorithm shown in Fig. 4.5 is modelled using matlab function blocks.

Table 5.1: Parameters for simulation study

Parameters	Values
System parameters	
Preferred feeder voltage $(V_{pf(L-L)})$	$400\angle 0^o$ V
Alternate feeder voltage $(V_{af(L-L)})$	$400\angle 0^o$ V
Backup generator voltage $(V_{gen(L-L)})$	400 V
Fundamental frequency	50 Hz
Preferred feeder resistance, inductance	$0.05\ \Omega, 0.01$ mH
Alternate feeder resistance, inductance	$0.05\ \Omega, 0.01$ mH
DSTATCOM parameters	
DC link voltage (V_{dc})	700 V
DC link capacitances $(C_{dc1} = C_{dc2})$	2000 μF
Filter parameters $(R_f,\ L_f)$	1 Ω, 5 mH
Hysteresis band for current controller (h_i)	0.2 A
$K_p,\ K_i$ values for dc-link voltage controller	140, 20
DVR parameters	
DC link voltage (V_{dcD})	800 V
Filter parameters (R_{se}, L_{se}, C_{se})	1 Ω, 1 mH, 2 μF
Hysteresis band for voltage controller (h_v)	5 V
Turns ratio of injection transformer	1 : 1
Load parameters	
L1 - Unbalanced load	$Z_{l1\ a} = 25 + j20\ \Omega$ $Z_{l1\ b} = 40 + j47\ \Omega$ $Z_{l1\ c} = 30 + j24\ \Omega$
- Nonlinear load	Diode bridge rectifier with R-L load $R = 20\ \Omega$, $L = 0.1$ H
L2 - Balanced linear load	$Z_{l2\ abc} = 13.5 + j4.5\ \Omega$
L3 - Balanced linear load	$Z_{l3\ abc} = 17 + j8.5\ \Omega$

The Table 5.1 gives the parameters used for the simulation study. The following four case studies are presented to test the power quality improvements in the custom power park.

- Simulation results for SSTS for load transferring between the preferred feeder and alternate feeder for improving the voltage quality of custom power park bus.
- Simulation results for DSTATCOM for improving the quality of current drawn from the feeders by the unbalanced non linear load L1.
- Simulation results for DVR which improves the voltage quality of most critical load (L3) under the condition when a sag/swell occur on the custom power park bus. This happens mainly due to transmission system faults because of which both the feeders are subjected to the disturbance.
- Simulation results for the operation of DVR and diesel generator during interruption.

Under normal conditions preferred feeder will be connected to the bus, and the breakers corresponding to all loads will be connected to the bus, DSTATCOM will be compensating the load L1 and DVR will be in idle mode, as shown in Table 4.3 the case 1 corresponds to the normal operating mode. When the operating modes are either case 1 or 2 or 3 preferred feeder will be supplying the loads and when operating mode changes to either 4 or 5 load the custom power park bus should be transferred to alternate feeder. When a transmission system fault occurs, both the feeders will be subjected to sag/swell i.e., case 6, DVR should operate to maintain the voltage across the most critical load. Under an interruption on both the feeders the diesel generator should supply the critical loads L2 and L3. During the start-up time of the diesel generator DVR has to maintain the voltage across the most critical load. The following sections explains the operation of the custom power park under various power quality disturbances with the help of simulation results.

The method used for sag/swell detection has fast detection time compared to single phase dq theory used in [14] and SRF theory used in [12]. Fig. 5.1 shows the comparison of different methods used for voltage sag/swell detection. A balanced sag of 40% is created on preferred feeder for $0.1\ s$ starting from $t = 0.1\ s$, the signal is compared with sag detection limit which is $0.9\ pu$ as shown. It can be seen that for the method used here i.e., modified SRF theory the voltage drops to the post sag value very fast compared to other methods, and when the sag is removed it takes a time which is less than other methods to go back to the normal value. Similarly in the case of an unbalanced

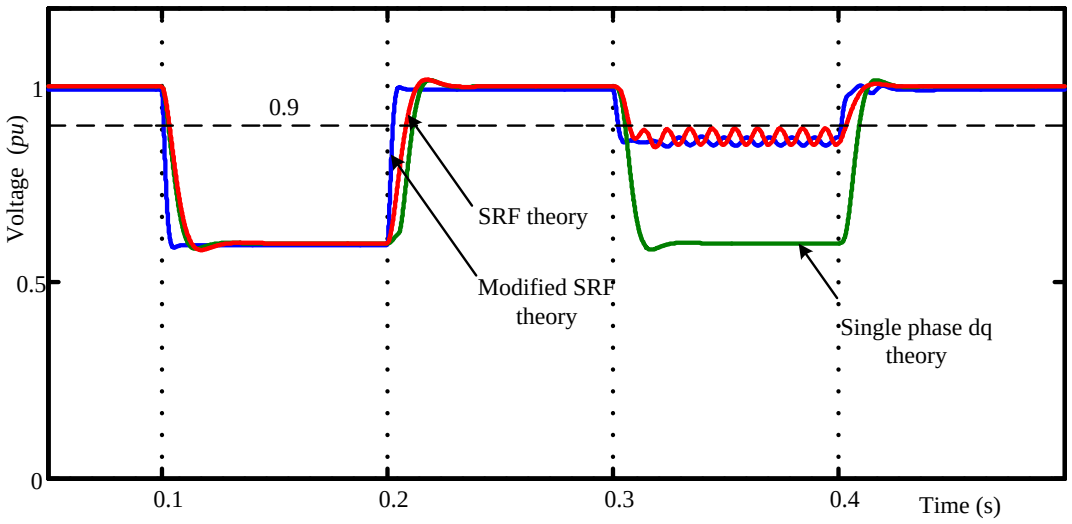

Figure 5.1: Voltage sag detection time comparison for sag at preferred feeder.

sag starting from $t = 0.2\ s$ is also shown, in this case also modified SRF theory has better detection time. So better performance is achieved with this sag/swell detection method.

5.1 Load Bus Transferring with SSTS

The custom power park bus should be transferred from preferred feeder to alternate feeder when some disturbance happens in the preferred feeder and it should be transferred back to the preferred feeder when the normal condition is restored in preferred feeder. In this section operation of the CPP for load transfer under various disturbances such as balanced sag on preferred feeder, balanced sag on both the feeders, unbalanced sag on preferred feeder and swell on preferred feeder are discussed.

Fig. 5.2 shows the fault detection signals for preferred and alternate feeders ($\overline{v}_{dp-pf}$ and $\overline{v}_{dp-af}$) and the transfer signals issued to the SSTS under various disturbances. It can be observed that if sag/swell occurs at any one of the feeders it will be transferred to the other and if it occurs on both the feeders the gating signals given to the SSTS's remains unchanged. The various cases are described below with the help of Fig. 5.3-5.10.

1. Sag on preferred feeder

The simulation was done for a 40% balanced voltage sag on preferred feeder starting

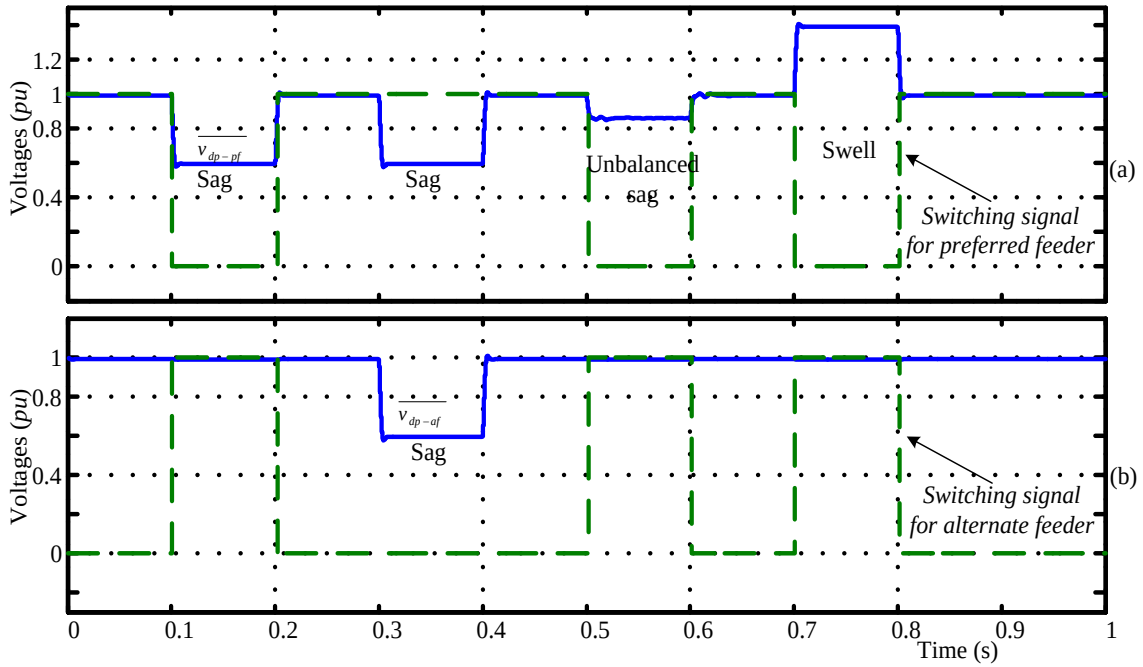

Figure 5.2: Fault detection and transfer signals during simulation: (a) Preferred feeder. (b) Alternate feeder.

from $t = 0.1\ s$ and it lasts till $t = 0.2\ s$. Fig. 5.3(a) shows the preferred feeder voltage which is under sag and Fig. 5.3(b) shows the alternate feeder voltage. From Fig. 5.3(c) it can be observed that the custom power park bus voltage is free from the sag except for a short duration which is taken for the detection of the sag. The Fig. 5.4(a) shows the preferred feeder current, during the sag the load currents will be supplied by the alternate feeder which is shown in Fig. 5.4(b) and the total load currents that drawn from the bus is continuous as shown in Fig. 5.4(c) irrespective of the load transfer between the feeders. The load currents are balanced and sinusoidal even though the load L1 is unbalanced and nonlinear because of the DSTATCOM which is connected in shunt with it injects the non linear and unbalance component of the current.

2. Sag on both feeders

This simulation was done for 40% sag on both the feeders starting from $t = 0.3\ s$ and it lasts till $t = 0.4\ s$. This operating mode corresponds to the case 6 discussed in Table 4.3. Under this condition preferred feeder will remains connected to the CPP bus which will get a voltage with 40% sag. The voltage and current waveforms of the feeders and CPP bus are shown in Fig.5.5(a)-(c) and 5.6(a)-(c) respectively. In this mode DVR will operate to maintain the voltage of the load L3 near to the nominal value. The current drawn by the loads L1 and L2 will reduce under this condition as shown in

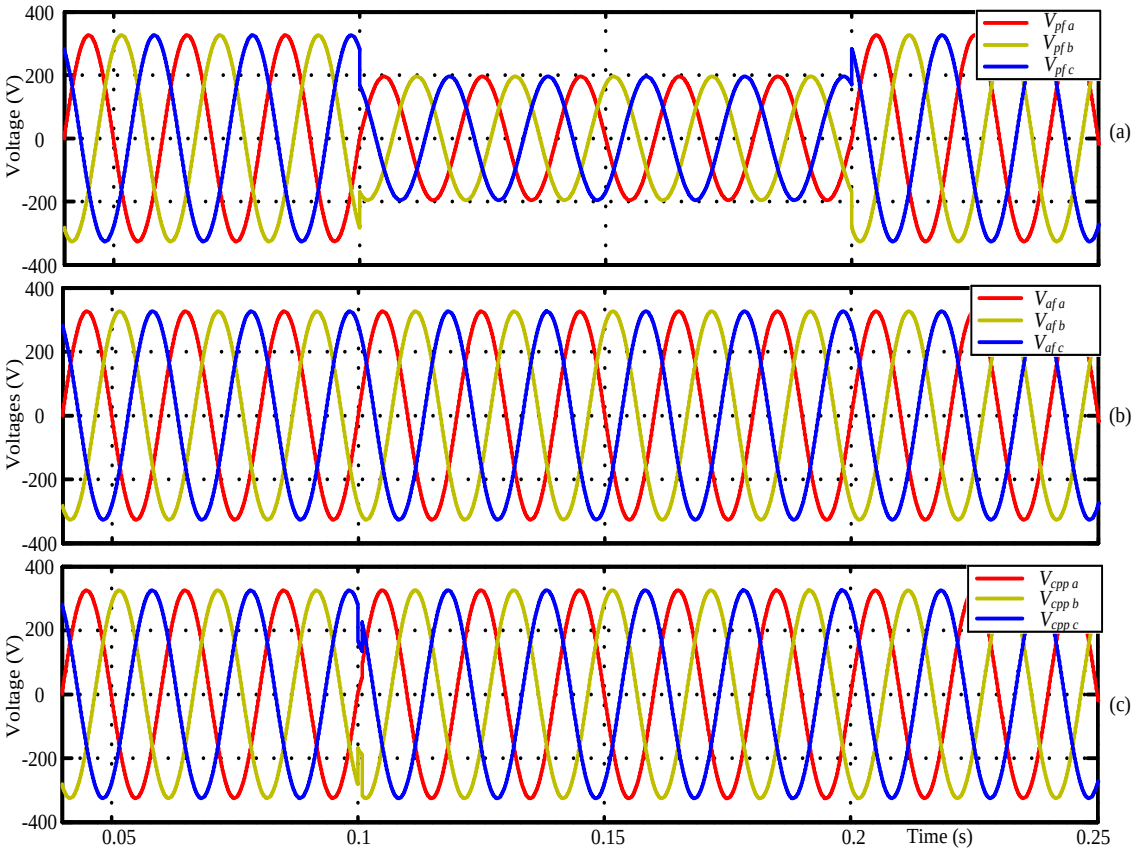

Figure 5.3: Sag on preferred feeder: (a) Preferred feeder voltage. (b) Alternate feeder voltage. (c) CPP bus voltage.

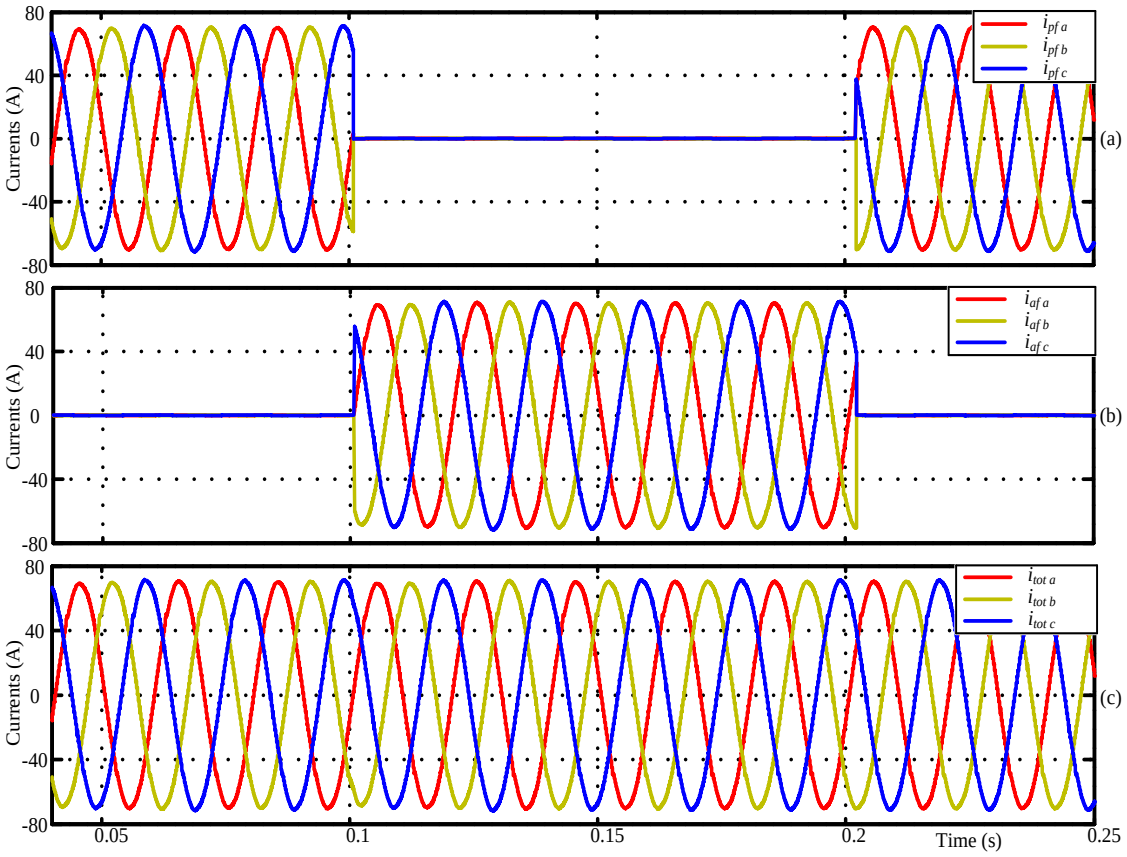

Figure 5.4: Sag on preferred feeder: (a) Preferred feeder current. (b) Alternate feeder current. (c) Total load current.

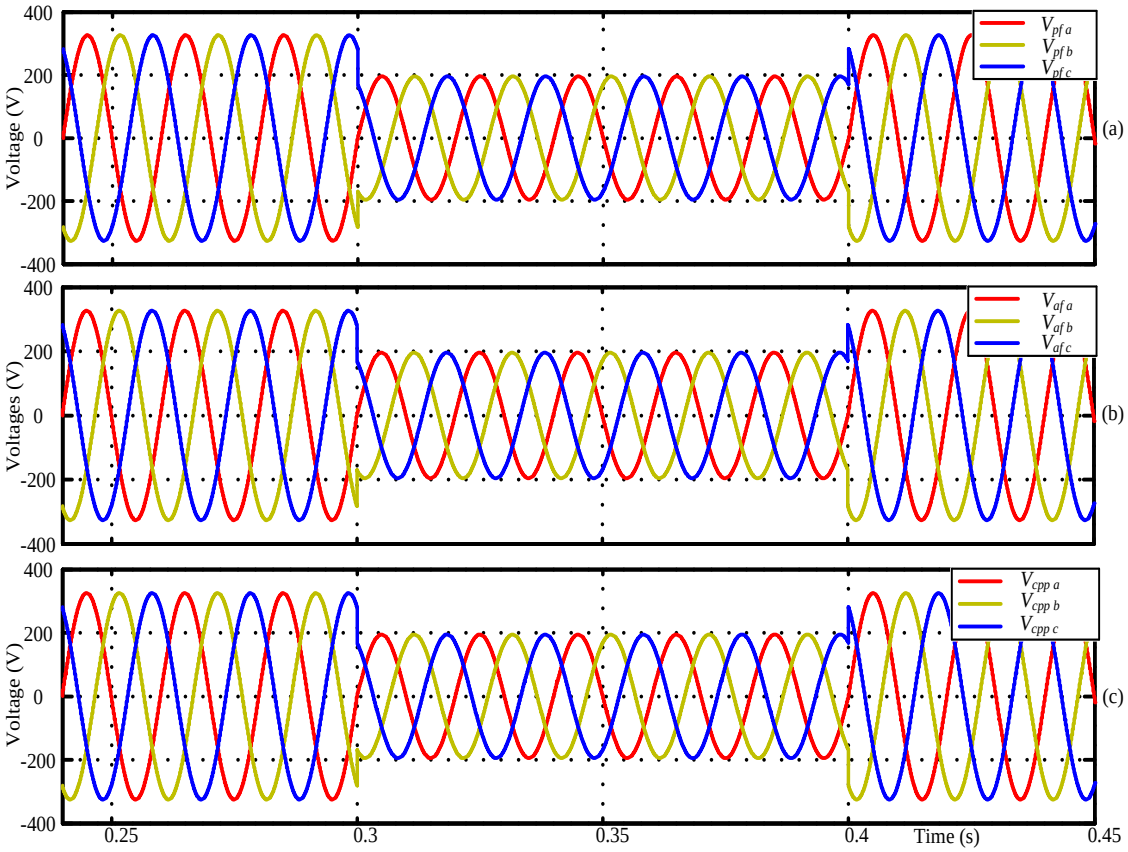

Figure 5.5: Sag on both feeders: (a) Preferred feeder voltage. (b) Alternate feeder voltage. (c) CPP bus voltage.

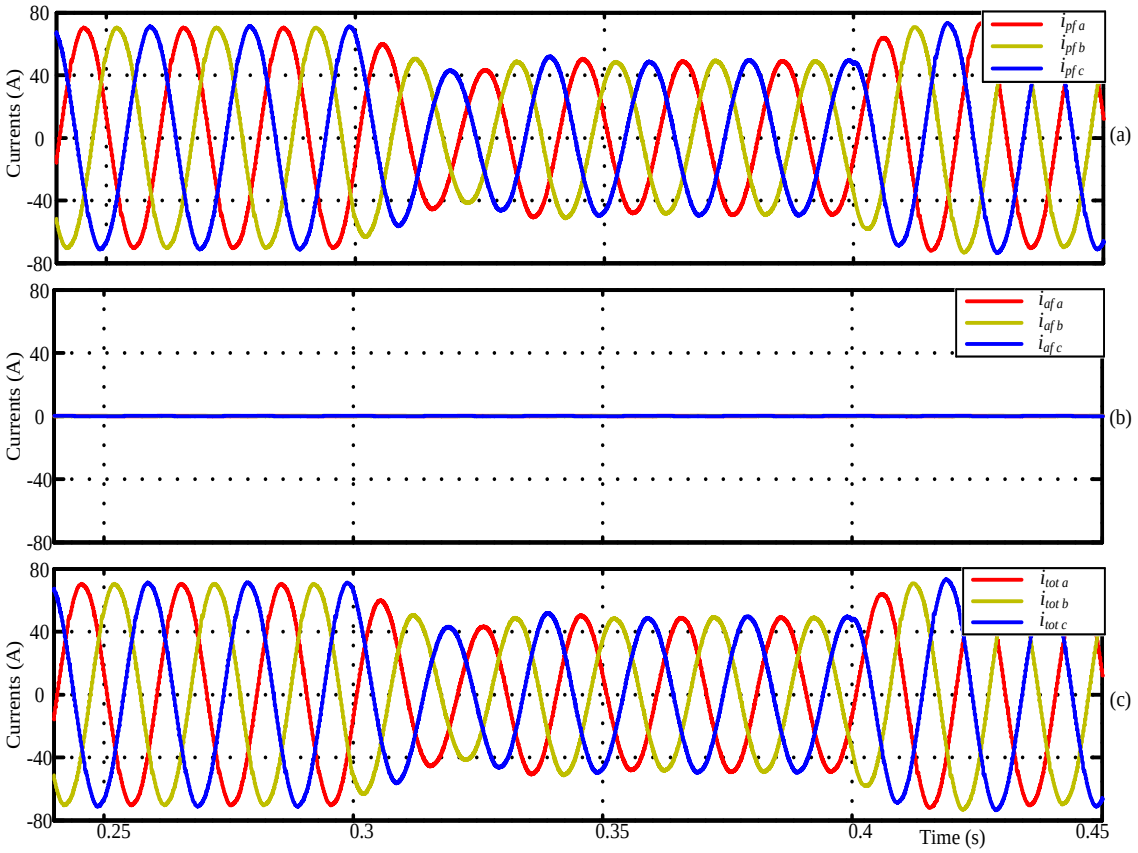

Figure 5.6: Sag on both feeders: (a) Preferred feeder current. (b) Alternate feeder current. (c) Total load current.

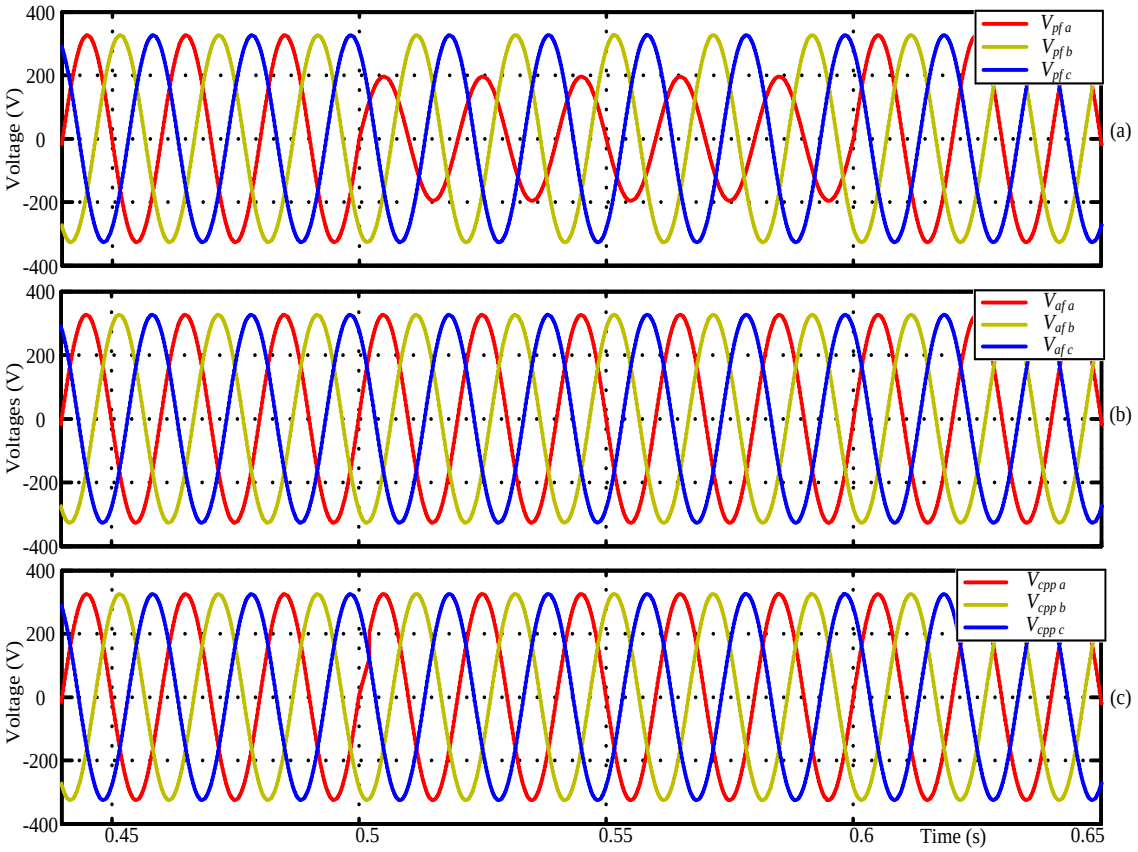

Figure 5.7: Unbalanced sag on preferred feeder: (a) Preferred feeder voltage. (b) Alternate feeder voltage. (c) CPP bus voltage.

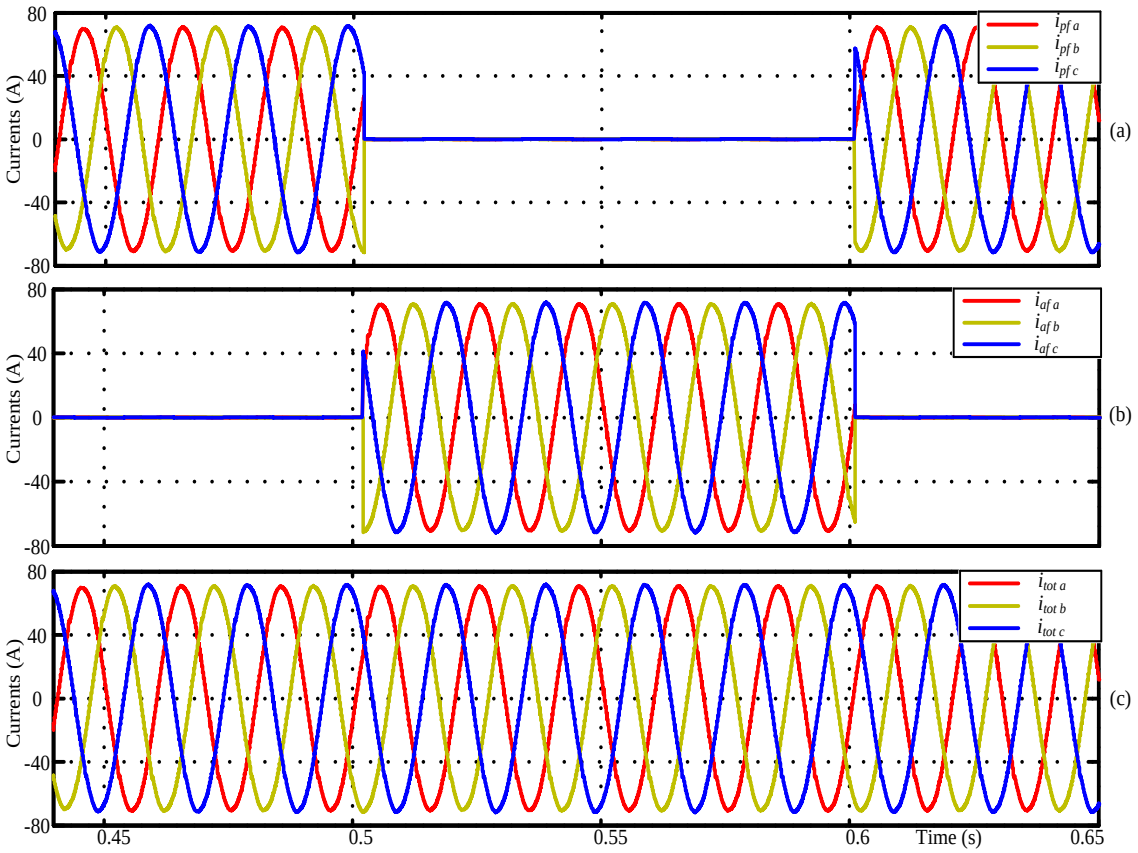

Figure 5.8: Unbalanced sag on preferred feeder: (a) Preferred feeder current. (b) Alternate feeder current. (c) Total load current.

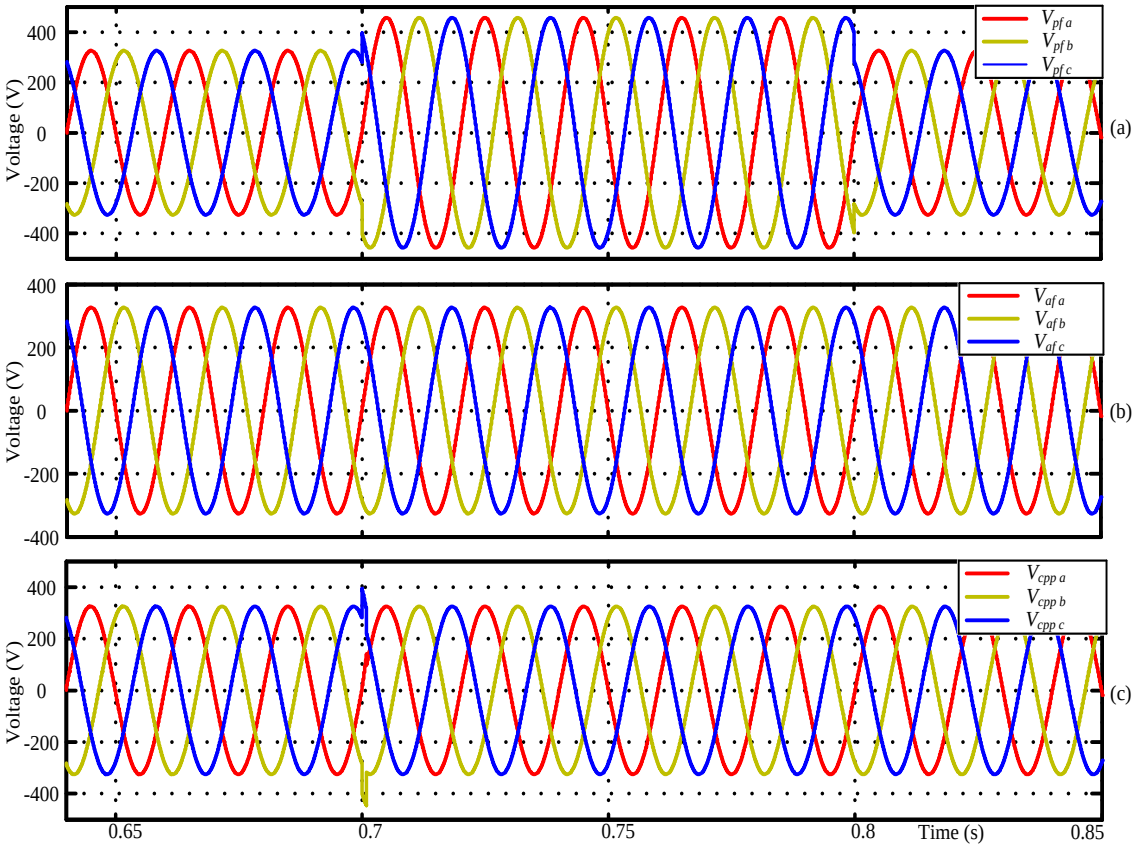

Figure 5.9: Swell on preferred feeder: (a) Preferred feeder voltage. (b) Alternate feeder voltage. (c) CPP bus voltage.

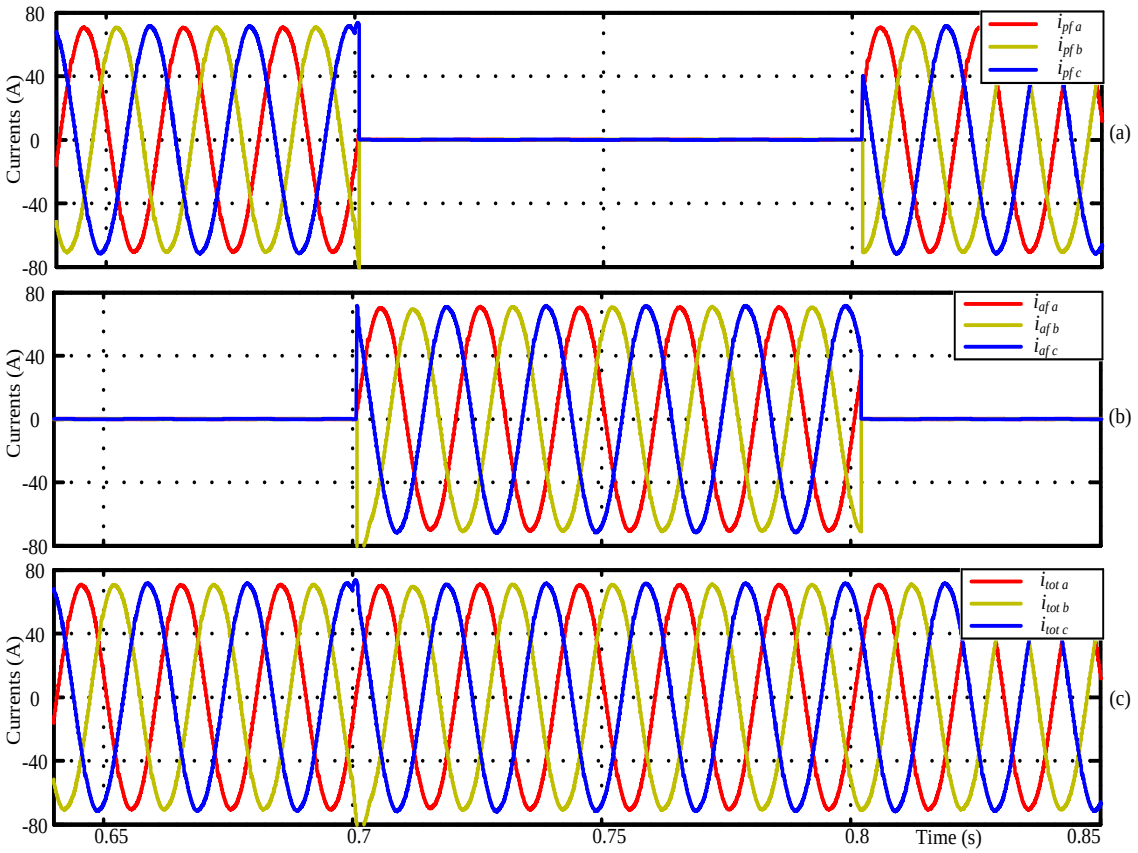

Figure 5.10: Swell on preferred feeder: (a) Preferred feeder current. (b) Alternate feeder current. (c) Total load current.

Fig. 5.6(c) as the voltage sag affects the CPP bus.

3. Unbalanced sag on preferred feeder

The next part of the simulation study is to evaluate the performance of the SSTS in transferring loads under unbalanced sag. A single phase sag of 40% is created in phase a of the preferred feeder staring from $t = 0.5\ s$ and it lasts till $t = 0.6\ s$. The voltage and current waveforms are as shown in Fig. 5.7(a)-(c) and 5.8(a)-(c) respectively. As soon as the unbalanced sag is detected at the preferred bus the CPP bus will be transferred to preferred feeder. From Fig. 5.7(c) it can be seen that the CPP bus voltage is free from the unbalanced sag at the preferred feeder as SSTS transfer it to the alternate feeder, and the load currents are continuous as in Fig. 5.8(c).

4. Swell on preferred feeder

The simulation was done for a 40% balanced voltage swell on preferred feeder starting from $t = 0.7\ s$ and it lasts till $t = 0.8\ s$. Fig. 5.9(a) shows the preferred feeder voltage which is under sag and Fig. 5.9(b) shows the alternate feeder voltage. From Fig. 5.9(c) it can be observed that the custom power park bus voltage is free from the swell except for a short duration which is taken for the detection of the swell. The Fig. 5.10(a) shows the preferred feeder current, during the swell the load currents will be supplied from the alternate feeder as shown in Fig. 5.10(b) and the total load currents that drawn from the bus is continuous as shown in Fig. 5.10(c) irrespective of the load transfer between the feeders.

From the above simulation results it can be observed that SSTS is effective in transferring loads between two feeders. A fast sag swell detection is achieved using modified SRF theory where the detection time is very much less than 1/5th of the cycle of system frequency.

5.2 Harmonic and Reactive Power Compensation Using DSTATCOM

As the load L1 contain unbalanced and DC loads it will produce harmonics and unbalance in the current drawn from the feeders which will give rise to distortion in CPP bus

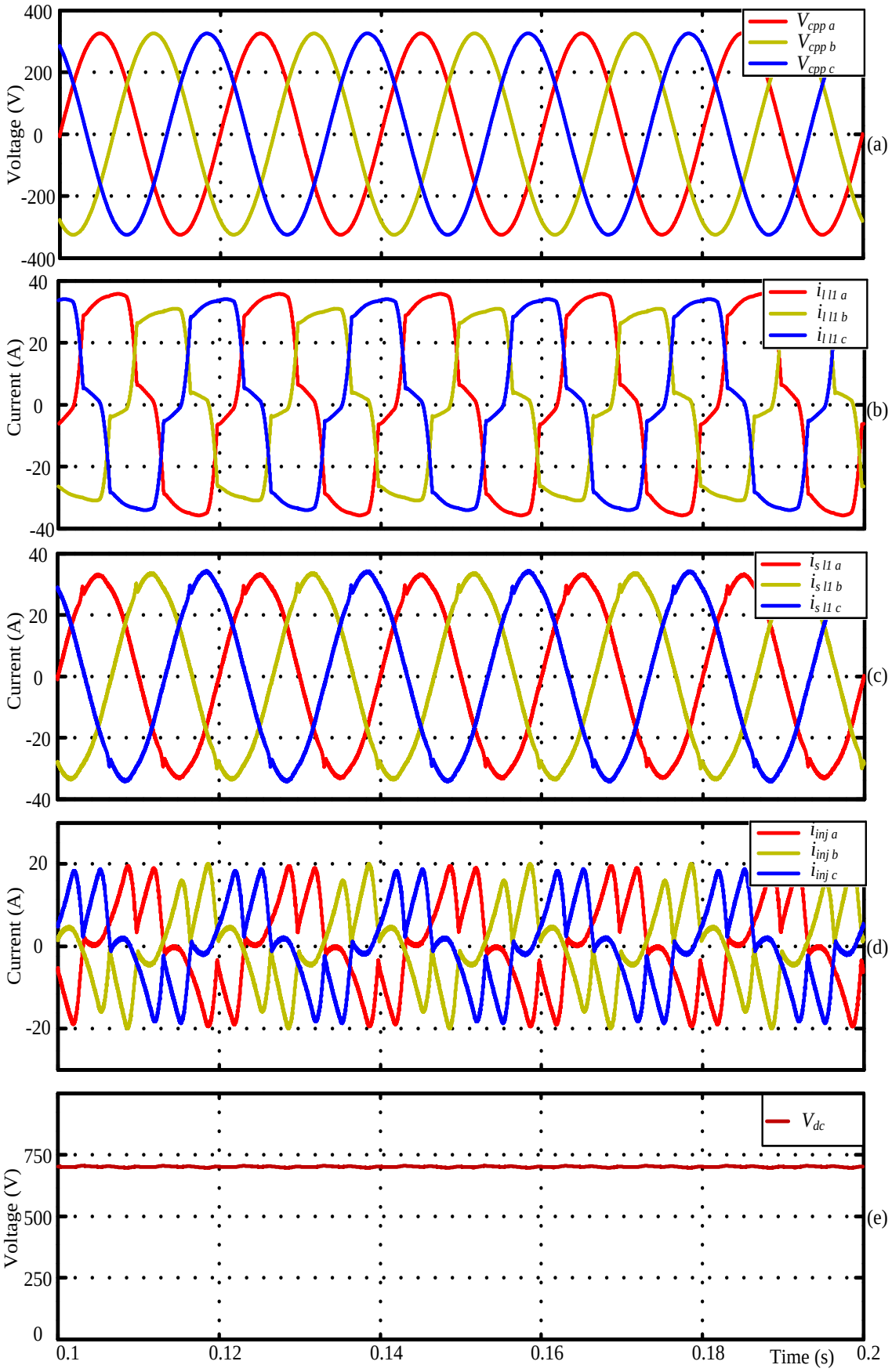

Figure 5.11: Waveforms illustrating operation of DSTATCOM: (a) CPP bus voltage. (b) L1 load currents. (c) L1 source currents. (d) Compensator injected currents. (e) DC link voltage.

voltage and other load currents because of the feeder impedance. A DSTATCOM which is operated in current control mode is connected in shunt with the load L1. This DSTATCOM mitigates the harmonics and unbalance in the load current and also it compensates for the reactive power required by the load L1. Instantaneous symmetrical component theory is used for generating the currents to be injected by the DSTATCOM. The generated reference is given to the hysteresis band PWM controller which will generate the switching pulses for the VSI. The Fig. 5.11(a) shows the CPP bus voltage at the PCC of L1 and DSTATCOM. The Fig. 5.11(b) shows the the L1 load current which is unbalanced and containing harmonics, Fig. 5.11(c) shows the current drawn by the load L1 from the CPP bus and Fig. 5.11(d) current injected by the DSTATCOM to compensate for the harmonics, unbalance and reactive power. The dc link voltage of the DSTATCOM is maintained at 700 V during the entire operating period as shown in Fig. 5.11(e).

The power quality improvements acheived by the connection of the DSTATCOM are the following:

- The THD of current drawn by phase a of the load L1 is 17.42% in the case if DSTATCOM is not there and that is reduced to 2.93% after DSTATCOM connection at the load terminal.
- The THD of the total current drawn from the feeders in phase a is reduced to 1.51% from 8.07% after DSTATCOM connection.

There is considerable reduction in THD of the feeder currents because of the DSTATCOM, hence THD can be kept below the limits specified by relevant standards [29].

5.3 Voltage Compensation Using DVR

DVR operates only when a fault occurs on both the feeders are under the voltage disturbance or when the feeder which is connected to the CPP bus has distorted voltage. DVR control scheme uses SRF based algorithm for generating the voltages that is to be injected. This reference voltage is given to the hysteresis band PWM controller for generating switching pulses for the VSI. This section discusses the operation of DVR under different operating conditions such as balanced voltage sag/swell, unbalanced sag and distorted voltage.

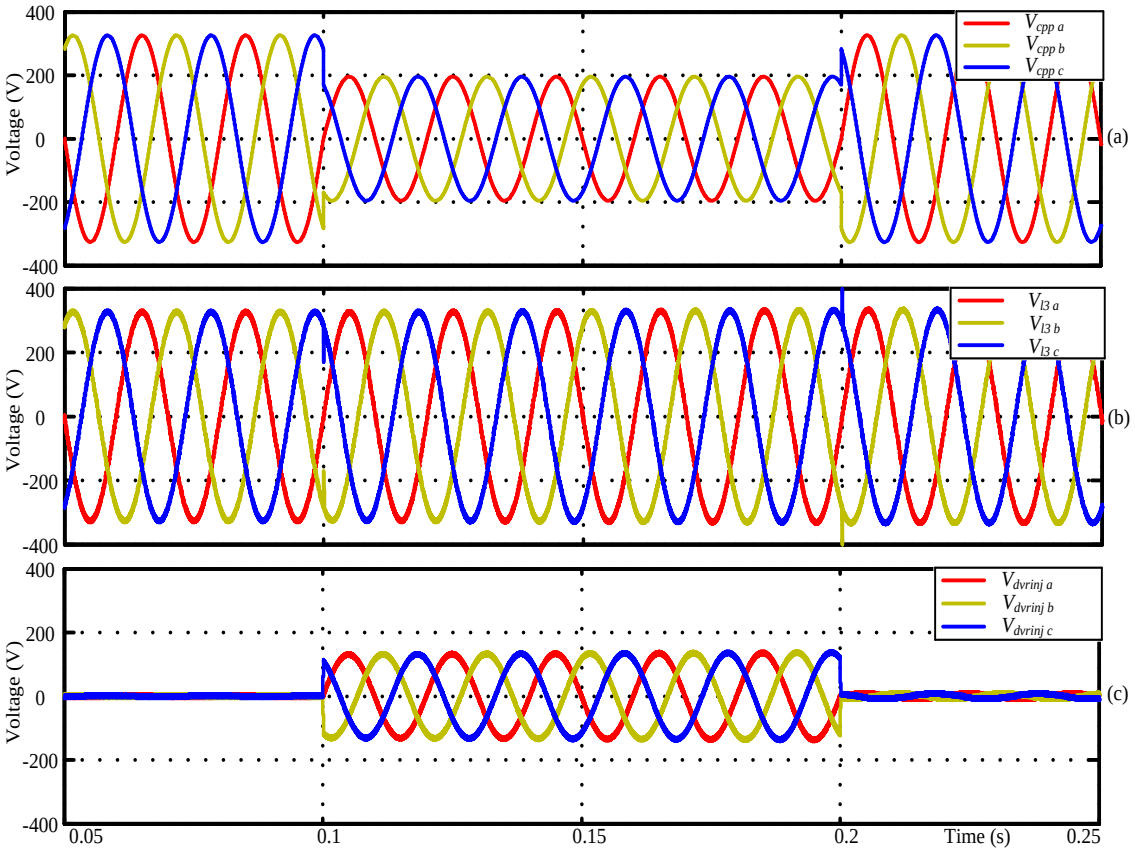

Figure 5.12: Sag on both feeders: (a) CPP bus voltage. (b) Voltage across the load L3. (c) DVR injected voltage.

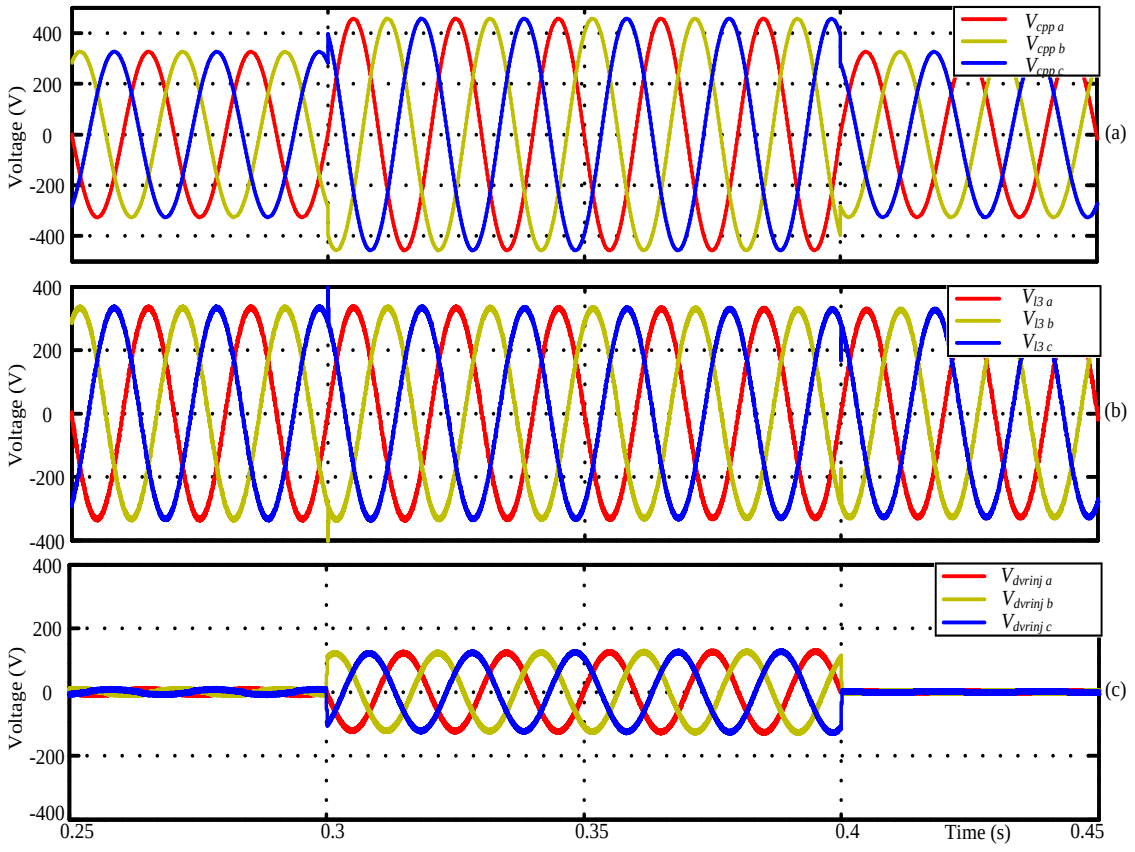

Figure 5.13: Swell on both feeders: (a) CPP bus voltage. (b) Voltage across the load L3. (c) DVR injected voltage.

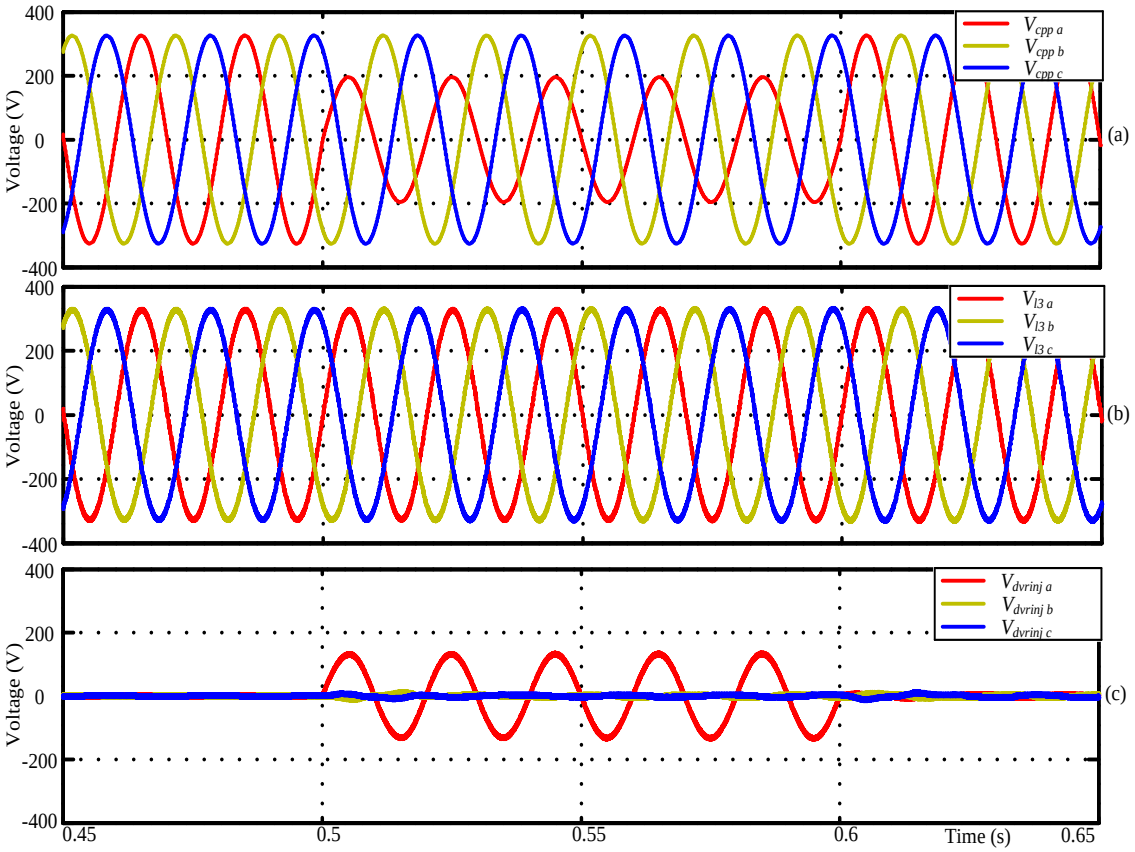

Figure 5.14: Unbalanced sag on both feeders: (a) CPP bus voltage. (b) Voltage across the load L3. (c) DVR injected voltage.

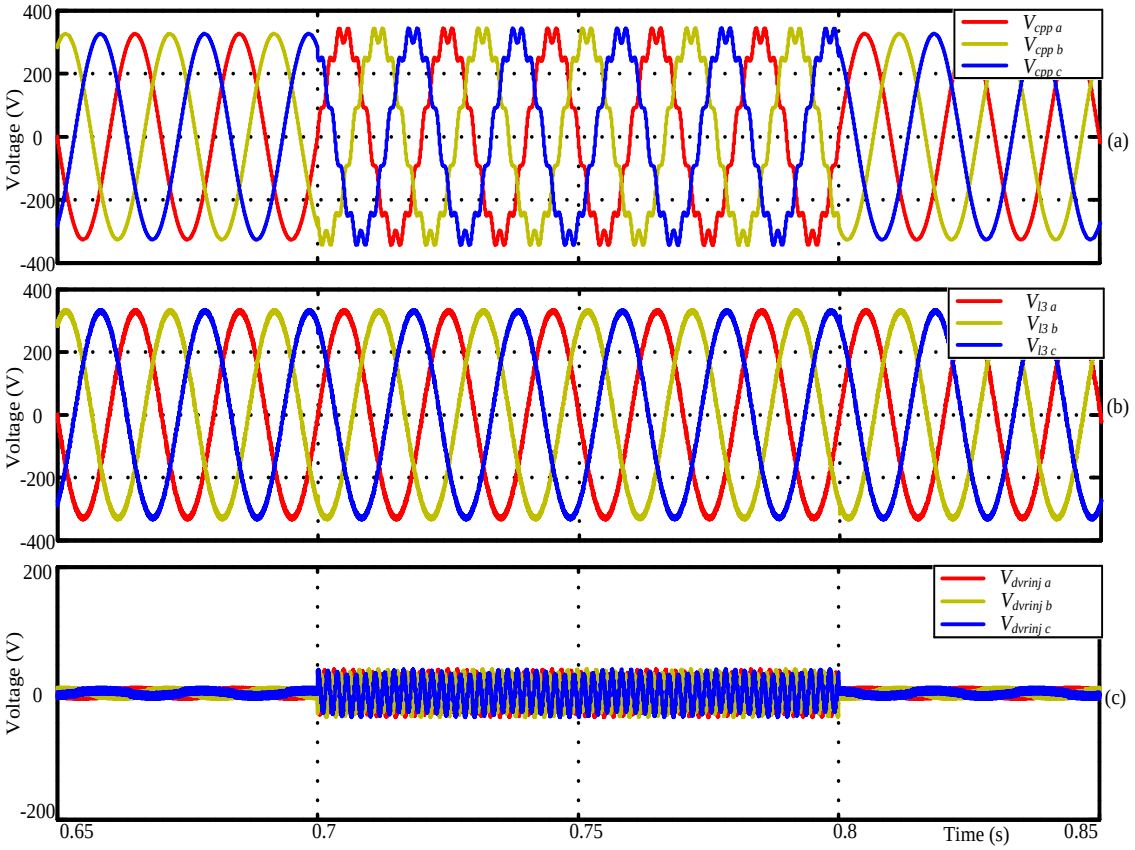

Figure 5.15: Distorted voltage with 11th harmonic on CPP bus: (a) CPP bus voltage. (b) Voltage across the load L3. (c) DVR injected voltage.

The Fig. 5.12(a) shows the CPP bus voltage when both the preferred and alternate feeders are affected by the voltage sag of 40% from $t = 0.1\ s$ to $t = 0.2\ s$. The load L3 will get a terminal voltage which is equal to the pre-fault value as shown in Fig. 5.12(b). The injected voltage by the DVR for compensating the sag is as shown in Fig. 5.12(c). So the most critical load L3 is not affected by voltage sag but during this duration other loads will get a voltage which is same as CPP bus voltage.

Fig. 5.13(a) shows the CPP bus voltage when both the feeders are subjected to swell of 40% starting from $t = 0.3\ s$ and it lasts till $t = 0.4\ s$. In this operating mode CPP bus will be connected to the preferred feeder and the L3 voltage is as shown in Fig. 5.13(b). The DVR will inject a voltage which is in phase opposition with the CPP bus voltage for compensating under this condition which is as in Fig. 5.13(c).

Next simulation study is conducted for evaluating the ability of DVR to inject voltage under unbalanced sag condition. Fig. 5.14(a) shows the CPP voltage when both the feeders are subjected to a 40% sag in phase a from $t = 0.5\ s$ to $t = 0.6\ s$. In this case the phase a of DVR injects a voltage to make the L3 voltage balanced. The voltage across the load L3 is as shown in Fig. 5.14(b) and dvr injcted voltage is as in Fig. 5.14(c).

The next part is to evaluate the performance of DVR for compensating the distortions in the feeder voltage. The CPP bus is connected to the preferred feeder, 11th order voltage harmonics are present in the feeder voltage for duration of $0.1\ s$ starting from $t = 0.7\ s$. Fig. 5.15(a) shows the CPP bus voltage which contain the voltage harmonics. DVR injects a voltage to compensate this harmonics and the load L3 will get a voltage which is free from distortion as in Fig. 5.15(b). The THD of the voltage across the L3 is reduced to 1.3% from 9.16% which is the THD of CPP bus voltage in this duration.

From the simulation results presented above it can be observed that DVR can compensate for the voltage quality disturbances which happens in both the feeders and it also keeps the THD of the voltage across the most critical load under the limits as per standards [29].

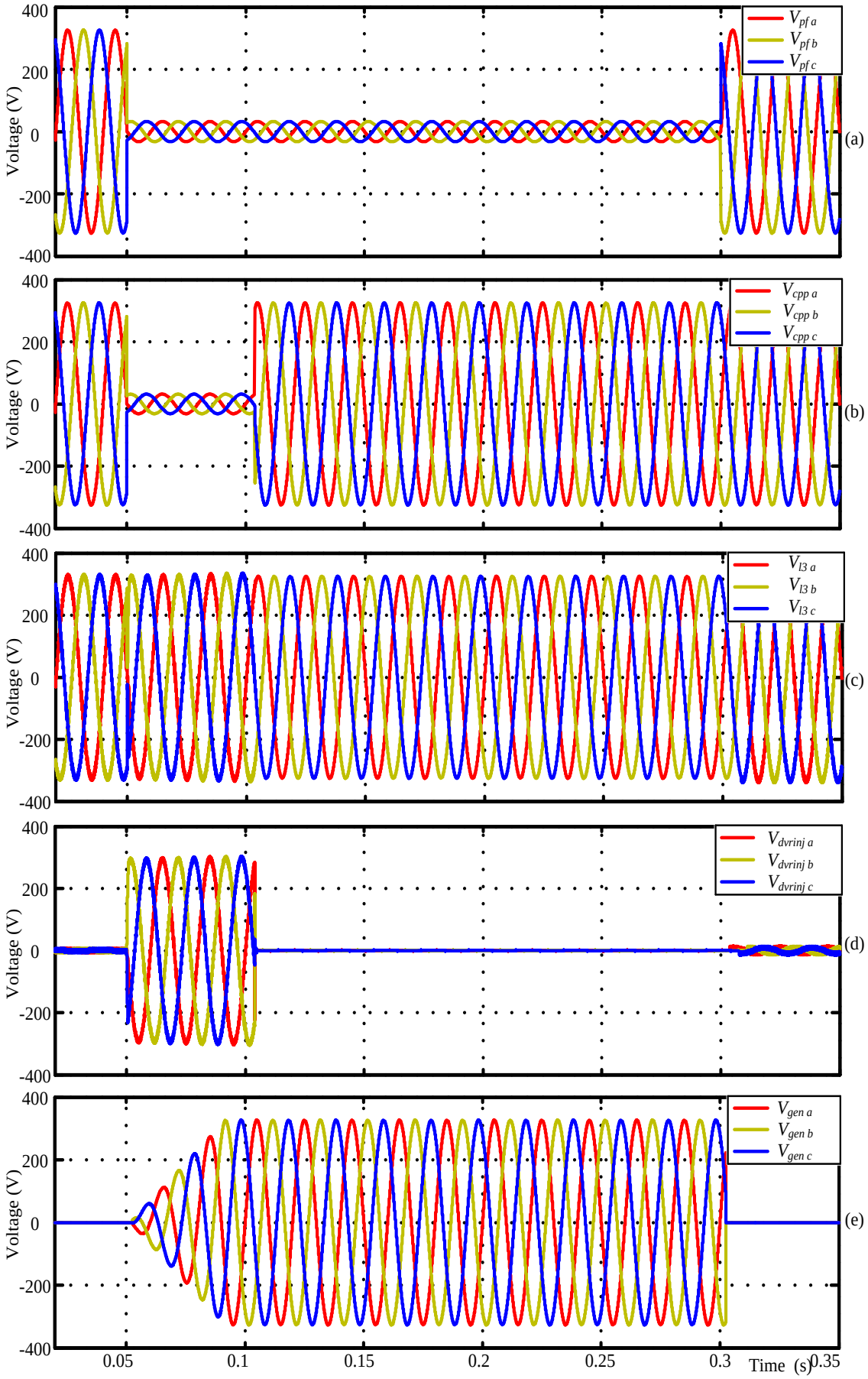

Figure 5.16: CPP voltages under total interruption: (a) Preferred feeder/Alternate feeder. (b) CPP bus. (c) Load L3. (d) DVR injected. (e) Diesel generator.

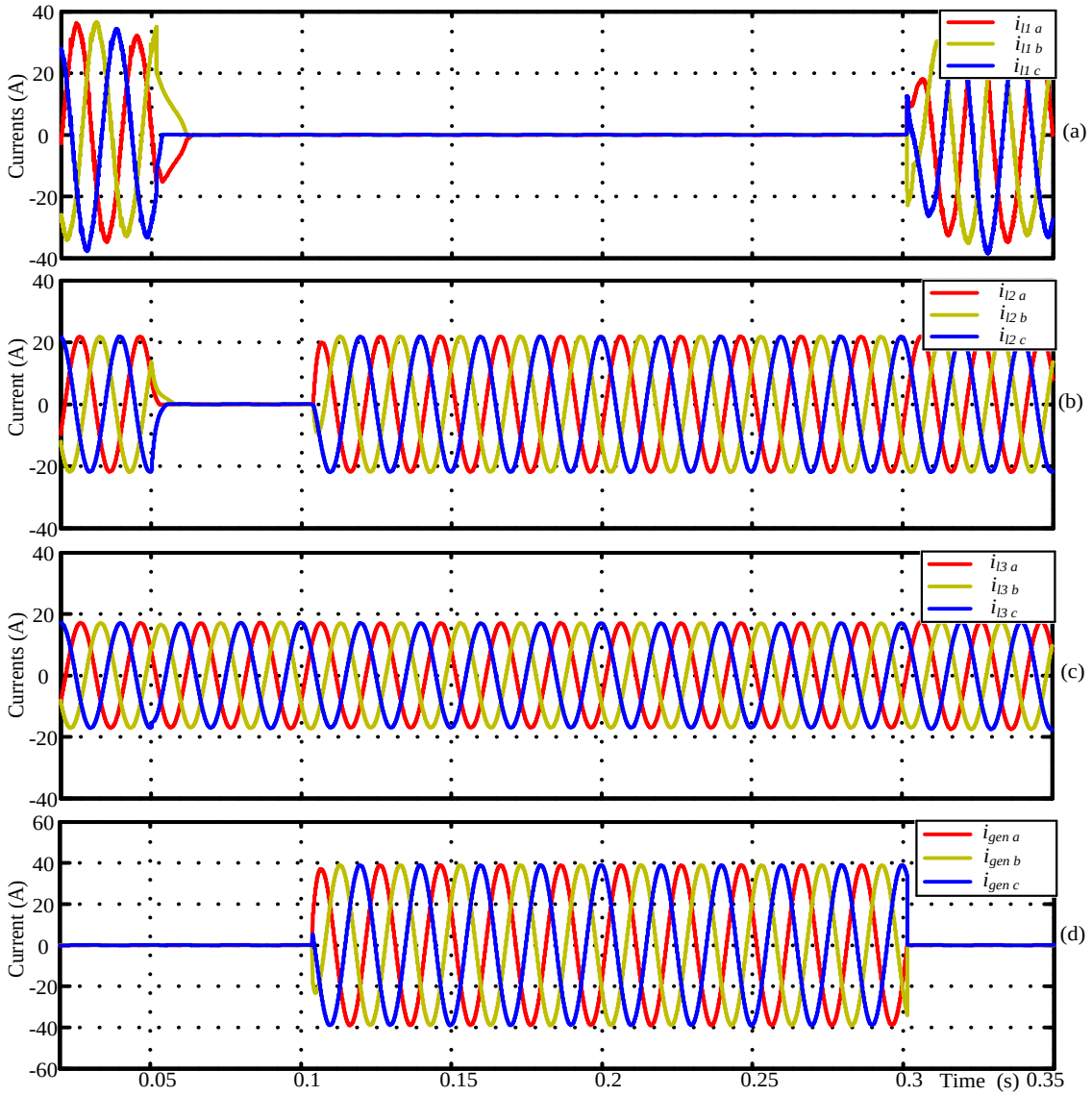

Figure 5.17: CPP currents under total interruption: (a) L1. (b) L2. (c) L3. (d) Diesel generator.

5.4 Operation of DVR and DG During Interruption

In the event when both the feeders got interrupted (i.e., more than 50% sag/swell on both the feeders) diesel generator has to supply the critical loads (L2 and L3). During the generation start-up time DVR will maintain the voltage across the most critical load (L3), after the start-up delay generator will be connected to the CPP bus and it will starts supplying the loads (L2 and L3). Fig. 5.16(a)-(e) shows the different voltages and Fig. 5.17(a)-(d) shows the different currents in the CPP for an interruption staring at $t = 0.05\ s$ and it lasts till $t = 0.3\ s$. In this study diesel generator for simplification is modelled as a controlled voltage source in which voltage will build up to the nominal value within few cycles after it gets a signal for starting (dg_start). It will issue the

ready signal (dg_ready) after the voltage reaching the nominal value (i.e., between 0.9 and $1.1\ pu$).

The interruption is started at $t = 0.05\ s$ at both preferred and alternate feeders as shown in Fig. 5.16(a), but the feeder will remains connected to the CPP bus to get a reference for the DVR injected voltage. During the period from $t = 0.05\ s$ to $t = 0.1\ s$ the generator voltage will build up as shown in Fig. 5.16(e) and DVR will inject a voltage as in Fig. 5.16(d) to maintain the voltage across the load L3. After DG start-up this will be connected to the CPP bus and the voltage at the CPP bus is as shown in Fig. 5.16(b) and DVR will be bypassed. The distinguishing feature of the load L3 is that it gets power even under interruption where as the L2 gets power only when some auxiliary generation is connected to the CPP bus.

Fig. 5.17 shows the different currents in the CPP. From Fig. 5.17(a) it is evident that the load L1 will get the power only when either of the feeder is restored. Fig. 5.17(b) shows the current of second load (L2), it can be observed that it gets power when either feeders or generator is connected to the CPP bus and the load current of L3 is continuous as in Fig. 5.17(c).

It is noted from the simulation results that the load L3 will get better grade power in the park, L2 will receive the next grade power and L1 will receive the least qualified power in the CPP and it is also evident that all the loads receive better quality power than the normal distribution system.

5.5 Summary

A high quality power compared to normal distribution system is achieved for all the loads in the CPP by suitable control of different devices. The loads in the CPP can be transferred from preferred feeder to alternate feeder if some sag/swell occurs in the preferred feeder. DSTATCOM compensates for the harmonic and reactive power drawn by the load L1. In the case when both feeders are subjected to sag/swell DVR maintains the voltage most sensitive load (L3) to a constant value. Under total power loss on both the feeders diesel generator which will start within few seconds used to supply the critical loads (L2 and L3).

CHAPTER 6

CONCLUSION

This chapter intends to summarize the work which has been carried out in this thesis and it also gives an idea about future works which can be carried out based ion this thesis.

6.1 Conclusion and Summary

A Custom power Park (CPP) model with a suitable control algorithms which work under distorted grid voltages are presented in this work. It has three Custom power devices, they are Solid State Transfer Switch (SSTS), Distribution Static Compensator (DSTATCOM) and Dynamic Voltage Restorer (DVR). The operation and control of each device under various power quality disturbances have been discussed in detail. The coordinated operation of the custom power devices is made possible to form a CPP with the help of fast control algorithm based on SRF theory. The SSTS selects the better quality feeder from the available feeders to supply loads in the park. The transfer time from one feeder to another is reduced with the help the control algorithm developed in this work. DSTATCOM operates to compensate for unbalanced and harmonic currents drawn by the loads in the park, and it can also supply a part of reactive power required by the loads. The voltage sags and swells affect the park bus only when both feeders of the CPP are under the disturbance, in this case DVR will compensate for the most sensitive loads in the park.

The effectiveness of the CPP to operate under various power quality disturbances such as voltage and current harmonics, balanced and unbalanced voltage sags/swells and voltage interruption has been investigated with the help of simulation study. The simulation results show that all the loads in the Custom Power Park are benefited with superior quality power supply than that available in normal distribution system. The major outcome of this work is the fast and effective control algorithm based on SRF for coordination of the custom power devices is presented in this work. The CPP model

presented can be used as a platform for testing and evaluating efficiency of models of all kind of custom power devices.

6.2 Scope for Future Work

Experimental validation of the working of custom power devices and the control algorithm should be done in order to verify the simulation results, this can be considered as the next step in this study.

DC energy storage for the DVR is considered as a simple voltage source in the simulation study, it can be replaced with some renewable energy based storage system which is more practical.

In this thesis the loads considered are static in nature, the study can be further extended by considering dynamic loads which is most common in almost all industries.

The diesel generator is normally has start-up time few minutes, if we use some distributed energy resources instead of this we can reduce this time as well as it will give big savings in terms of economy of operating a diesel generator.

REFERENCES

[1] N. Hingorani, "Overview of custom power applications," *IEEE - PES Summer Meeting Panel Session on Application of Custom Power Devices for Enhanced Power Quality, San Diego, CA*, 1998.

[2] A. El Mofty and K. Youssef, "Industrial power quality problems," in *Electricity Distribution, 2001. Part 1: Contributions. CIRED. 16th International Conference and Exhibition on (IEE Conf. Publ No. 482)*, vol. 2, june 2001, pp. 18–21.

[3] D. Flinn, C. Gilker, and S. Mendis, "Methods for identifying potential power quality problems," in *Rural Electric Power Conference, 1991. Papers Presented at the 35th Annual Conference*, Apr 1991, pp. C1/1–C1/5.

[4] A. de Almeida, L. Moreira, and J. Delgado, "Power quality problems and new solutions," *International Conference on Renewable Energies and Power Quality, Spain*, vol. 1, Mar 2003.

[5] A. Domijan, A. Montenegro, A. Keri, and K. E. Mattern, "Custom power devices: an interaction study," *Power Systems, IEEE Transactions on*, vol. 20, no. 2, pp. 1111–1118, May 2005.

[6] G. Satyaveer, A. Dixit, N. Mishra, and S. P. Singh., "Custom power devices for power quality improvement: a review," *International Journal of Research in Engineering and Applied Sciences (IJREAS)*, vol. 2, no. 2, pp. 1646–1659, Feb 2012.

[7] Y. Pal, A. Swarup, and B. Singh, "A review of compensating type custom power devices for power quality improvement," in *Power System Technology and IEEE Power India Conference, 2008. POWERCON 2008. Joint International Conference on*, Oct 2008, pp. 1–8.

[8] A. Ghosh and A. Joshi, "The concept and operating principles of a mini custom power park," *Power Delivery, IEEE Transactions on*, vol. 19, no. 4, pp. 1766–1774, Oct 2004.

[9] A. Ghosh, "Performance study of two different compensating devices in a custom power park," *Generation, Transmission and Distribution, IEE Proceedings-*, vol. 152, no. 4, pp. 521–528, July 2005.

[10] M. Emin Meral, A. Teke, and M. Tumay, "Overview of an extended custom power park," in *Power and Energy Conference, 2008. PECon 2008. IEEE 2nd International*, Dec 2008, pp. 1364–1368.

[11] A. Ghosh, R. Majumder, G. Ledwich, and F. Zare, "Power quality enhanced operation and control of a microgrid based custom power park," in *Control and Automation, 2009. ICCA 2009. IEEE International Conference on*, Dec 2009, pp. 1669–1674.

[12] A. Aghazadeh, R. Noroozian, A. Jalilvand, and H. Haeri, "Combined operation of dynamic voltage restorer with distributed generation in custom power park," in *Environment and Electrical Engineering (EEEIC), 2011 10th International Conference on*, May 2011, pp. 1–4.

[13] A. Tapia and N. Garcia, "Periodic steady-state solution of a custom power park using the limit cycle method," in *Power and Energy Society General Meeting, 2011 IEEE*, July 2011, pp. 1–6.

[14] B. Mohammed, K. Rao, R. Ibrahim, and N. Perumal, "Application of custom power park to improve power quality of sensitive loads," in *Power Electronics (IICPE), 2012 IEEE 5th India International Conference on*, Dec 2012, pp. 1–6.

[15] P. Manitha, V. J. Sankar, P. Anjana, V. Raveendran, and M. G. Nair, "Design and development of a mini custom power park," *{AASRI} Procedia*, vol. 7, no. 0, pp. 107 – 113, 2014, 2nd {AASRI} Conference on Power and Energy Systems (PES2013). [Online]. Available: http://www.sciencedirect.com/science/article/pii/S2212671614000389

[16] M. Moschakis and N. Hatziargyriou, "A detailed model for a thyristor-based static transfer switch," *Power Delivery, IEEE Transactions on*, vol. 18, no. 4, pp. 1442–1449, Oct 2003.

[17] H. Mokhtari, S. Dewan, and M. Travani, "Performance evaluation of thyristor based static transfer switch," *Power Delivery, IEEE Transactions on*, vol. 15, no. 3, pp. 960–966, Jul 2000.

[18] H. Mokhtari, M. R. Iravani, S. B. Dewan, P. Lehn, and J. A. Martinez, "Benchmark systems for digital computer simulation of a static transfer switch," *Power Engineering Review, IEEE*, vol. 21, no. 7, pp. 69–69, July 2001.

[19] H. J. Jung, I. Y. Suh, B. S. Kim, R. Y. Kim, S. Y. Choi, and J. H. Song, "A study on dvr control for unbalanced voltage compensation," in *Applied Power Electronics Conference and Exposition, 2002. APEC 2002. Seventeenth Annual IEEE*, vol. 2, 2002, pp. 1068–1073 vol.2.

[20] Y. Sillapawicharn and Y. Kumsuwan, "An improvement of synchronously rotating reference frame based voltage sag detection for voltage sag compensation applications under distorted grid voltages," in *Power Electronics and Drive Systems (PEDS), 2011 IEEE Ninth International Conference on*, Dec 2011, pp. 100–103.

[21] P. T. Cheng, C. C. Huang, C. C. Pan, and S. Bhattacharya, "Design and implementation of a series voltage sag compensator under practical utility conditions," *Industry Applications, IEEE Transactions on*, vol. 39, no. 3, pp. 844–853, May 2003.

[22] U. Miranda, L. Rolim, and M. Aredes, "A dq synchronous reference frame current control for single-phase converters," in *Power Electronics Specialists Conference, 2005. PESC '05. IEEE 36th*, June 2005, pp. 1377–1381.

[23] Mahesh K. Mishra and K. Karthikeyan, "An investigation on design and switching dynamics of a voltage source inverter to compensate unbalanced and nonlinear loads," *Industrial Electronics, IEEE Transactions on*, vol. 56, no. 8, pp. 2802–2810, Aug 2009.

[24] U. Rao, Mahesh K. Mishra, and A. Ghosh, "Control strategies for load compensation using instantaneous symmetrical component theory under different supply voltages," *IEEE Transactions on Power Delivery*, vol. 23, no. 4, pp. 2310–2317, 2008.

[25] H. Suryanarayana and Mahesh K. Mishra, "Fuzzy logic based supervision of dc link pi control in a dstatcom," in *India Conference, 2008. INDICON 2008. Annual IEEE*, vol. 2, Dec 2008, pp. 453–458.

[26] R. Salimin and M. Rahim, "Simulation analysis of dvr performance for voltage sag mitigation," in *Power Engineering and Optimization Conference (PEOCO), 2011 5th International*, June 2011, pp. 261–266.

[27] A. Pathan, S. Vanamane, and R. Chile, "Different control techniques of dynamic voltage restorer for power quality problems," in *Automation, Control, Energy and Systems (ACES), 2014 First International Conference on*, Feb 2014, pp. 1–6.

[28] U. Patil and A. Thorat, "Hysteresis voltage control technique in dynamic voltage restorer for power quality improvement," in *Energy Efficient Technologies for Sustainability (ICEETS), 2013 International Conference on*, April 2013, pp. 1149–1153.

[29] "Recommended practices and requirements for harmonic control in electrical power systems," *IEEE Standard 519-1992*, 1993.